NUMERICAL ASPECTS OF DENSITY FUNCTIONAL THEORY: CHARGE DENSITY EXPANSIONS AND CALCULATIONS OF ELECTROSTATIC INTERACTION ENERGIES

By

ISKHANDAR MD NASIR

Bachelor of Science

in Arts and Sciences

Oklahoma State University

Stillwater, Oklahoma

1984

Submitted to the Faculty of the Graduate College
of the Oklahoma State University
in partial fulfillment of the requirements
for the Degree of
MASTER OF SCIENCE
July, 1987

Thesis
1987
M478n
cop. 2

بسم الله الرحمن الرحيم

In the name of Allah, The Most Benificent, The Most Merciful.

OKLAHOMA STATE UNIVERSITY LIBRARY

NUMERICAL ASPECTS OF DENSITY FUNCTIONAL THEORY:
CHARGE DENSITY EXPANSIONS AND CALCULATIONS
OF ELECTROSTATIC INTERACTION ENERGIES

Thesis Approved:

Paul Wes Shaw
Thesis Advisor

A L Sallt

E E Lafon

Norman N. Durham
Dean of the Graduate College

1282852

ACKNOWLEDGEMENTS

Praise be to Allah, Most Beneficient, Most Merciful for all His bounties to His servant.

First of all I would like to express my sincere appreciation and thanks to my thesis advisor, Dr. Paul Westhaus for all his cooperations, guidance and assistance throughout the course of this work.

Appreciations is also expressed to both of my thesis committee, Dr Earl Lafon and Dr Larry Scott for all their beneficial comments and advice in the final preparation of this thesis. Appreciation was also dedicated to all faculty of the Physics Deparment at Oklahoma State University for sharing their knowledge and building my understanding in Physics.

Finally I would to express my special gratitude to my beloved wife Norizan Ishak and my child for giving me the supports and courages and comforts during the course of this work. Also I would like to all my friends especially Sanusi and family, Kamal Mohammad and Sallehuddin Sidek for their helps in the finishing touch of this thesis.

TABLE OF CONTENTS

LIST OF FIGURES

Figure Page

Figure Page

LIST OF TABLES

CHAPTER I

INTRODUCTION

It has been the ambition of the chemist and physicist working in the area of chemical physics to develop an easier approach in explaining the details of molecular interactions qualitatively and quantitatively. With this in mind, the Density Functional Theory (DFT) has been introduced and is lately becoming more popular. An interesting feature of the Density Functional Theory formalism is that it offers the possibility of invoking our chemical intuition in trying to understand the structure and energetics of molecules. This is primarily true because the focus of DFT is the ordinary three dimensional space, the space over which electron density is defined. In contrast to this is the traditional quantum chemistry approach where the sought-for ground state eigenfunction Ψ_o of the Hamiltonian is defined in the many-electron Hilbert space. Therefore as the systems become more and more complex, especially in treating molecular interactions, the problems which arise using traditional techniques tend to mushroom. Here, by traditional quantum chemistry techniques, we mean molecular orbital calculations extended perhaps by configuration interaction studies. Therefore the need to understand the Density Functional formalism becomes more obvious especially in solving many-body problems such as molecular interactions.

Within the DFT formalism, the remarkable achievement by Hohenberg and Kohn [1] establishes the fact that the total electronic energy of interaction for a given configuration of the fixed nuclei may be found by seeking the minimum value of an energy functional of the electron charge density. Indeed, the theory shows the existence of such a functional whose value is always an upper bound to the electronic energy for all imaginable choices of the electronic charge density. At the present time, DFT formalism provides a rigorous quantum mechanical framework in which calculations of properties and electronic energies of a collection molecules are possible within certain approximation. It is in fact the interaction energy of molecules or fragments of molecules in their electronic ground state that we hope to investigate. By the electronic energy of molecules or fragments of molecules, we mean the ground state electronic energy eigenvalue of the complete Hamiltonian of the system with all the nuclei of all the molecules fixed in place; that is, we seek the ground state electronic energy in the Born-Oppenheimer [2] approximation. In addition, we also need to add the Coulombic repulsion energy of the fixed nuclei to obtain the total energy of the entire system. The term "fragment of a molecule" or molecular fragment refers to a collection of nuclei whose internal coordinates do not change during the course of our consideration. The potential energy of interaction can be deduce as the difference between the total energy of the interacting system and the energy of each isolated fragment. Now, as the positions of the molecular fragments are changed, the total electronic and Coulombic repulsion energies of the system are

recalculated for each new configuration of the nuclei. The consequence of this is that a new potential energy is obtained for each new configuration of the nuclei. In other words, the potential energy itself depends on the position and orientation of the nuclei which make up the molecules. If we then plot the potential energy of interaction versus all the independent variables, the result is a potential energy surface. The intermolecular force, $\vec{F}_i$, on the i^{th} nucleus is related to the potential energy by

$$\vec{F}_i = -\vec{\nabla}_i V \qquad (1.1)$$

where V is the potential energy of interaction. In a word, we are considering the theory of intermolecular forces within the Density Functional formalism.

Let us analyse the problem by first expressing the Hamiltonian assuming that we have applied the Born-Oppenheimer approximation so that what we are interested in is just the electronic energy of the total Hamiltonian. Consider the general case where we have a system of F interacting molecular fragments indexed by f = 1,2,3.....F with a total of N electrons and A nuclei. Now each of the fragments can consist of either a single nucleus (i.e for atoms) or a number of nuclei (i.e for molecules) and some electrons. Say the f^{th} fragment consists of A_f labeled nuclei and N_f labeled electrons. Now, to specify this particular fragment in space explicitly we needs $3A_f$ nuclear coordinates. These nuclear coordinates can be divided into two sets. The first set consists of six external coordinates which are the center of mass coordinates $\vec{R}_f$ and the Euler angles $\vec{\Omega}_f$. The other set consists of $3A_f$-6 internal

coordinates which we write as $\{ \tau_f \}$. The electronics, Hamiltonian for the entire system can be written as:

$$\hat{H} = \sum_{f=1}^{F} \left\{ \sum_{i \epsilon \kappa_f} \left[\frac{-\hbar^2}{2m} \nabla_i^2 + \sum_{a \epsilon \eta_f} \frac{-Z_a e^2}{|\vec{r}_i - \vec{R}_a|} \right] + \sum_{\substack{i<j \\ i,j \epsilon \kappa_f}} \frac{e^2}{|\vec{r}_i - \vec{r}_j|} + \sum_{\substack{a<b \\ a,b \epsilon \eta_f}} \frac{Z_a Z_b e^2}{|\vec{R}_a - \vec{R}_b|} \right\}$$

$$+ \sum_{1 \le f < f \le F} \left\{ \sum_{i \epsilon \kappa_f} \sum_{a \epsilon \eta_{f'}} \frac{-Z_a e^2}{|\vec{r}_i - \vec{R}_a|} + \sum_{j \epsilon \kappa_f} \sum_{b \epsilon \eta_{f'}} \frac{e^2}{|\vec{r}_i - \vec{r}_j|} + \sum_{a \epsilon f} \sum_{b \epsilon f} \frac{Z_a Z_b e^2}{|\vec{R}_a - \vec{R}_b|} \right\} \qquad (1.2)$$

Note that in writing the Hamiltonian, we assume that all the electrons and nuclei in the system are labeled 1 to N and 1 to A respectively. Then we associate each set of the labeled electrons and nuclei with one of the fragments so that a particular set of labeled electrons and nuclei belong to a particular labeled fragment. All of these labeled electrons and nuclei belonged to one of the sets κ_f and η_f respectively where f is the fragment label and f = 1,2,...F.

Let us analyse the Hamiltonian [Eqn (1.2)] term by term. Note that in the first line we first consider the electrons and nuclei within a given fragment f and then sum over all the fragments. The first terms are the kinetic energies of all the electrons in the system. The second, third and fourth terms in the Hamiltonian are the electron-nucleus, electron-electron and nucleus-nucleus Coulombic interactions respectively within each fragment. Finally, in the second line the terms refer to the corresponding inter-fragment interactions. On the other hand if one carries out the summations over all the nuclei and electrons

within each fragment followed by the summations over all the fragments, then the Born-Oppenheimer Hamiltonian becomes

$$\hat{H} = \sum_{i=1}^{N} \frac{-\hbar^2}{2m} \nabla_i^2 + \sum_{i=1}^{N}\sum_{a=1}^{A} \frac{-Z_a e^2}{|\vec{r}_i - \vec{R}_a|} + \sum_{i<j}^{N} \frac{e^2}{|\vec{r}_i - \vec{r}_j|} + \sum_{a<b}^{A} \frac{Z_a Z_b e^2}{|\vec{R}_a - \vec{R}_b|} . \qquad (1.3)$$

In accord with the indistiguisability of electrons, the Hamiltonian is clearly symmetric in the electron particle labels. As we noted above each of the nuclear coordinates can be associated with a particular fragment f and expressed in terms of the center of mass coordinates $\vec{R}_f$, the Euler angles $\vec{\Omega}_f$ and the set of internal coordinates $\{ \tau_f \}$. We seek to determine the ground state energy by solving the eigenvalue problem

$$H\Psi_o(\vec{R}_f, \vec{\Omega}_f, \{\tau_f\}; x_1, x_2, \ldots x_N) =$$

$$E_o(\vec{R}_f, \vec{\Omega}_f, \{\tau_f\})\, \Psi_o(\vec{R}_f, \vec{\Omega}_f, \{\tau_f\}; x_1, x_2, \ldots x_N) \qquad (1.4)$$

as a function of the center of mass coordinates and Euler angles for all the fragments. Note the dependence of the energy on the internal coordinates of each fragment. This dependence can be written in the form

$$E = E_o(\vec{R}_1, \vec{\Omega}_1, \vec{R}_2, \vec{\Omega}_2, \ldots \vec{R}_F, \vec{\Omega}_F; \{\tau_1\}, \{\tau_1\}, \ldots \{\tau_F\}) . \qquad (1.5)$$

We envision E_o to be a function of the $\vec{R}$'s and $\vec{\Omega}$'s, but still parameterized by the τ's. Once we find the solution this ground state energy is substracted from the ground state energy of each of the isolated fragments each of which also surely depends on the internal coordinates of that fragment. The potential energy of interaction can be

written as:

$$V(\vec{R}_1,\vec{\Omega}_1,\vec{R}_2,\vec{\Omega}_2,\ldots\vec{R}_F,\vec{\Omega}_F;\ \{\tau_1\},\{\tau_1\},\ldots\{\tau_F\}\ ) =$$

$$E_o(\vec{R}_1,\vec{\Omega}_1,\vec{R}_2,\vec{\Omega}_2,\ldots\vec{R}_F,\vec{\Omega}_F;\ \{\tau_1\},\{\tau_1\},\ldots\{\tau_F\}\ ) - \sum_{f=1}^{F} E_o(\ \{\tau_f\}\ ) \qquad (1\cdot 6)$$

Note that the parametric dependence on the internal coordinates still survives in the structure of the potential energy surface. Finally one has to make note that some of the external coordinates are ignorable so that in practice the potential energy of interaction does not depend on all the external coordinates for the system. In particular, the potential energy surely cannot depend on the center of mass of the entire system or its orientation in space. Therefore, in general the potential energy of interaction actually depends on 6F-6 variables. On the other hand, there are also special cases where the fragments involved in the interactions are atoms or linear molecules in which cases the ignorable coordinates must be determined individually.

Now, let's suppose that we knew the normalized groundstate eigenfunction Ψ_o although in fact we generally do not. Then the ground state energy can be expressed as

$$E_o = \int \Psi_o^{\star}\, \hat{H} \Psi_o \, d\tau \qquad (1\cdot 7)$$

From this expression we can also write the ground state energy E_o within the pure state density matrix formalism [3]:

$$E_o = -\frac{\hbar^2}{2m} \int d^3 r \sum_{\xi} \nabla^2 \rho^{(1)}(\vec{r}, \xi; \vec{r}', \xi') \Big|_{\vec{r}'=\vec{r},\ \xi'=\xi} +$$

$$\int d^3r \sum_{a=1}^{A} \frac{-Z_a e^2}{|\vec{r} - \vec{R}_a|} \rho^{(1)}(r) + \frac{e^2}{2} \int d^3r_1 \int d^3r_2 \frac{\rho^{(2)}(\vec{r}_1, \vec{r}_2)}{|\vec{r}_1 \; \vec{r}_2|} +$$

$$\sum_{a<b}^{A} \frac{Z_a Z_b e^2}{|\vec{R}_a - \vec{R}_b|} \qquad (1\cdot 8)$$

where $\rho^{(1)}(\vec{r}, \xi; \vec{r}', \xi')$ is the full one-electron reduced density matrix, and $\rho^{(1)}(\vec{r})$ is defined as the sum over the spin coordinate ξ of diagonal elements

$$\rho^{(1)}(\vec{r}) = \sum_{\xi} \rho^{(1)}(\vec{r},\xi; \vec{r},\xi). \qquad (1\cdot 9)$$

Similarly, $\rho^{(2)}(\vec{r}_1, \vec{r}_2)$ are the diagonal elements of the two-electron reduced density matrix summed over the spin coordinates ξ_1 and ξ_2

$$\rho^{(2)}(\vec{r}_1, \vec{r}_2) = \sum_{\xi_1} \sum_{\xi_2} \rho^{(2)}(\vec{r}_1, \xi_1, \vec{r}_2, \xi_2; \vec{r}_1, \xi_1, \vec{r}_2, \xi_2) \; . \qquad (1\cdot 10)$$

In general, an n^{th} order "reduced" density matrix element arising from a pure-state wavefunction Ψ is

$$\rho^{(n)}(x_1,x_2 \ldots x_n; x_1',x'_2,\ldots x'_n) = \frac{N!}{n!\,(N-n)!} \int dx_{n+1}\, dx_{n+2} \ldots dx_N \; *$$

$$\Psi(x_1,x_2 \ldots x_n,x_{n+1} \ldots x_N)\; \Psi^{*}(x_1',x_2' \ldots x_n',x_{n+1} \ldots x_N) \qquad (1\cdot 11)$$

In the expression above the x's correspond to the spin and the ordinary 3-Dimensional space and spin coordinates of an electron i.e.

$$x \rightarrow \vec{r}, \xi$$

Given the exact ground state eigenfunction Ψ_o, one may in

principle calculate $\rho^{(1)}$ and $\rho^{(2)}$ straightfowardly and thus obtain E_o according to Eqn (1·8). The important thing to notice here is that even if one did not know the exact form of the ground state wavefunction, all one would need to know to obtain E_o are the elements of the one- and two-electron reduced density matrices. Can one use Eqn (1·8) by-passing explicit consideration of Ψ? One might suggest using trial densities for both the one- and two- electron reduced density matrices motivated by an extension of the Rayleigh Ritz variational principal [4] which states

$$E_o \leq \int \Psi^{\star}_{trial} H \Psi_{trial} \, d\tau \qquad (1\cdot12)$$

Then the extension of equation (1·12) would apparently become

$$E_o \leq \frac{-\hbar^2}{2m} \int d^3r \sum_{\xi} \nabla^2 \rho^{(1)}_{trial}(\vec{r}, \xi; \vec{r}', \xi') \Big|_{\vec{r}'=\vec{r},\, \xi'=\xi} + \int d^3r \sum \frac{-Z_a e^2}{|\vec{r} - \vec{R}_a|} \rho^{(1)}_{trial}(\vec{r}) + \int d^3r_1 \int d^3r_2 \frac{\rho^{(2)}_{trial}(\vec{r}_1, \vec{r}_2)}{|\vec{r}_1 - \vec{r}_2|} + \sum \frac{Z_a Z_b e^2}{|\vec{R}_a - \vec{R}_b|} \qquad (1\cdot13)$$

In other words, as one can vary the wavefunction in search for a minimum based on the Rayleigh-Ritz variational principle then one ought to be able to do the same thing using the reduced density matrices $\rho^{(1)}$ and $\rho^{(2)}$ provided both are derivable from a legitimate normalized trial wavefunction. This method was attempted in the past ignoring the proviso and problems of inconsistency arose because for some trial

functions the energy obtained was lower than the exact ground state energy E_o. This inconsistency tells us that in using the energy expression Eqn (1·8), one cannot freely vary the densities in search for the minimum. One must guarantee that the trial one- and two- electron density matrices are derivable from the same N-electron wavefunction. In other words, these density matrices have to be N-representable.

It was not until late 1964 that Hohenberg and Kohn proposed the remarkable theorem which states that for a given local potential $v(\vec{r})$ there does exist an energy functional $\epsilon(N,\rho_N)$ of the electron density $\rho_N(\vec{r})$ such that for all N representable densities $\rho_N(\vec{r})$, $\epsilon(N,\rho_N)$ is an upper bound of the exact electronic ground state eigenvalue $E_o(\underline{R})$. Thus

$$E_o(\underline{R}) \leq \epsilon(N,\rho_N;\underline{R}) \qquad (1\cdot 14)$$

with the equality sign being obtained for the true ground state density. Here, $\underline{R}$ stands for the collection of nuclear coordinates $\vec{R}_a$ and charges Z_a, a=1,2...A.

The remarkable point of the theorem is that in finding the ground state energy one just has to consider the diagonal elements of the one-electron reduced density matrix. This can be anticipated for the expectation value of the local potential energy term in Eqn (1·8)

$$\langle\Psi|\sum_{i=1}^{N}\sum_{a=1}^{A}\frac{-Z_a e^2}{|\vec{r}_i-\vec{R}_a|}|\Psi\rangle$$

which is written in terms of the diagonal elements of the one-electron reduced density matrix

$$\int d^3 r \sum \frac{-Z_\alpha e^2 \rho^{(1)}(\vec{r})}{|\vec{r} - \vec{R}_a|}$$

On the other hand, it is not at all obvious how the kinetic energy and the electrostatic repulsion energy terms may be expressed in terms of $\rho^{(1)}$. Unfortunately in their original paper Hohenberg and Kohn only proved the existence of the energy functional but did not give a precise form of it. If in fact we knew the form of the energy functional then the problem of determining the ground state energy and the density for a particular local potential --i.e. a particular configuration of the nuclei-- would be a matter of minimizing the functional. One can envision doing this by using trial densities $\rho^{(1)}(\vec{r})$ in the known functional; still one must guarantee that the trial $\rho^{(1)}(\vec{r})$'s are N-representable, but as shown by Gilbert [5] this is easily done. The bottle neck in this program remains not knowing the exact energy functional. Many efforts have been made by researchers in this area trying to find the exact form of the ground state energy functional $\epsilon(N, \rho; \underline{R})$. In fact, later developments [6] have shown that there is not just one functional but rather many such inequivalent functionals, all of which have the upper bound property. In a sense, Hohenberg and Kohn discovered the existence of one such energy functional which according to these later developments had the limitation of being defined over what have come to be called " v-representable " densities.

Now let us derive an exact form of the energy functional based on the approach suggested by Levy [7]. We begin with his definition of

energy functional

$$\epsilon(N, \rho_N; \underline{R}) = \min_{\{|\Psi\rangle_{\rho_N}\}} \{ {}_{\rho_N}\langle\Psi| H |\Psi\rangle_{\rho_N} \} \qquad (1.15)$$

Here, what we envision is a search throughout the set of normalized N-electron states $\{ |\Psi\rangle_{\rho_N} \}$, each of which yielding the given electron density

$$\rho_N(\vec{r}) = {}_{\rho_N}\langle\Psi| \sum \delta(\vec{r} - \vec{r}_i) |\Psi\rangle_{\rho_N}, \qquad (1.16)$$

for one or more optimum states $|\tilde{\Psi}\rangle_{\rho_N}$ for which the expectation value of H achieves a minimum. It then follows from the Rayleigh-Ritz variational principle that once the energy functional is obtained the subsequent search of $\epsilon(N, \rho_N; \underline{R})$ over all N-representable $\rho_N(r)$ for the minimum value of the functional will necessarily yield the exact eigenvalue $E_o(\underline{R})$. Consequently, one can then write the exact energy $E_o(\underline{R})$ in the following fashion:

$$E_o(\underline{R}) = \min_{\{\rho_N(\vec{r})\}} [\, \epsilon(N, \rho_N; \underline{R}) \,]$$

$$= \min_{\{\rho_N(\vec{r})\}} [\, \min_{\{|\Psi\rangle_{\rho_N}\}} \{ {}_{\rho_N}\langle\Psi| H |\Psi\rangle_{\rho_N} \} \,] \qquad (1.17)$$

From the expression above, one can notice that the computation of the ground state eigenvalue $E_o(\underline{R})$ is cast into a two-tier variational search procedure: the innermost being a search over a set of N electron state vectors, all of which are constrained to yield a specified density, and the outermost a search over all such N-electron densities.

Using the Hamiltonian given in equation (1.3) we find the energy

functional $\epsilon(N,\rho_N(r);\underline{R})$ to be

$$\epsilon(N, \rho_N; \underline{R}) = \{ \min_{|\Psi\rangle_{\rho_N}} \} \{ {}_{\rho_N}\langle\Psi| \sum_{i=1}^{N} \frac{-\hbar^2}{2m} \nabla_i^2 + \sum_{i=1}^{N}\sum_{a=1}^{A} \frac{Z_a e^2}{|\vec{r}_i - \vec{R}_a|}$$

$$\sum_{i<j}^{N} \frac{e^2}{|\vec{r}_i - \vec{r}_j|} + \sum_{a<b}^{A} \frac{Z_a Z_b e^2}{|\vec{R}_a - \vec{R}_b|} |\Psi\rangle_{\rho_N} \} \qquad (1.18)$$

$$= [\{|\Psi\rangle_{\rho_N}\} \{ {}_{\rho_N}\langle\Psi| \sum_{i=1}^{N} \frac{-\hbar^2}{2m} \nabla_i^2 + \sum_{i<j}^{N} \frac{e^2}{|\vec{r}_i - \vec{r}_j|} |\Psi\rangle_{\rho_N} \}$$

$$- \frac{e^2}{2} \int d^3r \int d^3r' \frac{\rho_N(\vec{r})\rho_N(\vec{r}')}{|\vec{r} - \vec{r}'|}]$$

$$+ \frac{e^2}{2} \int d^3r \int d^3r' \frac{\rho_N(\vec{r})\rho_N(\vec{r}')}{|\vec{r} - \vec{r}'|} + \sum_{a=1}^{A} [-Z_a e^2 \int d^3r \frac{\rho_N(\vec{r})}{|\vec{r} - \vec{R}_a|}] + \sum_{a<b} \frac{Z_a Z_b e^2}{|\vec{R}_a - \vec{R}_b|} \qquad (1.19)$$

The terms not depending upon the specific electronic wave function but only upon the charge density have been removed from the minimization prescription since the search is restricted to wavefunctions yielding the same charge density. Furthermore, the classical Coulombic self-interaction functional

$$J(\rho) = \frac{e^2}{2} \int d^3r \int d^3r' \frac{\rho_N(\vec{r})\rho_N(\vec{r}')}{|\vec{r} - \vec{r}'|} \qquad (1.20)$$

has been added and approriately subtracted in order to define the following functional

$$\epsilon_o(N, \rho_N) = [\ \{|\Psi\rangle_{\rho_N}\}\ \{{}_{\rho_N}\langle\Psi| \sum \frac{-\hbar^2}{2m}\nabla_i^2 + \sum \frac{e^2}{|\vec{r}_i - \vec{r}_j|}|\Psi\rangle_{\rho_N}\} - J(\rho_N(\vec{r}))\ ] \qquad (1.21)$$

Again, the construction of the $\epsilon_o(\rho_N, N)$ envisions a search over all N-electron state functions $|\Psi\rangle_{\rho_N}$ giving the specified electron density for one which minimizes the expectation value of the sum of electron kinetic energy and Coulomb repulsion operators. The complete energy functional $\epsilon(N, \rho_N; \underline{R})$ then becomes

$$\epsilon(N, \rho_N; \underline{R}) = \epsilon_o(N, \rho_N) + J(\rho_N(r)) + \sum_{a=1}^{A}[-Z_a e^2 \int d^3r \frac{\rho_N(r)}{|\vec{r} - \vec{R}_a|}] + \sum_{a<b}^{A} \frac{Z_a Z_b e^2}{|R_a - R_b|} \qquad (1.22)$$

Let suppose that in carrying out the minimization procedure we find the optimum N-electron wave function $|\tilde{\Psi}\rangle_{\rho_N}$ so that $\epsilon_o(N, \rho_N)$ becomes

$$\epsilon_o(N, \rho_N) = \{{}_{\rho_N}\langle\tilde{\Psi}| \sum \frac{-\hbar^2}{2m}\nabla_i^2 + \sum_{i<j}^{N} \frac{e^2}{|\vec{r}_i - \vec{r}_j|}|\tilde{\Psi}\rangle_{\rho_N}\} - J(\rho_N(\vec{r})) \qquad (1.23)$$

Then it is possible to define the kinetic energy functional $\epsilon_{o,k}$

$$\epsilon_{o,k}(N, \rho_N) = {}_{\rho_N}\langle\tilde{\Psi}|\frac{-\hbar^2}{2m}\nabla_i^2|\tilde{\Psi}\rangle_{\rho_N} \qquad (1.24)$$

and also to define the exchange-correlation energy functional as

$$\epsilon_{o,xc}(N, \rho_N) = {}_{\rho_N}\langle\tilde{\Psi}| \sum_{i<j}^{N} \frac{e^2}{|\vec{r}_i - \vec{r}_j|}|\tilde{\Psi}\rangle_{\rho_N} - J(\rho_N(\vec{r})) \qquad (1.25)$$

Note that at this point it is only $\epsilon_{o,xc}$ that can be defined. Only after the introduction of a model Hartree-Fock reference state $|\Phi\rangle$ may the individual terms, that is the exchange term

$$\epsilon_{o,x}(N,\rho_N) = {}_{\rho_N}\langle\Phi|\sum_{i<j}^{N} \frac{e^2}{|\vec{r}_i - \vec{r}_j|}|\Phi\rangle_{\rho_N} - J(\rho_N(\vec{r})) \quad (1.26)$$

and the correlational term

$$\epsilon_{o,c}(N,\rho_N) = {}_{\rho_N}\langle\tilde{\Psi}|\sum_{i<j}^{N} \frac{e^2}{|\vec{r}_i - \vec{r}_j|}|\tilde{\Psi}\rangle_{\rho_N} - \langle\Phi|\sum_{i<j}^{N} \frac{e^2}{|\vec{r}_i - \vec{r}_j|}|\Phi\rangle \quad (1.27)$$

be defined.

In finding the exact ground state energy, having obtained the form of the energy functional, one must carry out the minimization of this known energy functional with respect to the density $\rho(\vec{r})$. In other words, the exact ground state eigenvalue for a fixed configuration of the nuclei is then to be found in the search over all N electron densities $\rho_N(r)$ for the minimum value of the functional. Using the energy functional defined in Eqn (1.22), we have that

$$\begin{aligned} E_o(\underline{R}) &= \left\{\min_{\rho_N}\right\}\left[\epsilon(N,\rho_N;\underline{R})\right] \\ &= \left\{\min_{\rho_N}\right\}\left[\epsilon_o(N,\rho_N) + J(\rho_N)\right. \\ &\quad \left. + \sum_{a=1}^{A}\left(-Z_a e^2\int dr\,\frac{\rho_N(r)}{|\vec{r}-\vec{R}_a|}\right)\right] + \sum_{a<b}^{A}\frac{Z_a Z_b e^2}{|\vec{R}_a - \vec{R}_b|} \end{aligned} \quad (1.28)$$

Note that in carrying out the minimization of the functional, each different nuclear configuration ($\underline{R}$) results in a different N electron density denoted by $\tilde{\rho}_N(\underline{R})$. The ground state energy becomes

$$E_o(\underline{R}) = \epsilon_o(N, \tilde{\rho}_N(\underline{R})) + J(\tilde{\rho}_N(\underline{R})) + \sum_{a=1}^{A} [-Z_a e^2 \int d^3r \frac{\tilde{\rho}_N(\underline{R})}{|\vec{r} - \vec{R}_a|}]$$

$$+ \sum_{a<b}^{A} \frac{Z_a Z_b e^2}{|R_a - R_b|} \qquad (1.29)$$

Using Eqn (1.6) and realizing an expression similar to Eqn (1.29) obtains for each isolated fragment, we find the potential energy of interaction can be written as

$$V(\vec{R}_1, \Omega_1, \vec{R}_2, \Omega_2 \ldots R_F, \Omega_F; \{\tau_1\}, \{\tau_2\} \ldots \{\tau_F\}) =$$

$$\epsilon_o(N, \tilde{\rho}_N(\underline{R})) + J(\tilde{\rho}_N(\underline{R})) + \sum_{a=1}^{A} (-Z_a e^2 \int d^3r \frac{\tilde{\rho}(\underline{R})}{|\vec{r} - \vec{R}_a|})$$

$$- \sum_{f=1}^{F} \left\{ \epsilon_o(N, \tilde{\rho}_{N_f}(R_f^o) + J(\tilde{\rho}_{N_f}(R_f^o)) \right.$$

$$\left. + \sum_{a \in \{\eta_f\}} \left[-Z_a e^2 \int d^3r \frac{\tilde{\rho}_{N_f}(\vec{r}; \vec{R}_f^o)}{|\vec{r} - \vec{R}_a|} \right] \right\}$$

$$+ \sum_{1 \le f < f' \le F} \sum_{a \in \{\eta_f\}} \sum_{b \in \{\eta_{f'}\}} \frac{Z_a Z_b e^2}{|\vec{R}_a - \vec{R}_b|} . \qquad (1.30)$$

Each of the F independent minimizations carried out for the isolated molecules--the asymptotic positions being indicated by $\underline{R}_{o_f}$ --necessarily yields the ground state energy E_{o_f} and density $\tilde{\rho}_{N_f}$ for a molecular fragment. Each fragment is in fact specified by the nuclear configuration and charges

$$\underline{R}_{o_f} = \{R_a^o, Z_a\}, \; a \in \{\eta_f\} \qquad (1.31)$$

and the number of electrons N_f. Of course, there is the obvious

restriction that

$$\sum_{f=1}^{F} N_f = N \qquad (1.32)$$

In addition, we must also presume that the partition of the N electrons among the F isolated molecules is the one yielding the lowest total sum of their electronic energies. Finally, we note that only the inter-fragments nuclear repulsion energy terms survive in taking the energy difference in Eqn (1.6).

Any N representable charge density may be written in terms of superimposing the optimum densities of the molecular fragments and then allowing that charge distribution to relax. In this manner we can write the variational density appearing in Eqn (1.30) as

$$\rho_N(\vec{r}) = \sum_{f=1}^{F} \tilde{\rho}_{N_f}(\vec{r}\,; \vec{R}_f, \vec{\Omega}_f, \{\tau_f\}) + \Delta\rho(\vec{r}) \qquad (1.33)$$

where the translated optimum density for molecule f is

$$\tilde{\rho}_{N_f}(\vec{r}\,; \vec{R}_f, \vec{\Omega}_f, \{\tau_f\}) = \tilde{\rho}_{N_f}(\vec{r}\,; \vec{R}_f^{\circ}, \vec{\Omega}_f^{\circ}, \{\tau_f^{\circ}\}) \Big|_{\substack{\vec{R}_f^{\circ} \to \vec{R}_f \\ \vec{\Omega}_f^{\circ} \to \vec{\Omega}_f \\ \{\tau_f^{\circ}\} \to \{\tau_f\}}} \qquad (1.34)$$

Note that Eqn (1.34) defines $\Delta\rho$ in terms of the variational charge density $\rho_N(\vec{r})$ and the exact molecular charge densities $\tilde{\rho}_{N_f}(\vec{r})$ assumed found in the asymptotic optimizations. The fact that $\Delta\rho$ can be defined in this manner assists us in doing the computation because we may then use those charge densities for all the molecular fragments found by the traditional quantum chemistry calculations and focus

attention on $\Delta\rho$ which is to be found variationally. Of course, we must also make sure that due to charge conservation

$$\int d^3r\, \Delta\rho(\vec{r}) = 0 \qquad (1.35)$$

Using the expression Eqn (1.33) for the density $\rho_N(\vec{r})$, we can then write the original statement of Eqn (1.30) in terms of $\Delta\rho$ and express the potential energy of interaction as a search over the N representable $\Delta\rho$'s

$$\begin{aligned}
&V(R_1, \Omega_1, R_2, \Omega_2, \ldots R_F, \Omega_F; \{\tau_1\}, \{\tau_2\} \ldots \{\tau_F\}) \\
&= \{\Delta\rho\}^{\min} \left\{ \left[\epsilon_0\left(N, \left[\sum_{f=1}^{F} \tilde{\rho}_{N_f} + \Delta\rho\right]\right) - \sum_{f=1}^{F} \epsilon_0(N_f, \tilde{\rho}_{N_f}) \right] \right. \\
&+ e^2 \int d^3r\, \Delta\rho(r) \int d^3r' \left[\frac{\sum_{f=1}^{F} \tilde{\rho}_{N_f}(\vec{r}') + \sum_{f=1}^{F} \sum_{a\in n_f} \left(-Z_a \delta(\vec{r}' - \vec{R}_a)\right) + \frac{\Delta\rho(\vec{r}')}{2}}{|\vec{r} - \vec{r}'|} \right] \Bigg\} \\
&+ \sum_{1\le f<f'\le F} \left\{ e^2 \left[\int d^3r \int d^3r' \frac{\tilde{\rho}_{N_f}(\vec{r})\, \tilde{\rho}_{N_{f'}}(\vec{r}')}{|\vec{r} - \vec{r}'|} \right] + \sum_{a\in n_f} \sum_{b\in n_{f'}} \frac{Z_a Z_b e^2}{|\vec{R}_a - \vec{R}_b|} \right. \\
&\left. + \sum_{a\in n_f} \left(-Z_a \int \frac{d^3r\, \tilde{\rho}_{N_{f'}}(\vec{r})}{|\vec{r} - \vec{R}_a|} \right) + \sum_{b\in n_f} \left(-Z_b \int \frac{d^3r\, \rho_{N_f}(\vec{r})}{|\vec{r} - \vec{R}_b|} \right) \right\}
\end{aligned} \qquad (1.36)$$

Since we have assumed already that the charge densities of the isolated molecules are known, the variational search in Eqn (1.36) concerns only terms inside the first curly brackets and results in an optimum $\Delta\rho$ and a minimum value of this bracket. The terms outside the first curly brackets can be identified as the electrostatic interaction energy due to the rigid (i.e. frozen) charge density of the isolated fragments. This

electrostatic energy can be evaluated at the outset. The terms inside the variational search in $\Delta\rho$ can be classified as quantum corrections (involving the functionals $\epsilon_o(N, \rho)$) and induction energy.

In practice to find the potential energy of interaction given in Eqn (1.36) is virtualy impossible for two reasons. Firstly, is the difficulty in finding the exact energy functional $\epsilon_o(N, \rho_N)$. Secondly, is the difficulty in carrying out the search for the optimum $\Delta\rho$. What is clearly needed is a way of approximating density functional calculations. We shall adopt the Gordon-Kim (GK) [8] approach. In the Gordon-Kim model, in addition to using an approximate functional for $\epsilon_o(N, \rho_N)$, the variational search over $\Delta\rho$ is never carried out to obtain the optimum charge density. Rather, with the charge densities for the isolated molecular fragments obtained from the traditional quantum chemical calculations, the charge density for the interacting system is approximated simply as the superposition of those molecular charge densities, rigidly translated and rotated with each molecule. In other words, we set $\Delta\rho (\vec{r}) = 0$ and thereby yield the possibility of computing induction energy. To be sure in the GK model, the potential energy of interaction becomes simply

$$V(\underline{R}) = \epsilon_o\Big(N, \sum_{f=1}^{F} \tilde{\rho}_{N_f}\Big) - \sum_{f=1}^{F} \epsilon_o\big(N_f, \tilde{\rho}_{N_f}\big)$$
$$+ \sum_{1\le f<f'\le F} \left\{ e^2 \left[\int d^3r \int d^3r' \frac{\tilde{\rho}_{N_f}(\vec{r})\tilde{\rho}_{N_{f'}}(\vec{r}')}{|\vec{r}-\vec{r}'|} \right] + \sum_{a\in\eta_f}\sum_{b\in\eta_{f'}} \frac{Z_a Z_b e^2}{|\vec{R}_a - \vec{R}_b|} \right.$$
$$+ \sum_{a\in\eta_f} \left(-Z_a \int \frac{d^3r\, \tilde{\rho}_{N_{f'}}(\vec{r})}{|\vec{r}-\vec{R}_a|} \right) + \sum_{b\in\eta_{f'}} \left(-Z_b \int \frac{d^3r\, \tilde{\rho}_{N_f}(\vec{r})}{|\vec{r}-\vec{R}_b|} \right) \tag{1.37}$$

Even after doing this approximation, the point still remains that none of these functionals ϵ_o, ϵ_{ok}, ϵ_{ox}, ϵ_{oc} is known explicitly in term of N and ρ. Thus, Gordon and Kim suggested that each of the energy functionals above be approximated by the corresponding one obtained from the extended electron gas. In other words they consider the asymptotic limit ($N \to \infty$) for each of the energy functionals:

$$\epsilon_{o,K}(N,\rho_N) \to \lim_{N\to\infty} \epsilon_{o,K}(N,\rho_N) = \epsilon_{o,K}^{EG}(\rho) \cong (3/10)(3\pi^2)^{3/2} \int d^3r \rho^{5/3} \quad (1.38)$$

$$\epsilon_{o,x}(N,\rho_N) \to \lim_{N\to\infty} \epsilon_{o,x}(N,\rho_N) = \epsilon_{o,x}^{EG}(\rho) \cong -(3/4)(3/\pi)^{2/3} \int d^3r \rho^{4/3} \quad (1.39)$$

$$\epsilon_{o,c}(N,\rho_N) \to \lim_{N\to\infty} \epsilon_{o,c}(N,\rho_N) = \epsilon_{o,c}^{EG}(\rho) \cong \int d^3r \rho E_{corr}(\rho) \quad (1.40)$$

Here the extended electron gas Hartree-Fock state on which the $\epsilon_{o,k}$ and $\epsilon_{o,x}$ approximate expressions are built is the Slater determinant of plane waves filling the Fermi sea [9]. Corrections to these formulas based upon density gradient expansions are given below. Explicit expressions of the integrand $E_{cor}(\rho)$ for various ranges of the density ρ are given by Parker, Snow, and Pack [10]. With $r_s = (4\pi a_o^3 \rho/3)^{-1/3}$ where a_o is the Bohr radius, we have in atomic Rydberg units:

for high density, $r_s \leq 0.7$

$$E_{corr}(r_s) = -0.0311 \ln r_s - 0.048 + 0.009 r_s \ln r_s - 0.01 r_s \quad (1.41)$$

for intermediate density, $0.7 < r_s < 10$

$$E_{corr}(r_s) = -0.06156 + 0.01898 \ln r_s \qquad (1.42)$$

for low density, $r_s \geq 10$

$$E_{corr}(r_s) = -0.438 r_s^{-1} + 1.325 r_s^{-3/2} - 1.47 r_s^{-2} - 0.4 r_s^{-5/2} \qquad (1.43)$$

In using the above expressions the density is not a constant as in the extended (i.e. infinite) electron gas. Instead for finite electron systems ρ is considered a function of position. Finally, then the potential energy of interaction in the GK model becomes

$$V(\vec{R}_1, \vec{\Omega}_1, \vec{R}_2, \vec{\Omega}_2 \ldots \vec{R}_F, \vec{\Omega}_F : \{\tau_1\}, \{\tau_2\} \ldots \{\tau_F\})$$

$$= \left\{ \left[\epsilon_{0,K}^{EG}\left(\sum_{f=1}^{F} \tilde{\rho}_{N_f} \right) - \sum_{f=1}^{F} \epsilon_{0,K}^{EG}\left(\tilde{\rho}_{N_f}\right) \right] \right.$$

$$+ \left[\epsilon_{0,x}^{EG}\left(\sum_{f=1}^{F} \tilde{\rho}_{N_f} \right) - \sum_{f=1}^{F} \epsilon_{0,x}^{EG}\left(\tilde{\rho}_{N_f}\right) \right]$$

$$\left. + \left[\epsilon_{0,c}^{EG}\left(\sum_{f=1}^{F} \tilde{\rho}_{N_f} \right) - \sum_{f=1}^{F} \epsilon_{0,c}^{EG}\left(\tilde{\rho}_{N_f}\right) \right] \right\}$$

$$+ \sum_{1 \leq f < f' \leq F} \left[e^2 \iint d^3r\, d^3r' \frac{\tilde{\rho}_{N_f}(\vec{r})\, \rho_{N_{f'}}(\vec{r}')}{|\vec{r} - \vec{r}'|} \right.$$

$$+ \sum_{a \in n_f} \int d^3r \frac{-Z_a e^2 \tilde{\rho}_{N_{f'}}(\vec{r})}{|\vec{r} - \vec{R}_a|} + \sum_{b \in n_{f'}} \int d^3r \frac{-Z_b e^2 \tilde{\rho}_{N_f}(\vec{r}')}{|\vec{r} - \vec{R}_b|}$$

$$+ \sum_{a \in \eta_f} \sum_{b \in \eta_{f'}} \frac{Z_a Z_b e^2}{|\vec{R}_a - \vec{R}_b|} \Bigg] \qquad (1.44)$$

Gordon and Kim found in their original calculations that dispersion energies were not accurately given by the electron gas model itself. Thus they devised a "Drude Model" (essentially coupled oscillators) to account for the long range interaction energy and attempted to join these results to the shorter range electron gas result. There are two sources for error in adopting the extended electron gas energy expressions. Besides the inhomogeneity of the density leading to gradient expansion corrections, one also needs to make corrections because the system considered has a finite number of electrons. Recent work by Pearson and Gordon [11] is directed toward including gradient correction terms in the kinetic energy functional. Pioneering work by Rae [12] introduced a finite N correction to the Gordon-Kim model in his consideration of the self-exchange energy. Waldman and Gordon [13] considered the possibility of correcting all three functionals for finite N by simply introducing a scaling coefficient depending on N and determined by comparing the extended electron gas results with the self-consistent-field results for N-electron atoms and ions. However, they concluded that with the explicit inclusion of the dispersion energies via the Drude model, the correlation energy functional should be neglected. As a result Waldman and Gordon obtain finite N corrections only for the kinetic and exchange energy functionals in the form of N-dependent multiplicative factors of $\epsilon_{ok}(\rho)$ and $\epsilon_{ox}(\rho)$.

Other modifications of these functionals, notably by Parr and his co-workers, have also been proposed. The latest review by Parr [14] shows all the correction terms to the extended electron gas energy functionals. In his review, the expression for the kinetic energy functional take the form

$$T[\rho] = T_0[\rho] + T_2[\rho] + T_4[\rho] \qquad (1.45)$$

where T_0 is the kinetic energy of the free electron gas (the Thomas-Fermi [15]) result and is given in Eqn (1.38). T_2 is 1/9 of the original Weizsacker correction [16] and in atomic units is

$$T_2[\rho] = 1/9\ T_W[\rho] = \frac{1}{9}\left(\frac{1}{8}\int d^3r \frac{|\vec{\nabla}\rho(\vec{r})|^2}{\rho(\vec{r})}\right) \qquad (1.46)$$

T_4 is the fourth order correction as given by Hodges [17], namely

$$T_4[\rho] = \frac{1}{540}(3\pi^2)^{-2/3}\int d^3r\,\rho^{1/3}\left[\left(\frac{\nabla^2\rho}{\rho}\right)^2 - \frac{9}{8}\left(\frac{\nabla^2\rho}{\rho}\right)\left(\frac{\nabla\rho}{\rho}\right)^2 + \frac{1}{3}\left(\frac{\nabla\rho}{\rho}\right)^4\right] \qquad (1.47)$$

The exchange functional takes the form

$$K[\rho] = K_0[\rho] + K_2[\rho] \qquad (1.48)$$

where $K_0[\rho]$ is the exchange energy of the free electron gas (the Dirac [18] result) and is given in Eqn (1.39). K_2 is

$$K_2[\rho] = -3/4\ (3/\pi)^{1/3}\beta\int d^3r \frac{|\vec{\nabla}\rho(\vec{r})|^2}{\rho^{4/3}(\vec{r})} \qquad (1.49)$$

where β is a constant of the order of 10^{-3} which can be determined in several ways. One way is known $X_{\alpha\beta}$ method. Alternatively, taking β=0 if one lets the coefficient of the Dirac exchange result depend on the

number of electrons N, then one gets the exchange energy of the Xα theory [19] defined as

$$K_{x\alpha}(\rho) = C_{x\alpha}(N) \int \rho^{4/3} d^3r \qquad (1.50)$$

Further refinements introduce coefficients which depend on N for all these various terms. Finally, the correlation energy functional take takes the form shown in Eqn ($^{1.41-1.43}$). A bibliography of these functional modifications is included in the Appendix. E.

The central problem attacked in this thesis is the representing of the electron density $\rho(\vec{r})$ as a linear combination of elementary functions. Having done this we ultimately wish to use these expansion in computing the potential energy surfaces using Gordon-Kim model. However, even though the explicit form of the potential energy of interaction based on the Gordon-Kim model has been given above (Eqn (1.44)), in carrying out the calculations in this thesis we will consider only the electrostatic part of the energy expression. In other words, we are considering only the Coulombic interaction energy

$$V_{COUL}(R) = \sum_{1\le f<f'\le F} \left\{ e^2 \left[\int d^3r \int d^3r' \frac{\tilde{\rho}_{N_f}(\vec{r})\,\rho_{N_{f'}}(\vec{r}')}{|\vec{r}-\vec{r}'|} \right.\right.$$

$$+ \sum_{a\in\eta_f} \left(-Z_a \int \frac{d^3r\, \tilde{\rho}_{N_{f'}}(\vec{r})}{|\vec{r}-\vec{R}_a|} \right) + \sum_{b\in\eta_{f'}} \left(-Z_b \int \frac{d^3r\, \tilde{\rho}_{N_f}(\vec{r})}{|\vec{r}-\vec{R}_b|} \right.$$

$$\left.\left. + \sum_{a\in\eta_f} \sum_{b\in\eta_{f'}} \frac{Z_a Z_b e^2}{|\vec{R}_a - \vec{R}_b|} \right\} \qquad (1.51)$$

The electrostatic energy by itself is in fact playing a bigger role in the understanding of the structure of large molecules and their interactions with smaller reactants. Here we have in mind the "Molecular Electrostatic Potentials" (MEP) introduced by Tomasi [20] in the early 1970's. One computes the electrostatic potential using the total charge density of a molecule and examines those regions where this potential is rather large. This idea was used subsequently by many groups in predicting, for example, the conformation of bio-polymers or the reaction site of a drug. Two sources of particular note are the 1982 review article by Tomasi and the volume Chemical Applications of Atomic and Molecular Electrostatic Potentials edited by Politzer and Truhlar [21] appearing in 1981. Beyond MEP, however, these expansions of $\rho(\vec{r})$ which we investigate in this thesis will be used in the complete density functional calculations for the total electronic energy of interaction. From there on, by using the complete form of the energy expression and obtaining the electronic energies for various configurations of the nuclei, we hope to determine the potential energy surface.

Let us next outline our approach to the problem of computing the electrostatic interaction energy using Eqn (1.51). Basically there are three major tasks that we need to do to be able to compute the electrostatic interaction energy. These can be summarizes as follows:

1) Obtain the charge densities at various points in space for the isolated molecular fragments involved in the interaction. The way we handle this problem is by numerically tabulating the charge densities at

various points in space knowing the wave function of the particular molecular fragment. This is discussed in detail in Chapter 2.

2) Fit the charge densities of each isolated fragment as linear combination of Slater-type functions. The fitting routine is discuss in Chapter 3 and our experience in using the routine is discussed in Chapter 4.

3) Evaluate the electrostatic energy of interaction for the water-dimer using the Slater function expansions of the charge density of a water molecule. The results are discussed in Chapter 5.

CHAPTER II

GENERATING CHARGE DENSITIES FOR ATOMS AND MOLECULES AND EXPANDING $\rho(\vec{r})$ IN SPHERICAL SLATER FUNCTIONS

As mentioned in the previous chapter, the first task in determining the electrostatic interaction energy between two or more interacting molecular fragments is to obtain the electronic charge density for each individual fragment. The charge density can be obtained either from experiment or it can be generated knowing the wavefunction for the particular fragment. We will generate the densities using the Hartree-Fock (HF) approximate wavefunctions [22] . We will limit ourselves to a single Slater determinant wave function obtained from a self-consistentfield calculation.

Consider a wavefunction of the form of a single Slater determinant

$$\Delta_o = \frac{1}{\sqrt{N!}} \begin{vmatrix} \psi_{\lambda_1}(x_1) & \psi_{\lambda_2}(x_1) & \cdots\cdots & \psi_{\lambda_N}(x_1) \\ \psi_{\lambda_1}(x_2) & \psi_{\lambda_2}(x_2) & \cdots\cdots & \psi_{\lambda_N}(x_2) \\ & & & \\ \psi_{\lambda_1}(x_N) & \psi_{\lambda_2}(x_N) & \cdots\cdots & \psi_{\lambda_N}(x_N) \end{vmatrix} \qquad (2.1)$$

Here the ψ's are the orthonormal molecular spin orbitals obtained as solution of the coupled Hartree-Fock equations. The orthonormality among the molecular spin orbitals can be written as

$$\int dx\, \psi^{*}_{\lambda_i}(x)\, \psi_{\lambda_j}(x)$$

$$= \int d^3r \sum_{\xi} \psi^{*}_{\lambda_i}(r, \xi)\, \psi_{\lambda_j}(r, \xi) = \delta_{\lambda_i \lambda_j} \qquad (2.2)$$

"x_i" denotes the space and spin coordinates of electron i. The determinant can also be written in a more compact form

$$\Delta_o = \frac{1}{\sqrt{N!}} \sum_{\substack{i_1 i_2 \cdots i_N}} (-1)^{\sigma_p} P_{12.....N} \left(\prod \psi_{\lambda_i}(x_i) \right)$$

$$= A(N) \left(\prod \psi_{\lambda_i}(x_i) \right) \qquad (2.3)$$

where the P's are operators which permute the particle labels among themselves and the sum is over all N! such permutations. Here, the operator

$$A(N) = \frac{1}{\sqrt{N!}} \sum_{\substack{i_1 i_2 \cdots i_N}} (-1)^{\sigma_p} P_{12.....N} \qquad (2.4)$$

is called the antisymmetrizer. Given any wave function Ψ, we can obtain the corresponding one-electron density matrix as

$$\rho^{(1)}(x_1, x_1') = N \int dx_2 \ldots dx_N\, \rho(x_1, x_2 \ldots x_N; x_1', x_2, \ldots x_N) \qquad (2.5)$$

where the full density matrix

$$\rho(x_1, x_2 \ldots x_N; x_1', x_2', \ldots x_N') = \langle x_1, x_2, \ldots x_N | \Psi \rangle \langle \Psi | x_1', x'_2, \ldots x_N' \rangle$$

$$= \Psi(x_1, x_2, \ldots x_N)\, \Psi^{*}(x_1', x_2', \ldots x_N') \qquad (2.6)$$

Using the wavefunction Ψ given in Eqn (2·1), we get

$$\rho^{(1)}(x_1,x_1') = N \int dx_2 \ldots dx_N \frac{1}{\sqrt{N!}} \begin{vmatrix} \psi_{\lambda_1}(x_1) & \psi_{\lambda_2}(x_1) & \ldots & \psi_{\lambda_N}(x_1) \\ \psi_{\lambda_1}(x_2) & \psi_{\lambda_2}(x_2) & \ldots & \psi_{\lambda_N}(x_2) \\ & & & \\ \psi_{\lambda_1}(x_N) & \psi_{\lambda_2}(x_N) & \ldots & \psi_{\lambda_N}(x_N) \end{vmatrix}$$

$$\frac{1}{\sqrt{N!}} \begin{vmatrix} \psi_{\lambda_1}(x_1') & \psi_{\lambda_2}(x_1') & \ldots & \psi_{\lambda_N}(x_1') \\ \psi_{\lambda_1}(x_2) & \psi_{\lambda_2}(x_2) & \ldots & \psi_{\lambda_N}(x_2) \\ & & & \\ \psi_{\lambda_1}(x_N) & \psi_{\lambda_2}(x_N) & \ldots & \psi_{\lambda_N}(x_N) \end{vmatrix}^{\star} \qquad (2\cdot7)$$

Expanding the determinant we get $(N!)^2$ terms, each term is made up of the product of 2N spin orbitals. The factors may be paired-off according to particle labels and thus generally involve two different orbital labels so that one can write

$$\rho^{(1)}(x_1,x_1') = \frac{1}{(N-1)!} \left\{ \ldots + \psi_{\mu_1}(x_1)\psi^{*}_{\mu_1'}(x_1')\psi_{\mu_2}(x_2)\psi^{*}_{\mu_2'}(x_2)\ldots\psi_{\mu_N}(x_N)\psi_{\mu_N'}(x_N) + \ldots \right\} \qquad (2\cdot8)$$

However, using the orthonormality of the spin orbitals in carrying out the integrations over dx_i i=2.....N, for a term in Eqn (2·8) not to vanish, the orbital label of each $\psi_{\mu_i}(x_i)$ has to match up with its conjugate $\psi^{\star}_{\mu'}(x_i)$, i = 2,3,....N. The matching of the (N-1) orbital labels for particles 2,3....N forces orbital labels of particle 1 to match

also in the non-vanishing terms. In short all the orbital labels have to match for the integral not to vanish. Now, with a particular orbital λ_j assigned to particle 1 $\psi_{\lambda_j}(x_1)\,\psi^*_{\lambda_j}(x_1')$, one can still permute the matched orbital labels on the remaining of the (N-1) factors in

$$\prod_{k=2}^{N} \psi_{\mu_k}(x_k)\,\psi^*_{\mu_k}(x_k), \quad \mu_k \in \{\lambda_1 \ldots \lambda_{j-1}, \lambda_{j+1} \ldots \lambda_N\} \tag{2.9}$$

among the (N-1) particles k=2,3...N. This can be done in (N-1)! ways. Then, cancelling the factors of the (N-1)! and considering all choices for the orbital assigned to particle 1, we are left with

$$\rho^{(1)}(x_1, x_1') = \sum_{\lambda} \psi_\lambda(x_1)\,\psi^*_\lambda(x_1') \tag{2.10}$$

with the summation over the occupied spin orbitals which make up the Slater determinant. The density can be deduced from here by letting x'=x and summing over the spin coordinates. Thus, dropping the particle label "1", we write

$$\rho(\vec{r}) = \sum_{\xi} \rho(\vec{r},\xi;\vec{r},\xi) = \sum_{\lambda} \sum_{\xi} \psi_\lambda(x)\,\psi^*_\lambda(x) \tag{2.11}$$

In practice each molecular spin orbital for the single determinant Hartree-Fock state is written as the product of a spatial and a spin factor

$$\psi_\lambda(\vec{r}) = \Psi_\Lambda(\vec{r})\,\chi_{m_s}(\xi) \tag{2.12}$$

and is express as linear combination of atomic orbitals (LCAO). Thus,

$$\psi_\lambda(\vec{r},\xi) = \sum_{a} c_{a\lambda}\,\phi_a(\vec{r},\xi) \tag{2.13}$$

where ϕ_a is an atomic spin orbital also factored as

$$\phi_a = \Phi_A(\vec{r})\,\chi_{m_s}(\xi) \qquad (2.14)$$

Φ_A is a member of the spatial orbital basis set and is of the form of Slater- or Gaussian- type functions or some other functions used to expand the atomic orbitals. Notationwise we use Greek and Latin letters in refering to molecular and atomic orbitals respectively, and lower case and capitals in reference to spin and spatial orbitals. In the general LCAO expansion, the density given in Eqn (2.10) becomes

$$\rho(\vec{r}) = \sum_{\xi}\Big\{\sum_{\lambda}\Big[\sum_{a} C_{a\lambda}\phi_\lambda(\vec{r},\xi)\Big]\Big[\sum_{b} C^*_{b\lambda}\phi^*_\lambda(\vec{r},\xi)\Big]$$

$$= \sum_{\xi}\sum_{a}\sum_{b}\phi_a(\vec{r},\xi)\,P_{ab}\,\phi^*_b(\vec{r},\xi) \qquad (2.15)$$

Here, P_{ab} is an element of the so-called Hartree-Fock density matrix:

$$P_{ab} = \sum_{\lambda} C_{a\lambda}\,C^*_{b\lambda} \qquad (2.16)$$

In particular for a closed-shell HF wavefunction with the ansatz that the molecular spin orbitals factor as in Eqn (2.12), we find

$$\psi_\lambda = \Psi_\Lambda(\vec{r})\,\chi_{m_s}(\xi) = \sum_a C_{a\lambda}\phi_a$$

$$= \sum_A\sum_{m_s'} C_{A m_s' \Lambda m_s}\,\Phi_A(\vec{r})\,\chi_s^{m_s}(\xi)$$

$$= \sum_A\sum_{m_s'} C_{A\Lambda}\,\delta_{m_s m_s'}\,\Phi_A(\vec{r})\,\chi_s^{m_s}(\xi)$$

$$= \Big\{\sum_A C_{A\Lambda}\,\Phi_A(\vec{r})\Big\}\chi_s^{m_s}(\xi) \qquad (2.17)$$

Then with the understanding that each of the spatial orbitals Λ is doubly

occupied $\rho(\vec{r})$ becomes

$$\rho(\vec{r}) = \sum_{\xi} \left\{ \sum_{\lambda} \left(\left[\sum_{A} C_{A\Lambda} \Phi_A(\vec{r}) \right] \chi_s^{m_s}(\xi) \right) * \left(\left[\sum_{B} C_{B\Lambda}^{*} \Phi_B^{*}(\vec{r}) \right] \chi_s^{m_s *}(\xi) \right) \right\}$$

$$= \sum_{A} \sum_{B} \left(\sum_{\Lambda} C_{A\Lambda} C_{B\Lambda} \right) \Phi_A(\vec{r}) \Phi_B^{*}(\vec{r}) * \sum_{m_s} \sum_{\xi} \chi_s^{m_s}(\xi) \chi_s^{m_s *}(\xi)$$

$$= 2 \sum_{A} \sum_{B} \Phi_A(\vec{r}) P_{AB} \Phi_B^{*}(\vec{r}) \qquad (2.18)$$

Here A and B run over the atomic spatial orbitals and

$$P_{AB} = \sum_{\Lambda} C_{A\Lambda} C_{B\Lambda}^{*} \qquad (2.19)$$

To this point $\rho(\vec{r})$ has been the number density of electrons. Realizing that it is the charge density which enters directly into our electrostatic energy calculations, we subsequently let $\rho(\vec{r})$ stand for electronic charge density. The two densities are of course, related by a factor of (-e)

We have written a Fortran computer program based on Eqn (2.18) that will compute the charge density at any point in space given all the necessary input parameters. The input parameters are the atomic spatial orbitals Φ_Λ themselves and the expansion coefficients $C_{A\Lambda}$. The basis functions are Slater-type orbitals (STO) of the form

$$\Phi_A(\vec{r} - \vec{R}_A) = R_n(|\vec{r} - \vec{R}_A|) Y_l^m(\theta_A, \phi_A) \qquad (2.20)$$

where

$$R_n(r) = (2n!)^{-1/2} (2\zeta)^{n+1/2} r^{n-1} e^{-\zeta r} \qquad (2.21)$$

ζ is the optimum exponent determined in the SCF calculation and $Y_l^m(\theta_A,\phi_A)$ is a normalized spherical harmonics centered at $\vec{R}_A$. Thus, each spatial orbital basis function is determined by its center $\vec{R}_A$ and the three quantum number n,l,m. The output of this program is the charge density $\rho_o(\vec{r})$ at a set of selected points $\vec{r}_I$.

The points $\vec{r}_I$ are selected to lie along certain lines (e.g. bond directions) and in certain planes (e.g. the molecular plane) and on certain spheres (e.g. spheres centered at the nuclei). It is important that we select a "representative" sample of points in order that the tabulated charge density values accurately reflect the structure of the charge distribution. One of our aims is to understand better how such a representative sample of points is to be selected. Anticipating that the fitting program (to be discussed in Chapter III) requires the tabulated charge density at the minimal number of symmetry related points, we can limited the points $\vec{r}_I$ to reflect the spatial symmetry of the atom or molecule under consideration. In the case of atoms we need only be concerned with the positioning of the points along the given line. For diatomic molecules the selected points need to be chosen only in a particular half-plane. Again, of course, we must be concerned with

which points are selected in the half-plane. However, for general molecules--even small molecules like H_2O--only experience can dictate how best to select the set of representative points, which lie along lines, in planes, and on spheres.

We try to fit the tabulated charge density by a linear superposition of spherical Slater-type functions (STF)

$$\rho(\vec{r}) = \sum_{i=1}^{n} q_i \frac{\beta_i^{n_i+3}}{4\pi(n_i+2)!} |\vec{r}-\vec{R}_i|^{n_i} e^{-\beta_i|\vec{r}-\vec{R}_i|} \qquad (2.22)$$

Each of the spherical Slater functions

$$\frac{\beta_i^{n_i+3}}{4\pi(n_i+2)!} |\vec{r}-\vec{R}_i|^{n_i} e^{-\beta_i|\vec{r}-\vec{R}_i|} \qquad (2.23)$$

is specified by its position $\vec{R}_i$, inverse range β_i, and the power n_i associated with the prefactor. The numerical factor

$$\frac{\beta_i^{n_i+3}}{4\pi(n_i+2)!} \qquad (2.24)$$

insures that each Slater function is normalized so that

$$\int d^3r \left\{ \frac{\beta_i^{n_i+3}}{4\pi(n_i+2)!} |\vec{r}-\vec{R}_i|^{n_i} e^{-\beta_i|\vec{r}-\vec{R}_i|} \right\} = 1. \qquad (2.25)$$

q_i is the fractional charge associated with this particular Slater function. As we shall explain in the next chapter, the inverse range β_i, charge q_i and the location $\vec{R}_i$ are chosen by a least square fitting procedure of the linear superposition to the numerical data of the charge density. Some constraints may be imposed on the fitting procedure. The fact that

$$\int d^3r \, \rho(\vec{r}) = Q \qquad (2.26)$$

where Q is the total electronic charge of the atom or molecule, implies that we may want to require

$$\sum_{i=1}^{n} q_i = Q. \qquad (2.27)$$

Some interesting features about the Slater function include that we can represent a point charge at position $\vec{R}$ in the form

$$q\delta(\vec{r}-\vec{R}) = \lim_{\beta\to\infty} \left\{ \frac{q\beta^{n+3}}{4\pi(n+2)!} |\vec{r}-\vec{R}|^n e^{-\beta|\vec{r}-\vec{R}|} \right\} \qquad (2.28)$$

Furthermore, although each Slater function is spherically symmetric, by pairing these functions together and imposing constraints on their positions and coefficients one can simulate the directional behavior of a p-type function. To illustrate this directional behavior consider placing two Slater functions at "a" and "-a" along the zaxis. In doing so, we impose the constraint that the coefficients have the same magnitude but opposite sign. Consider then

$$f_n(\vec{r};a) = \left\{ r_+^n e^{-\beta r_+} - r_-^n e^{-\beta r_-} \right\} \qquad (2.29)$$

where

$$r_\pm = \sqrt{x^2+y^2+(z\mp a)^2} = \sqrt{r^2+a^2\mp 2ar\cos\theta} \qquad (2.30)$$

and note that one can write this combination of Slater functions as

$$f_n(\vec{r};a) = (-1)^n \frac{\partial^n}{\partial\beta^n} \left\{ e^{-\beta r_+} - e^{-\beta r_-} \right\} \qquad (2.31)$$

Now, consider the behavior of $f_n(\vec{r},\vec{a})$ for $\vec{r} >> a$; the distances may be conventionally written

$$r_\pm = r\left[1 + a^2/r^2 \mp 2a/r\cos\theta\right]^{1/2}$$

$$= r\left[1 + a/r\left(a/r \mp 2\cos\theta\right)\right]^{1/2} \qquad (2.32)$$

Using a Taylor series expansion, we can write

$$\left(1+a/r\left(a/r \mp 2\cos\theta\right)\right)^{1/2} \simeq 1 + \tfrac{1}{2}\, a/r\left(a/r \mp 2\cos\theta\right) \qquad (2.33)$$

so that

$$r_\pm \simeq r\left(1 + \tfrac{1}{2}\, a/r\left(a/r \mp 2\cos\theta\right)\right) \qquad (2.34)$$

Then

$$f_n(\vec{r};a) = (-1)^n \frac{\partial^n}{\partial\beta^n}\left\{e^{-\beta r\left[1+\frac{1}{2}a/r(a/r-2\cos\theta)\right]}\right.$$

$$\left. - e^{-\beta r\left[1+\frac{1}{2}a/r(a/r+2\cos\theta)\right]}\right\}$$

$$= (-1)^n \frac{\partial^n}{\partial\beta^n}\left\{e^{-\beta r\left(1+\frac{1}{2}a^2/r^2\right)}\left[e^{\beta a\cos\theta} - e^{-\beta a\cos\theta}\right]\right\}$$

$$= (-1)^n \partial^n/\partial\beta^n\left\{e^{-\beta r\left(1+\frac{1}{2}a^2/r^2\right)}\left[2\sinh(\beta a\cos\theta)\right]\right\}. \qquad (2.35)$$

Since a/r is also small we have, assuming βa is small, that

$$\simeq (-1)^n \partial^n/\partial\beta^n\, e^{-\beta r}\left(2\beta a\cos\theta\right)$$

$$= 2\beta a\cos\theta\left(r^n - nr^{n-1}\right)e^{-\beta r} \qquad (2.36)$$

The "cos θ" dependence is the signature of the p-like orbital behavior along the z-axis. We can offset the centers of two Slater functions along any line and obtain the desired directed lobe behavior.

There are various other reasons for choosing the Slater type functions (STF) in expanding the charge density. First of all is the use of these functions in evaluating the integrals in closed form in the electrostatic energy calculation. One might raise the question of why not use the exact expansion Eqn (2·18) for the charge density instead of fitting $\rho(\vec{r})$ to linear combination of spherical Slater-type functions, since Slater-type orbitals with the same radial functions appear directly in Eqn (2·21). The answer is mainly because the orbitals appear as bilinear forms in $\rho(\vec{r})$ with some terms having orbitals on two different centers; this leads to the problem of evaluating four-centers integrals in calculating the electrostatic repulsion integrals. Furthermore, there are many terms in the exact expansion (Eqn (2·18)) of the charge density; that is given N basis functions , there will be $N(N+1)/2$ terms and $[N(N+1)/2]^2$ integrals to evaluate. These problems do not arise when one expands the charge density as a linear superposition of spherical Slater-type functions, since as is shown in Appendix A, the electrostatic energy of interaction can be expressed in closed form.

Another reason for expanding the charge density in terms of spherical STF's is their behavior at the centers where they are placed. If one examines

$$\lim_{\vec{r}\to\vec{R}} \vec{\nabla}\left(e^{-\alpha|\vec{r}-\vec{R}|}\right) \qquad (2.37)$$

he finds this limit does not exist. This can be shown by noting that

$$\lim_{\vec{r}\to\vec{R}} \vec{\nabla}\left(e^{-\alpha|\vec{r}-\vec{R}|}\right) = \lim_{\vec{r}\to\vec{R}} -\alpha\left(\frac{\vec{r}-\vec{R}}{|\vec{r}-\vec{R}|}\right) e^{-\alpha|\vec{r}-\vec{R}|}$$

$$= \lim_{\vec{r}-\vec{R}} -\alpha\,\widehat{|\vec{r}-\vec{R}|}\, e^{-\alpha|\vec{r}-\vec{R}|} \qquad (2.38)$$

Now, since the unit vector depends on the angles ϕ,θ, the limit will depend on the direction of approach to the center. This type of behavior is indeed characteristic of the charge density at the nucleus of the atom and is due to the singularity in the Coulomb potential energy. Thus, the set of the STF's used to fit the charge density will satisfy this so-called cusp condition. Futhermore the atomic shell- like structure can also be formed using a linear superposition of these functions with various powers in the prefactors $|\,r - R\,|^n$. In a nut shell, most of the characteristic behaviors of the charge density can be satisfied by expanding the charge density in terms of spherical STF's.

We conclude this chapter with a brief review of other attempts at fitting the charge density. Rys et al [23] and Yanez et al [24] suggest a fit in terms of a linear combination of Gaussian functions. Yanez and his collaborators express the charge density in the form

$$\rho_0(\vec{r}) = \sum_j p_j \Omega_j(\vec{r})$$

$$\Omega_j = \sum_k d_{jk}\, g_k(\gamma_k, |\vec{r}-\vec{R}_j|) \qquad (2.39)$$

where

$$g_k(\gamma_k, |\vec{r}-\vec{R}_j|) = (\gamma_k/\pi)^{3/2} \exp\left[-\gamma_k(\vec{r}-\vec{R}_j)^2\right] \qquad (2.40)$$

The basis function Ω_j can be either a contracted or a primitive Gaussian function but each is associated with a single center. In fitting the charge density, besides making sure that the basis functions be normalized

$$\int \Omega_j \, d^3r = 1 \qquad (2.41)$$

they also imposed a constraint so that the summation of the optimum p_j's will be equal to the number of electrons

$$\sum_j p_j = N \qquad (2.42)$$

Furthermore, knowing that in a molecular environment atoms have the tendency to expand led them to introduce scaling so that

$$\rho'(\vec{r}) = \sum_A p_A s_A^3 \Omega_A (s_A |\vec{r} - \vec{R}_A|) \qquad (2.43)$$

where s_A is a scale factor for atom A. The scale factors may also be varied in the least squares fitting procedure and may or may not be associated with the electron number constraint. Even though formally they suggested using contracted Gaussians in the expansion, in practice they limit themselves to the primitive Gaussian of the form given in Eqn (2.40). On the other hand, besides investigating Gaussian-type expansions, Rys et al also suggest that polynomials in $\vec{r}_i$ defined on an interval (a_i, b_i) be used in expanding the charge density

$$\Omega_i = [r_i - \tfrac{1}{2}(a_i + b_i)]^{n_i} \quad a_i \leq r_i \leq b_i \qquad (2.44)$$

The purpose of using polynomial functions is to reduce the computational time during the optimization procedure. In both the methods of Rys et al

and Yanez et al, a least squares fitting procedure is used so that

$$\epsilon = \int d^3r \, (\rho_o - \rho_{fit})^2 \qquad (2.45)$$

is a minimum subject to the normalization constraint and perhaps some other constraints. This leads to optimum values of the parameters.

Again expanding the charge density in terms of linear combinations of Gaussian functions Hall and Smith [25] suggest that since the main interest is the energy, the criteria for finding the optimum parameters in the set of Gaussian functions should be based on minimizing the difference between the exact and the fitted electric field. Thus they seek, by least squares fitting, to minimize

$$\eta = \frac{1}{8\pi} \int (\vec{\nabla}\phi - \vec{\nabla}\phi^*)^2 d^3r \qquad (2.46)$$

The expression on the right can be transformed and written in terms of the fitted charge density $\rho^*(r)$ and the exact charge density $\rho(r)$,

$$\delta = \frac{1}{2} \int dr_1 \int dr_2 \frac{(\rho(1) - \rho^*(1))(\rho(2) - \rho^*(2))}{|\vec{r}_1 - \vec{r}_2|} \qquad (2.47)$$

In short, Eqn (2.47) is a least squares fitting of the electron density with $1/|r_1 - r_2|$ as a weighing function.

In comparing the methods of expanding charge density in terms of Slater or Gaussian functions, we find that one major shortcoming of using the Gaussian functions is that they do not have the cusp behavior at the center of Gaussian. Therefore fitting the charge density very close to the nucleus may be inaccurate due to this behavior. This

problem was noted by Smith and Hall in their paper. On the other hand, as we have already seen, Slater type functions do have required cusp behavior at the center.

Finally, one should note that there are other methods of representing the charge distributions, most notably the point charge model. The difference between this model and the models that we discussed previously is that, instead of fitting the given density directly using spatially extended functions such as Slaters or Gaussians, the electrostatic potential due to this density may be fit in terms of a linear combination of point charges. In this model, the electrostatic potential at certain discrete points $\{ \vec{R}_\alpha \}$ in space is found exactly using

$$V(R_\alpha) = \int d^3 r \frac{\rho(\vec{r})}{|\vec{r} - \vec{R}_\alpha|} \qquad (2.48)$$

Then, using this same formula except that the density $\rho(\vec{r})$ is replaced by

$$\rho_{PC}(r) = \sum q_i \, \delta(r - R_i) \qquad (2.49)$$

one obtains

$$V_{fit}(\vec{R}_\alpha) = \sum \frac{q_i}{|\vec{R}_\alpha - \vec{R}_i|} \qquad (2.50)$$

Momany [26], Cox and William [27], Ray et al [28] use a least squares fitting over a finite grid $\{ R_\alpha \}$ to minimize

$$\tau = \sum_{R_\alpha} | V_{fit}(R_\alpha) - V(R_\alpha) |^2 \qquad (2.51)$$

with the optimum choice of the parameters $\{ q_i, \vec{R}_i \}$. One major

problem of this method is that since the point charge potential diverges at the $\vec{R}_i$'s, the final result depends on the choice of grid. Alternatively, Brobjer and Murrell [29] prefer to determine the positions and the charges of the point charge model by fitting the molecular multipole moments obtained either from experiment or by calculation.

CHAPTER III

MATHEMATICAL ASPECT OF THE FITTING TECHNIQUE

In this chapter, our discussion will be focused upon the fitting procedure. As discussed in the previous chapter, we generate the charge density at selected points in space from a known wave function of the molecular fragment. Our task next is to fit this tabulated charge density in terms of a linear superposition of spherical Slater-Type Functions (STF). Mathematically, we write

$$\rho(\vec{r}) = \sum_{i=1}^{\eta} \alpha_i \, | \vec{r} - \vec{R}_i |^{n_i} \, e^{-\beta_i | \vec{r} - \vec{R}_i |} \equiv \rho_{fit}(\alpha_i \, \beta_i \, \gamma_i \, ; \vec{r}) \qquad (3.1)$$

where we have absorbed the q_i into α new linear fitting parameter

$$\alpha_i \equiv q_i \frac{\beta_i^{n_i+3}}{4\pi(n_i+2)!} \qquad (3.2)$$

In general, α_i, β_i, γ_i, i=1,2,.....η are determined using the least squares fitting minimization procedure described below. The fitted function ρ_{fit} can be thought of as not only a function of $\vec{r}$ but also a function of all 3η parameters involved in the fitting. Anticipating however that not all the α's, β's and γ's are independent, we write

$$\rho_{fit}(\alpha, \beta, \gamma \, ; \vec{r}) = \rho_{fit}\{ [\alpha_1 (a_1, a_2, \ldots . a_{n_A}), \alpha_2 (a_1, a_2, \ldots . a_{n_A}) \ldots \alpha_{N_A} (a_1, a_2, \ldots . a_{n_A}); \beta_1 (b_1, b_2, \ldots b_{n_B}), \beta_2 (b_1, b_2, \ldots b_{n_B}), \ldots \ldots \ldots \beta_{N_B} (b_1, b_2, \ldots b_{n_B}); \gamma_1 (c_1, c_2, \ldots c_{n_C}), \gamma_1 (c_1, c_2, \ldots c_{n_C}), \ldots \gamma_{N_C} (c_1, c_2 \ldots . c_{n_C})] : \vec{r}) \qquad (3.3)$$

Therefore, a total of 3η or less parameters are needed to be determined in the fitting routine. We have gathered the parameters into sets so that the set α consists of only the α_i:

$$\alpha = \{ \alpha_i \; i=1,2,...N_A \} \qquad (3.4)$$

Similarly, for the sets β and γ

$$\beta = \{ \beta_i \; i=1,2,...N_B \} \qquad (3.5)$$

and

$$\gamma = \{ \gamma_i \; i=1,2,...N_C \} \qquad (3.6)$$

Note that $N_A = N_B = N_C = \eta$. Now, within each of the given sets, one has the option of varying all the parameters at once or holding some fixed (i.e. "frozen") and allowing only a subset to vary. Futhermore, within these sets { α }, { β } and { γ }, one may also relate some of the parameters among themselves, say, because of symmetry constraints. These relationships among the parameters then allow us to express them in terms of smaller sets of parameters, the a's for the α's, b's for the β's and c's for the γ's. The a's, b's and c's are our independent parameters. In other words, each of the parameters α_i, β_j, and γ_k is written as a function of another set of parameters a_i, b_j, and c_k, respectively so that one has

$$\alpha_i = \alpha_i (a_1, a_2,....a_{n_A}) \qquad i=1,2,....N_A; \; n_A \leq N_A \qquad (3.7)$$

$$\beta_i = \beta_i (b_1, b_2,....b_{n_B}) \qquad i=1,2,....N_B; \; n_B \leq N_B \qquad (3.8)$$

$$\gamma_i = \gamma_i (c_1, c_2,....c_{n_C}) \qquad i=1,2,....N_C; \; n_B \leq N_B \qquad (3.9)$$

Consider the subset of parameters in the set α that are allow to

vary. We denote this subset by

$$\alpha^{\star} = \{ \alpha_{i_1}, \alpha_{i_2}, \ldots \alpha_{i_{M_A}} \} \equiv \{ \alpha_1^{\star}, \alpha_2^{\star}, \ldots \alpha_{M_A}^{\star} \} \qquad (3.10)$$

Similarly we denote the subsets of the β and γ parameters that are allowed to vary by $\beta^{\star}$ and $\gamma^{\star}$:

$$\beta^{\star} = \{ \beta_{i_1}, \beta_{i_2}, \ldots \beta_{i_{M_B}} \} \equiv \{ \beta_1^{\star}, \beta_2^{\star}, \ldots \beta_{M_B}^{\star} \} \qquad (3.11)$$

$$\gamma^{\star} = \{ \gamma_{i_1}, \gamma_{i_2}, \ldots \gamma_{i_{M_C}} \} \equiv \{ \gamma_1^{\star}, \gamma_2^{\star}, \ldots \gamma_{M_C}^{\star} \} \qquad (3.12)$$

Note that the subscripts i_1, i_2,... correspond to the place labels on the parameters that are allowed to vary in the sets α, β and γ. But not all of the parameters in the sets $\alpha^{\star}$, $\beta^{\star}$ and $\gamma^{\star}$ are independent. Some of them are related to one another within the same set where these relationships are expressed in terms of the independent parameters, the a's, b's and c's. Therefore, for the α parameters out of n_A independent parameters in the set a, in general only a subset of them is allowed to vary; we denote this subset by

$$a^{\star} = \{ a_{j_1}, a_{j_2}, \ldots a_{j_{m_a}} \} = \{ a_1^{\star}, a_2^{\star}, \ldots a_{m_a}^{\star} \}; \quad m_a \leq n_a \qquad (3.13)$$

Similarly, for the β and γ parameters, only a subset of the independent parameters, that is the b's and c's, is allowed to vary. Let these independent parameter sets be denoted

$$b^{\star} = \{ b_{j_1}, b_{j_2}, \ldots b_{j_{m_b}} \} = \{ b_1^{\star}, b_2^{\star}, \ldots b_{m_b}^{\star} \}; \quad m_b \leq n_b \qquad (3.14)$$

b

$$c^{\star} = \{ c_{j_1}, c_{j_2}, \ldots c_{j_{m_c}} \} = \{ c_1^{\star}, c_2^{\star}, \ldots c_{m_c}^{\star} \}; \quad m_c \leq n_c \qquad (3.15)$$

The relationship between the elements in the sets α^*, β^* and γ^* and the independent parameters a^*, b^* and c^* can be expressed schematically

$$\alpha^* = \alpha^* (a^*) \qquad (3.16)$$

$$\beta^* = \beta^* (b^*) \qquad (3.17)$$

$$\gamma^* = \gamma^* (c^*) \qquad (3.18)$$

It is the set of independent parameters, the a^*'s, b^*'s and c^*'s which are the independent variables used in the fitting routine. Once we get the optimum value of all these independent parameters we can compute α^*'s, β^*'s and γ^*'s according to the above scheme. One advantage of the option relating parameters to some other independent parameters appears in symmetry considerations of the charge density. We can guarantee that symmetry-related parameters are constrained to be equal in fitting the charge densities having symmetry properties; this is especially useful in fitting molecular charge densities. Another advantage of this option is that one can reduce the number of parameters involved in the fitting routine. One then hopes that the fitting routine will converge faster

The dependence of the center of the Slater function $\vec{R}_i$ on the γ parameter occurs explicitly in the form

$$\vec{R}_i (\gamma_i) = \vec{R}_{io} + \gamma_i \hat{r} (\theta, \phi) \qquad (3.19)$$

Here R_{io} is the initial center for the Slater function and $\hat{r}(\theta, \phi)$ defines the direction along which line the center may be changed. The

angles θ_i and ϕ_i are specified a priori. The fitting routine optimizes the parameter γ_i (which may be negative or positive) as the function "slides along" the specified line.

Finally, we impose the normalization or charge conservation constraint that

$$\int d^3 r\, \rho_{fit}(\vec{r}) = N\,(-e) \qquad (3.20)$$

In principle this single additional constraint may be included in the least squares optimization by the Lagrange multiplier technique. We found such an approach impractical however. Rather, among the set of α parameters that are not explicitly varied we chose a subset

$$\underline{\alpha} = \{ \alpha_{k_1}, \alpha_{k_2}, \ldots\ldots \alpha_{k_{Nfix}} \} = \{ \underline{\alpha}_1, \underline{\alpha}_2, \ldots \underline{\alpha}_{Nfix} \} \qquad (3.21)$$

which is nevertheless allowed to change in order to satisfy the above constraint. Using Eqn (3.1) for $\rho_{fit}(r)$ we obtain explicitly

$$\int d^3 r\, \rho_{fit}(\vec{r}) =$$

$$= \int d^3 r \left[\sum_{i=1}^{N} \alpha_i \left| \vec{r} - \vec{R}_i(\gamma_i) \right|^{n_i} e^{-\beta_i \left| \vec{r} - \vec{R}_i(\gamma_i) \right|} \right]$$

$$= \sum_{i=1}^{N} \alpha_i \frac{4\pi\,(n_i + 2)!}{\beta^{n_i + 3}} = N\,(-e) \qquad (3.22)$$

Then making the ansatz that

$$\underline{\alpha}_1 = \underline{\alpha}_2 = \ldots \underline{\alpha}_{Nfix} = \underline{\alpha} \qquad (3.23)$$

we found that each of these "nornalization fixed" α's is given

$$\underline{\underline{\alpha}}_j = \frac{1}{Nfix}\left[\frac{\beta^{n_i+3}}{4\pi\,(n_i+2)!}\right]\left[N(-e) - \sum_{i=1}^{N}{}' \alpha_i \left[\frac{\beta^{n_i+3}}{4\pi\,(n_i+2)!}\right]\right] \qquad (3.24)$$

Here we envision all these parameters in the relatively small set α to be equal by symmetry. The sum $\sum'$ in Eqn (3.24) is over all the other α's (including the frozen one) not in $\underline{\underline{\alpha}}$. As a consequence the $\underline{\underline{\alpha}}$'s are functions of the α's and β's to be varied, i.e. the set α^* and β^*. In turn, the $\underline{\underline{\alpha}}$'s depend on the independent variational parameters in the sets a^* and b^*. Schematically we write

$$\underline{\underline{\alpha}} = \underline{\underline{\alpha}}\left[\alpha^*(a^*),\ \beta^*(b^*)\right] = \underline{\underline{\alpha}}(a^*, b^*) \qquad (3.25)$$

Consider that there are a total of P data $\{\rho_o(\vec{r}_I), \vec{r}_I, I=1,2....P\}$ that we want to fit. Let us write ρ_{fit} in the form

$$\rho_{fit}(\alpha, \beta, \gamma ; \vec{r}_I) = \sum_{i=1}^{\eta} f_i(\alpha_i, \beta_i, \gamma_i ; \vec{r}_I) \quad I=1,2,....P$$

where

$$f_i(\alpha_i, \beta_i, \gamma_i ; \vec{r}_I) = \alpha_i \left|\vec{r} - \vec{R}_i(\gamma_i)\right|^{n_i} e^{-\beta_i \left|\vec{r} - \vec{R}_i(\gamma_i)\right|} \qquad (3.26)$$

The least squares fitting procedure to determine the parameters requires us to minimized the function

$$\Phi(\alpha, \beta, \gamma) \equiv \sum_{I=1}^{P}\left[\rho_o(\vec{r}_I) - \sum_{i=1}^{\eta} f_i(\alpha_i, \beta_i, \gamma_i ; \vec{r}_I)\right]^2 \qquad (3.27)$$

Let define the set η

$$\eta = \{\alpha^* \cup \beta^* \cup \gamma^*\} \qquad (3.28)$$

to be the union of all $M = M_A+M_B+M_C$ parameters that are unfrozen. Similarly, let define the set λ as the union of all $m = m_a+m_b+m_c$ independent parameters

$$\lambda = \{ a^* \cup b^* \cup c^* \} \qquad (3.29)$$

As mentioned before the α's, β's and γ's explicitly occuring in Eqn (3.27) are functions of the independent a's, b's, and c's. In the spirit of focusing upon the independent unfrozen parameters we write

$$\Phi(\lambda) \equiv \sum_{I=1}^{P} [\rho_o(\vec{r}_I) - \rho_{fit}(\lambda ; \vec{r}_I)]^2 \qquad (3.30)$$

where $\rho_{fit}(\lambda ; \vec{r}_I)$ is defined in equation (3.26). In carrying out the minimization procedure of equation (3.40), one also has to consider the normalization constraint so that, as stated above, the a^* and b^* appear not only in α^* and β^* but also in α.

To carry out the minimization of $\Phi(\lambda)$, consider changing λ to $\lambda + \Delta\lambda$. In doing so, let us think of the set λ as an mx1 column matrix made up of the completely independent a^*, b^* and c^* with $m = m_a+m_b+m_c$. Note that the column matrix λ is is constructed in such a way that the a^*'s are arrange first followed by the b^*'s and the c^*'s i.e

$$\lambda^T = (a_1^*, a_2^* \ldots a_{m_a}^*, b_1^*, b_2^* \ldots b_{m_b}^*, c_1^*, c_2^* \ldots c_{m_c}) \qquad (3.31)$$

Similarly, consider the set $\Delta\lambda$ represented by another m x 1 column matrix. For a given point λ in the parameter space, our immediate goal is to find $\Delta\lambda$ such that

$$\Phi (\lambda + \Delta\lambda) < \Phi (\lambda)$$

where

$$\Phi (\lambda + \Delta\lambda) = \sum_{I=1}^{P} [\rho_o(\vec{r}_I) - \rho_{fit}(\lambda + \Delta\lambda; \vec{r}_I)]^2 \qquad (3.32)$$

What we would ultimately like is to find the global minimum of $\Phi(\lambda)$. In practice we must be content with a stepwise procedure for continually reducing $\Phi(\lambda)$. To begin our discussion we consider a Taylor series expansion of $\Phi(\lambda+\Delta\lambda)$ about the point λ. Considering only up to the first order terms, we get

$$\Phi (\lambda + \Delta\lambda) \simeq \Phi_{approx} (\lambda + \Delta\lambda) = \sum_{I=1}^{P} [\rho_o(\vec{r}_I) - \rho_{fit}(\lambda; \vec{r}_I) - \sum_{j=1}^{m} \frac{\partial \rho_{fit}}{\partial \lambda_j} \Big|_{\lambda} \Delta\lambda_j]^2 \qquad (3.33)$$

Carrying out the indicated multiplication we have

$$\Phi_{approx} (\lambda + \Delta\lambda) = \sum_{I=1}^{P} \{ (\rho_o(r_I) - \rho_{fit}(\lambda; r_I))^2 - 2 \sum_{i=1}^{m} (\rho_o(\vec{r}_I) - \rho_{fit}(\lambda; \vec{r}_I)) \frac{\partial \rho_{fit}}{\partial \lambda_i} \Big|_{\lambda} \Delta\lambda_i + \sum_{i=1}^{m} \sum_{j=1}^{m} \frac{\partial \rho_{fit}}{\partial \lambda_i} \Big|_{\lambda} \frac{\partial \rho_{fit}}{\partial \lambda_j} \Big|_{\lambda} \Delta\lambda_i \Delta\lambda_j \} \qquad (3.34)$$

or in matrix form

$$\Phi_{approx}(\lambda + \Delta\lambda) = A_o - 2Q^T \Delta\lambda + \Delta\lambda^T C \Delta\lambda \qquad (3.35)$$

Here, A_o is a scalar

$$A_o = \sum_{I=1}^{P} \left[\rho_o(\vec{r}_I) - \rho_{fit}(\lambda; \vec{r}_I) \right]^2 = \Phi(\lambda) \qquad (3.36)$$

while Q is an m x 1 matrix whose i^{th} element is

$$Q_i = \sum_{I=1}^{P} \left(\rho_o(\vec{r}_I) - \rho_{fit}(\lambda; \vec{r}_I) \right) \frac{\partial \rho_{fit}}{\partial \lambda_i} \Big|_{\lambda} \qquad (3.37)$$

and C is a symmetric m x m matrix whose ij^{th} element is

$$C_{ij} = \sum_{I=1}^{P} \frac{\partial \rho_{fit}}{\partial \lambda_i} \Big|_{\lambda} \frac{\partial \rho_{fit}}{\partial \lambda_j} \Big|_{\lambda} \qquad (3.38)$$

Note that the partial derivative with respect to the λ's can be written in the explicit form

$$\frac{\partial \rho_{fit}}{\partial \lambda_j} \Big|_{\underset{\sim}{\lambda}} = \begin{cases} \frac{\partial}{\partial a_j^*} \rho_{fit} \\ \frac{\partial}{\partial b_j^*} \rho_{fit} \\ \frac{\partial}{\partial c_j^*} \rho_{fit} \end{cases} \qquad (3.39)$$

where

$$\frac{\partial \rho_{fit}}{\partial a_j^*} = \sum_{i=1}^{M_A} \left(\frac{\partial \rho_{fit}}{\partial \alpha_i^*} \right) \left(\frac{\partial \alpha_i^*}{\partial a_j^*} \right) \qquad (3.40)$$

$$\frac{\partial \rho_{fit}}{\partial b_j^*} = \sum_{i=1}^{M_B} \left(\frac{\partial \rho_{fit}}{\partial \beta_i^*} \right) \left(\frac{\partial \beta_i^*}{\partial b_j^*} \right) \qquad (3.41)$$

$$\frac{\partial \rho_{fit}}{\partial c_j^*} = \sum_{i=1}^{M_c} \left(\frac{\partial \rho_{fit}}{\partial \gamma_i^*} \right) \left(\frac{\partial \gamma_i^*}{\partial c_j^*} \right) \qquad (3.42)$$

In the spirit of our remarks concerning th e normalization constraint it should be appreciated that

$$\frac{\partial \rho_{fit}}{\partial \alpha_i^*} = \frac{\partial}{\partial \alpha_i^*} \rho_{fit} \left[\ldots \alpha_i^* \ldots \bar{\bar{\alpha}} (\ldots \alpha_i^* \ldots) \ldots \right] \qquad (3.43)$$

and

$$\frac{\partial \rho_{fit}}{\partial \beta_i^*} = \frac{\partial}{\partial \beta_i^*} \rho_{fit} \left[\ldots \beta_i^* \ldots \bar{\bar{\alpha}} (\ldots \beta_i^* \ldots) \ldots \right] \qquad (3.44)$$

Therefore the approximation to the exact $\Phi(\lambda+\Delta\lambda)$ is quadratic in $\Delta\lambda$; Written in more explicit form Eqn (3.35) becomes

$$\Phi_{approx}(\lambda+\Delta\lambda) = A_0 - 2 \sum_{i=1}^{m} Q_i \Delta\lambda + \sum_{i=1}^{m} \sum_{j=1}^{m} \Delta\lambda_i C_{ij} \Delta\lambda_j \qquad (3.45)$$

The minimum of $\Phi_{approx}(\lambda+\Delta\lambda)$ can be found by taking the partial derivatives with respect to $\Delta\lambda_k$, k=1,2....m and equating each of them to zero:

$$\frac{\partial \Phi_{approx}}{\partial \Delta\lambda_k} = -2Q_k + \sum_{j=1}^{m} C_{kj} \Delta\lambda_j + \sum_{i=1}^{m} \Delta\lambda_i C_{ik} = 0$$

$$\text{for } k = 1, 2, \ldots m. \qquad (3.46)$$

But $C_{ik}=C_{ki}$ implies that

$$\frac{\partial \Phi_{approx}}{\partial \Delta\lambda_k} = -2Q_k + 2 \sum_{j=1}^{m} C_{kj} \Delta\lambda_j = 0$$

$$\text{for } k = 1, 2 \ldots m. \qquad (3.47)$$

In matrix form we can write this set of m equations

$$C\,\Delta\lambda = Q \qquad (3.48)$$

Now, if C^{-1} exists then the unique solution is

$$\Delta\lambda = C^{-1}Q \qquad (3.49)$$

and therefore

$$\begin{aligned}\Phi_{approx}(\lambda+\Delta\lambda) &= \Phi_{approx}(\lambda + C^{-1}Q)\\ &= A_0 - 2\underset{\sim}{Q}^T C^{-1}Q + Q^T(C^{-1})^T C C^{-1}Q\\ &= A_0 - Q^T C^{-1}Q = \Phi(\lambda) - Q^T C^{-1}Q \qquad (3.50)\end{aligned}$$

If C^{-1} is positive definite then clearly

$$\Phi_{approx}(\lambda+\Delta\lambda) < \Phi(\lambda) \qquad (3.51)$$

and moreover this value is the minimum value of $\Phi_{approx}(\lambda)$.

But what we have done is to minimize Φ_{approx}. What we are interested in doing is to find $\Delta\lambda$ which ensures

$$\Phi(\lambda+\Delta\lambda) < \Phi(\lambda) \qquad (3.52)$$

In general the solution $\Delta\lambda = C^{-1}Q$ which minimize Φ_{approx} does not guarantee the inequality (Eqn (3.52)) be satisfied. However, we can adapt this approach to our real purpose by letting

$$\Delta\lambda = \sigma R^{-1}Q \qquad (3.53)$$

where R^{-1} is a positive definite matrix and σ is a positive number. For

then it can be shown that the inequality (Eqn (3.52)) can be satisfied with an appropriate choice for σ. Indeed, one can then express $\Phi(\lambda+\Delta\lambda)$ using the definition for $\Delta\lambda$ in Eqn (3.53) as

$$\Phi(\lambda+\Delta\lambda) = A_0 - 2Q^T\sigma R^{-1}Q + \sigma^2 Q^T(R^{-1})^T C R^{-1}Q + O(\sigma^2)$$

$$= A_0 - 2\sigma Q^T R Q + O(\sigma^2) \qquad (3.54)$$

When σ is small enough then the linear term in Eqn (3.54) must dominate to the extent that all the higher order terms can be considered negligible. Consequently, one can write

$$\Phi(\lambda+\Delta\lambda) \simeq A_0 - 2\sigma Q^T R Q < A_0 = \Phi(\lambda) \qquad (3.55)$$

which implies

$$\Phi(\lambda+\Delta\lambda) < \Phi(\lambda) \qquad (3.56)$$

With the redefinition of $\Delta\lambda$ according to Eqn (3.53), the question that arises is how to pick R^{-1} and σ and therefore $\Delta\lambda$ in an optimal way. At this point we are going to use the Marquardt algorithm [30] to find R^{-1} and σ. Basically, the Marquardt algorithm is a compromise between the steepest descent and the Gauss method in the least squares fitting procedure. To begin with, consider

$$R = [C + \Lambda B^2] \qquad (3.57)$$

where the matrix B can be any symmetric, positive definite and non-singular m x m matrix and Λ is some constant. The matrix C is

defined as in Eqn (3.38) and is Hermitian (in fact it was symmetric since all its element are real). To be specific the recommend choice of the matrix B is given by the prescription

$$B_{ij} = \left\{ \begin{array}{l} \sqrt{c_{ii}} \text{ , if } \sqrt{c_{ii}} \geq \epsilon \\ 1 \text{ , if } \sqrt{c_{ii}} < \epsilon \\ 0 \text{ , for } i \neq j \end{array} \right\} \text{for } i = j \qquad (3.58)$$

where $\epsilon = 10^{-6}$ in the appropriatiate units. Eqn (3.57) can also be written in the form

$$R = B[\, B^{-1} C B^{-1} + \Lambda \,] B \qquad (3.59)$$

Since C is symmetric then the term $B^{-1}CB^{-1}$ is also symmetric. Let

$$S = U^T [\, B^{-1} C B^{-1} \,] U \qquad (3.60)$$

where U is an orthogonal tranformation matrix and S is the diagonal matrix of the eigenvalues of $B^{-1}CB^{-1}$. Thus, since

$$B^{-1} C B^{-1} = U S U^T \qquad (3.61)$$

we have for R

$$\begin{aligned} R &= B[\, U S U^T + \Lambda U U^T \,] B \\ &= BU[\, S + \Lambda \,] U^T B^T \end{aligned} \qquad (3.62)$$

Then a little matrix algebra lead to the required inverse:

$$\begin{aligned} R^{-1} &= (U^T B^T)^{-1} [\, S + \Lambda 1 \,]^{-1} (BU)^{-1} \\ &= (B^T)^{-1} U [\, S + \Lambda 1 \,]^{-1} U^T B^{-1} \\ &= (B^{-1})^T (U^{-1})^T [\, S + \Lambda 1 \,]^{-1} U^{-1} B^{-1} \\ &= (U^{-1} B^{-1})^T [\, S + \Lambda 1 \,]^{-1} U^{-1} B^{-1} \\ &= G^T [\, S + \Lambda 1 \,]^{-1} G \end{aligned} \qquad (3.63)$$

where

$$G = U^{-1}B^{-1} \qquad (3.64)$$

Note that the requirement that R^{-1} be positive definite is that for all vectors X,

$$X^T R^{-1} X > 0 \qquad (3.65)$$

Clearly

so that R^{-1} is positive definite provided $[\ S + \Lambda 1\ ]^{-1}$ is positive definite. This in turn will be true provided

$$\Lambda > -S_{min} \qquad (3.66)$$

that is, Λ must be larger than the negative of the smallest eigenvalue of $B^{-1}CB^{-1}$. Therefore the elements of the sought-for matrix R are

$$(R^{-1})_{ij} = \sum_{k\ell} (G^T)_{ik} \left\{ [S + \Lambda 1]^{-1} \right\}_{k\ell} G_{\ell j} \qquad (3.67)$$

The fact that

$$[S + \Lambda 1]^{-1}$$

is diagonal implies

$$(R^{-1})_{ij} = \sum_{k} G_{ki} (S_k + \Lambda)^{-1}_k G_{kj} \qquad (3.68)$$

Let summarize the Marquardt algorithm step by step.

1) Start with an initial guess for the Λ, σ and the elements of the matrix λ. Marquardt suggest to put $\Lambda = 0.01$ and $\sigma = 1.00$

2) Construct the matrices B and C which are defined in Eqn (3.58) and Eqn (3.38) respectively.

3) At the start of the ith iteration , find the matrix R^{-1} defined in Eqn (3.68).

$$R_i^{-1} = (C_i + \Lambda B_i^2) = G^T [S + \Lambda 1]^{-1} G \ .$$

(Note that the subcript i here and below labels the i^{th} iteration.)

4) Using the result for R_i in step (3) and letting $\sigma_i = 1$, find

$$\Delta\lambda_i = \sigma_i R_i^{-1} Q_i$$

Let

$$\lambda^{(1)} = \lambda_i + \Delta\lambda_i$$

and evaluate

$$\Phi^{(1)} \equiv \Phi (\lambda^{(1)}) \ .$$

5) If $\Phi^{(1)} < \Phi_i \equiv \Phi(\lambda_i)$, then accept $\lambda_{i+1} = \lambda^{(1)}$ and replace Λ with the maximum of the two numbers 0.01Λ or ϵ where ϵ is a small positive number, say 10^{-7}. Then return to step 2 and begin the next iteration.

6) If $\Phi^{(1)} \geq \Phi_i$ and

$$\frac{[(\Delta\lambda)^T]^2}{[(Q^T Q) \{ (\Delta\lambda)^T (\Delta\lambda) \}]} < 0.5$$

then replace Λ with 10Λ and return to step 3. Otherwise replace σ by $\sigma/2$ and return to step 4 evaluating

$$\Phi(\lambda + \sigma R^{-1} Q_i)$$

which according to our proof must, for small enough σ, eventually become less than $\Phi(\lambda_i)$.

Once this condition is satisfied accept $\lambda_{i+1} = \lambda_i + \Delta\lambda_i$

The iteration procedure continues until $\Delta\lambda$--that is all the $\Delta\lambda$ components--are smaller than a preassigned constant. The final point λ_f

in the parameter space is then accepted as giving the optimum Φ and thus the "best fit" to the data $\{ \rho_o(r_I) \}$.

CHAPTER IV

GETTING THE BEST FIT TO THE CHARGE DENSITY

With the fitting routine tools available (i.e. fitting method and computer program) which have been discussed in the previous chapter, the question that arises next is how one can utilize these tools to the maximum capacity in order to get the best fit to a given tabulated charge density. Therefore, our attention in this chapter will be focused on guiding the reader toward finding an optimum fit to the charge density. Frankly speaking, from the experience that we have, this is not an easy task. Indeed, most of our research time has been spent on just fitting the charge density. In retrospect, we hope that we can at least devise some guidelines based upon this experience on how to fit the charge density for any molecular fragment. The importance of getting a good fit is obvious since we are going to use the fitted density in the energy computations; our calculations indicate the energy is very sensitive to the fit.

Of course, the charge density depends upon the approximate wave function for the fragment. Beyond that, the numerical representation of this density depends on our choice of points at which to tabulate it. In Chapter II we discussed the various geometric figures which we may use to arrange the points. Still one has to learn by experience how best to set up the parameters for these figures, such as the length of a line or

the radius of a sphere on which the points are arranged. Despite the importance of ensuring the the tabulated density is "representative", our focus here is on optimizing the α, β and γ parameters in fitting a given tabulation of the charge density.

As we have mentioned in the Chapter III, in fitting the charge densities our main objective is to minimize the function

$$\Phi(\alpha,\beta,\gamma) = \sum_{I=1}^{P} \left(\rho_o(\vec{r}_I) - \rho_{fit}(\alpha,\beta,\gamma;\vec{r}_I) \right)^2$$

In other words, we search for the sets of parameters α, β and γ in the parameter space so that Φ (α,β,γ) is a minimum. The sought-for minimum is the global minimum in the parameter space and not a local minimum. The distinction is that the global minimum is the absolutely smallest value of Φ, whereas a local minimum refers to a relative minimum in the parameter space within the vicinity of the initial guess of the parameters. One can think of the surface Φ as embedded within a multi-dimensional parameter space whose dimension equals the number of independent parameters used in fitting the charge density. We anticipate many local minima on this multi-dimensional surface and out of these local minima only the one having the absolutely lowest value is the global minimum. Finding the set of parameters that will lead to Φ being the global minimum is not easy. The reason is because the very structure of the program (i.e. the Marquardt algorithm) forces Φ to converge to a near minimum; but this does not imply we have reached the global minimum. In fact given so many local minima, chances are small the global minimum is actually found. It is therefore important that one should start with a good initial guess to the parameters so as to

get, if not the best, at least a very good fit. We hope to present in this chapter a method of doing this. Each resulting fit can be characterised by a root mean square (RMS) value

$$(\Delta\rho)_{RMS} = \sqrt{\Phi(\alpha,\beta,\gamma)/P-1}$$

Presumably the smaller $(\Delta\rho)_{RMS}$ the better the fit.

Basically, all the factors which affect the convergence of the fitting routine fall under two categories:

1) The number, type and initial location of spherical Slater Functions used to expand the charge densities. Note that we distinguish the different types of Slater functions by the power n_i on $|\vec{r} - \vec{R}|^{n_i}$. Thus we need to plan a' priori on constructing inner shells, lone pairs directed bonds, etc. by a judicious choice of the expansion functions.

2) The initial guess to and the manipulations of the parameters, i.e all the α's, β's and γ's. Among these possibilities are included such options as:

a) Freeze some of the parameters and optimize only the remaining subset. For instance, we might begin by superimposing atomic densities to form the molecular expansion, keeping the inner shell atomic parameters frozen and allowing only the valence shell parameters to be reoptimized.

b) Relate the some of parameters to one another , thus reducing the total number of independent variables. Symmetry consideration, for instance, reduce the number of independent parameters involved in the optimization. Another way of reducing the number of parameters is by

using subsets of "even-tempered" functions in which the β parameters are related to one another. Typically, within a given subset we require $\beta_{i+1} = d\beta_i$ where d is a fixed ratio factor.

c) Impose the normalization constraint on different choices of the $\underline{\underline{\alpha}}$ parameters

All of these manipulations on the parameters have been discussed in the previous chapter. Changing any one of the factors mentioned above in the fitting routine will lead to a different set of "optimum" parameters α, β and γ corresponding to a different local minimum.

Before presenting an illustration of our method, let us mention some guidelines that we use in fitting the charge densities of the neon atom and the water molecule. We presume these will become part of the general guidelines.

1) With the charge density to be fitted is generated from Hatree-Fock orbitals ψ_λ's written as a LCAO of STO's, we look at the elements of the density matrix associated with a given center and consider those elements whose values are large (say >0.1). From the location of these elements in the density matrix we deduce the types and the initial exponents of the Slater functions on a given center. The computer program that we have written to generate $\rho_o(\vec{r})$ from the Hartree-Fock wavefunction isolates the elements in the density matrix that are large enough (say >0.1).

2) We try to use as few parameters as possible to begin with. This can be done by using the concepts of even-tempered functions and symmetry. Then, as needed, and guided by our comments above, we add one or two

additional functions at a time in an attempt to reduce $(\Delta\rho)_{RMS}$.

3) We use the results of previous fits and see whether one can freeze some of the parameters that one is sure of. Also we check whether there are any improvement to the previous fit by adding just one new function at a time.

4) We plot the charge density difference $\Delta\rho=\rho_{fit}-\rho_o$ (and, for atoms $r^2\Delta\rho$, the radial charge density difference) to get a visual insight into how well the fit spatially reflects the actual charge density. Sometimes almost equally good $(\Delta\rho)_{RMS}$ values are found for two different fits where one clearly does not spatially mimic the true density. In such instances this fit can be eliminated from attempts at further refinements by our visual inspection.

5) For fitting charge densities of molecules, we first center the functions on nuclei; then we try adding some functions along the bonds and in the region of lone pairs. We also have the option that the centers of these functions are allow to slide back and forth along the bond. We have used these options to fit the charge density of the water molecule and make incremental improvements in the successive fits.

Listed Table I thru IV are the results of several fits to the neon charge density. Each table presents three different convergent fits illustrating various factors which affect the optimization routine. From these results one can conclude that the "optimum" parameters in fitting a given tabulated charge density are not unique. The set of points to be fit is the same for all the different fits in Table I thru IV. We fit 121 points equally spaced 0.05 a.u. apart along a given line begining at the

TABLE I

COMPARING FITS USING DIFFERENT INITIAL GUESS TO BETA PARAME

NAME	i	n_i	BETA I ( )	BETA F ( )	CHARGE (q)	RMS
FIT 1	1	2	8.17317	6.647	-4.50032	1.30E-02
	2	1	38.5607	20.4538	0.35769	
	3	0	18.6251	18.6266	-2.4102	
	4	2	4.28342	4.2834	-3.4472	
FIT 2	1	2	7.12658	6.98474	-3.86389	4.89E-03
	2	1	45.1088	31.7256	0.01529	
	3	0	18.0662	19.7124	-2.03346	
	4	2	4.05819	4.40599	-4.11793	
FIT 3	1	2	6.12958	6.60143	-5.13395	2.02E-03
	2	1	25.1088	28.825	0.02489	
	3	0	19.0662	19.6592	-2.05002	
	4	2	4.05819	3.83593	-2.84092	

TABLE II

COMPARING FITS USING DIFFERENT # OF FIXED BETA PARAMETER

NAME	i	n_i	INIT. BETA	FINAL BETA	CHARGE (q)	RMS
FIT 5	1	2	7.12658	6.98474	-3.86389	4.89E-03
ALL	2	1	45.1088	31.7256	0.01529	
BETA	3	0	18.0662	19.7124	-2.03346	
FREED	4	2	4.05819	4.40599	-4.11793	
FIT 6	1	2	7.12658	6.2955	-5.90009	1.21E-02
ONE	2	1	45.1088	19.7955	0.57722	
BETA	3	0	18.0662	18.0662	-2.64152	
FIXED	4	2	4.05819	3.48537	-2.03561	
FIT 4:	1	2	7.12658	6.49209	-5.04272	1.36E-02
TWO	2	1	45.1088	19.7647	0.58014	
BETA	3	0	18.0662	18.0662	-2.64152	
FIXED	4	2	4.05819	4.05819	-2.8959	

TABLE III

COMPARING FITS USING DIFFERENT # OF SLATER FUNCTION

NAME	i	n_i	INIT. BETA	FINAL BETA	CHARGE (q)	RMS
FIT 7	1	2	7.12658	6.98474	-3.86389	4.89E-03
FOUR	2	1	45.1088	31.7256	0.01529	
SLATER	3	0	18.0662	19.7124	-2.03346	
FUNCT.	4	2	4.05819	4.40599	-4.11793	
FIT 8	1	2	7.13738	7.1898	-20.1803	8.26E-02
FIVE	2	1	29.9629	15.9272	5.90839	
SLATER	3	0	18.0822	11.7398	-9.62635	
FUNCT.	4	2	4.05713	7.71514	0.19196	
	5	2	8.80599	8.5358	13.7063	
FIT 9	1	2	7.13738	7.22602	-60.3589	7.20E-03
SIX	2	1	29.9629	20.7308	0.37261	
SLATER	3	0	18.0822	18.5159	-2.45372	
FUNCT.	4	2	4.05713	4.93756	-23.927	
	5	2	8.80599	7.499	44.5888	
	6	2	5.006	5.54416	31.7782	

TABLE IV

COMPARING FITS USING DIFFERENT TYPES OF SLATER FUNCTION

NAME	i	n_i	INIT. BETA	FINAL BETA	CHARGE (q)	RMS
FIT 10	1	2	7.12658	6.87312	-4.18175	3.92E-03
	2	2	35.1088	47.3045	0.01036	
	3	0	18.0662	19.7283	-2.02855	
	4	2	4.05819	4.30895	-3.80007	
FIT 11	1	2	7.12658	6.98474	-3.86389	4.89E-03
	2	1	45.1088	31.7256	0.01529	
	3	0	18.0662	19.7124	-2.03346	
	4	2	4.05819	4.40599	-4.11793	
FIT 12	1	1	7.12658	33.0949	0.00037	2.91E-01
	2	1	45.1088	17.953	2.37344	
	3	0	18.0662	14.8003	-4.80522	
	4	2	4.05819	4.16347	-7.56859	

origin. The self consistent field wave function that we use to generate the charge density at this selected set of points is given by Clementi [31]. In fitting the charge density we try to illustrate the factors that can lead the fitting routine to converge to a different point in the parameter space. The set of γ parameters is not allowed to vary since all the Slater functions remain centered on the Neon nucleus. Furthermore, one should note the computer program chooses all the initial variable α parameters based on the initial guesses of the β parameters by performing a linear fit. Therefore, in this and all atomic cases, one would normally have to make initial guesses only for the β parameters. The initial guesses for the β parameters and the final convergent values for the β's and charge q's along with the $(\Delta\rho)_{RMS}$ are shown for for different fits in Table I thru IV.

The first three fits (Table I) illustrate that choosing different initial guesses for the β (thus a different set of α) parameters leads to different convergence points in the parameter space; thus one obtains different results even though the number and types of Slater functions are the same. Fig 1 presents $\Delta\rho(\vec{r}) = \rho_{fit} - \rho_o$ and Fig 2 $r^2\Delta\rho(\vec{r})$, each as a function of r, for the three fits listed in Table I. While all three fits are acceptable (the amplitudes of all three are less than $0.08e/(bohr)^3$ in Fig 1 and $0.02e/(bohr)$ in Fig 2) Fits 2 and 3 appear much better than Fit 1 (in Red). Visual inspection of Fits 2 and 3 leads us to prefer Fit 3 (in Green) although the distinction is not this time as striking. These conclusions are consistent with the $(\Delta\rho)_{RMS}$ results found in Table 1.

origin. The self consistent field wave function that we use to generate the charge density at this selected set of points is given by Clementi [31]. In fitting the charge density we try to illustrate the factors that can lead the fitting routine to converge to a different point in the parameter space. The set of γ parameters is not allowed to vary since all the Slater functions remain centered on the Neon nucleus. Furthermore, one should note the computer program chooses all the initial variable α parameters based on the initial guesses of the β parameters by performing a linear fit. Therefore, in this and all atomic cases, one would normally have to make initial guesses only for the β parameters. The initial guesses for the β parameters and the final convergent values for the β's and charge q's along with the $(\Delta\rho)_{RMS}$ are shown for for different fits in Table I thru IV.

The first three fits (Table I) illustrate that choosing different initial guesses for the β (thus a different set of α) parameters leads to different convergence points in the parameter space; thus one obtains different results even though the number and types of Slater functions are the same. Fig 1 presents $\Delta\rho(\vec{r}) = \rho_{fit} - \rho_o$ and Fig 2 $r^2\Delta\rho(\vec{r})$, each as a function of r, for the three fits listed in Table I. While all three fits are acceptable (the amplitudes of all three are less than $0.08e/(bohr)^3$ in Fig 1 and $0.02e/(bohr)$ in Fig 2) Fits 2 and 3 appear much better than Fit 1 (in Red). Visual inspection of Fits 2 and 3 leads us to prefer Fit 3 (in Green) although the distinction is not this time as striking. These conclusions are consistent with the $(\Delta\rho)_{RMS}$ results found in Table 1.

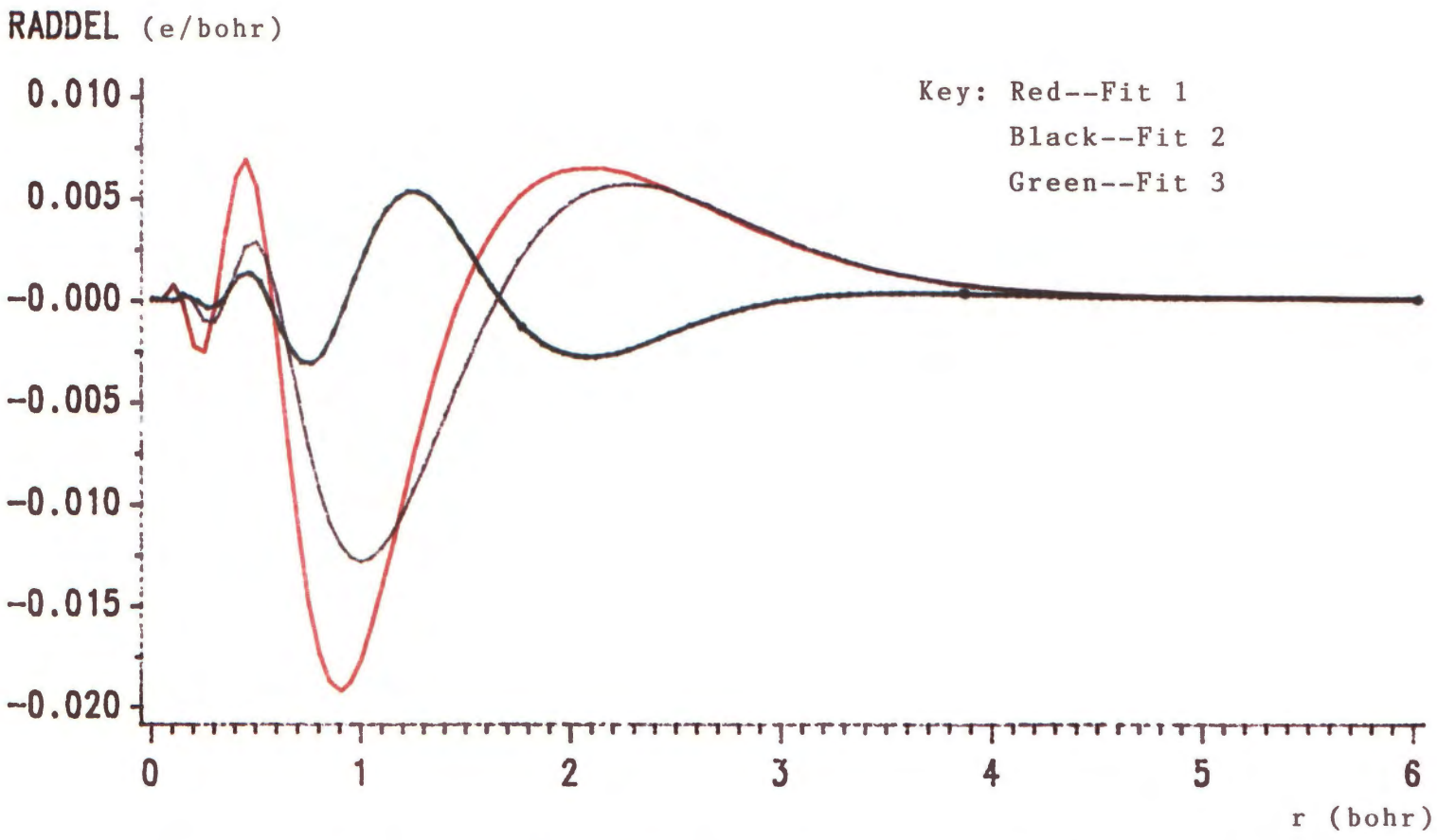

Figure 2. Plots of radial charge density difference ($r^2\Delta\rho$) versus the radial distance (r) for Neon atom for three fits listed in Table 1.

In a similar manner Fits 4 thru 6 (Table II) illustrate that using the same functions as before, one again obtains different fits by freezing one or more of the β parameters, keeping the initial guesses the same for all of them. The corresponding plots of $\Delta\rho$ and $r^2\Delta\rho$ are presented in Fig. 3 and Fig. 4 respectively. From the figures we see that Fit 4 (in Black) is somewhat superior to both Fit 5 (in Red) and Fit 6 (in Green). Indeed, Fit 4 is obtained by optimizing all four β parameters while Fits 5 and 6 freeze one and two β parameters respectively. As expected better $(\Delta\rho)_{RMS}$ values are obtained with fewer β parameters frozen. Of course, the routines take longer (more CPU time) to converge with more free parameters.

Fits 7 thru 9 illustrate that using different numbers of Slater functions leads to yet another set of results. These results are presented in Table III and the plots of $\Delta\rho$ and $r^2\Delta\rho$ are given in Figures 5 and 6. Obviously Fit 8 (in Red) may be immediately discarded from consideration; indeed its $(\Delta\rho)_{RMS}$ value is more than an order of magnitude greater than those for Fits 7 and 9. The point to be made here is that from the visual inspection alone candidate Fits for further improvements can be either kept or rejected. Of the remaining two the fit involving the four Slater functions (in Black) is visually superior than the six Slater functions (in Green). Again this conclusion is supported by the $(\Delta\rho)_{RMS}$ values in Table III. While intuition might suggest the better fit always obtains with the larger number of expansion functions, such a conclusion is clearly erroneous. There are in fact other factors--indeed those mentioned before--which play a crucial

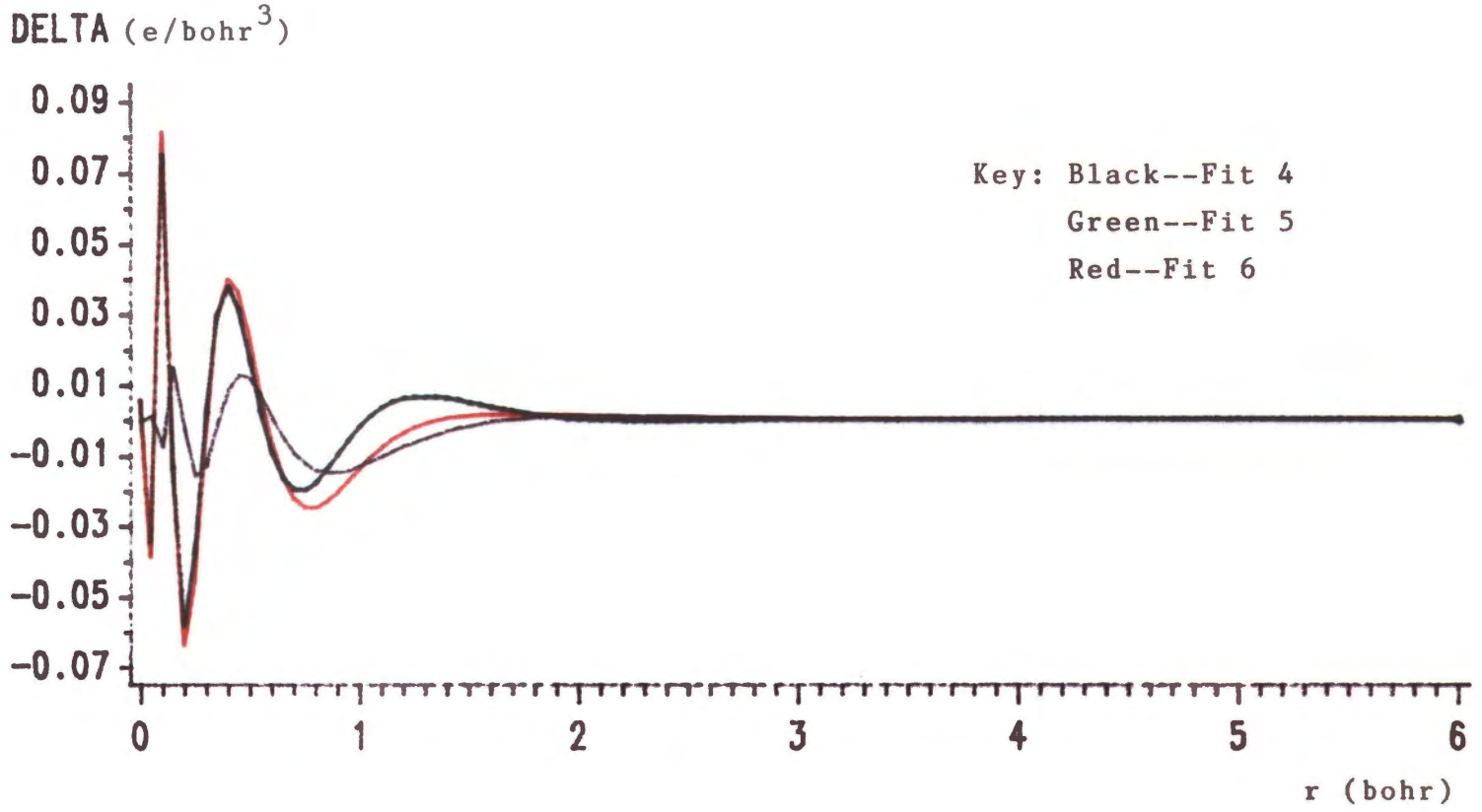

Figure 3. Plots of charge density difference ($\Delta\rho$) versus the radial distance (r) for Neon atom for three fits listed in Table 2.

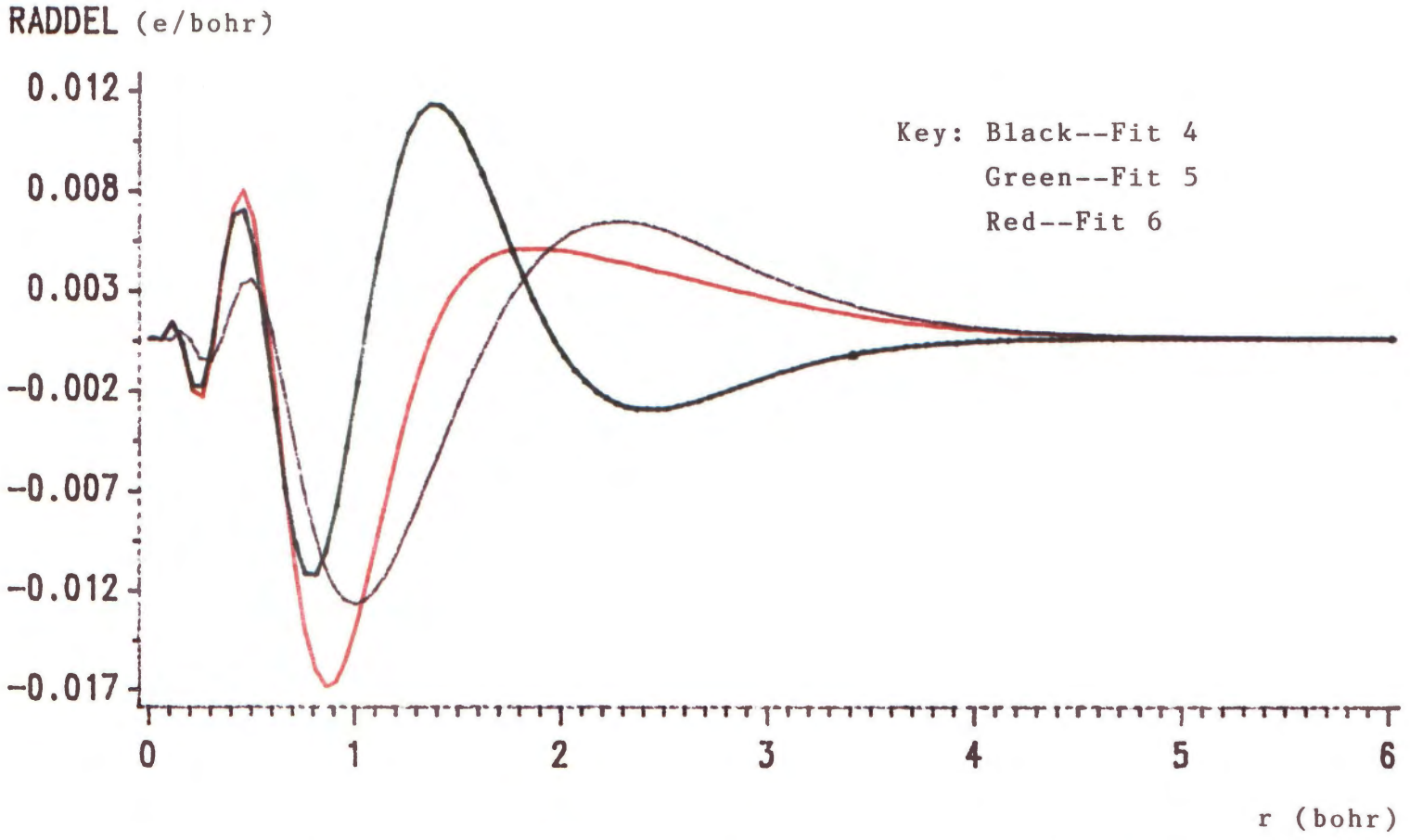

Figure 4. Plots of radial charge density difference ($r^2\Delta\rho$) the radial distance (r) for Neon atom for three fits listed in Table 2.

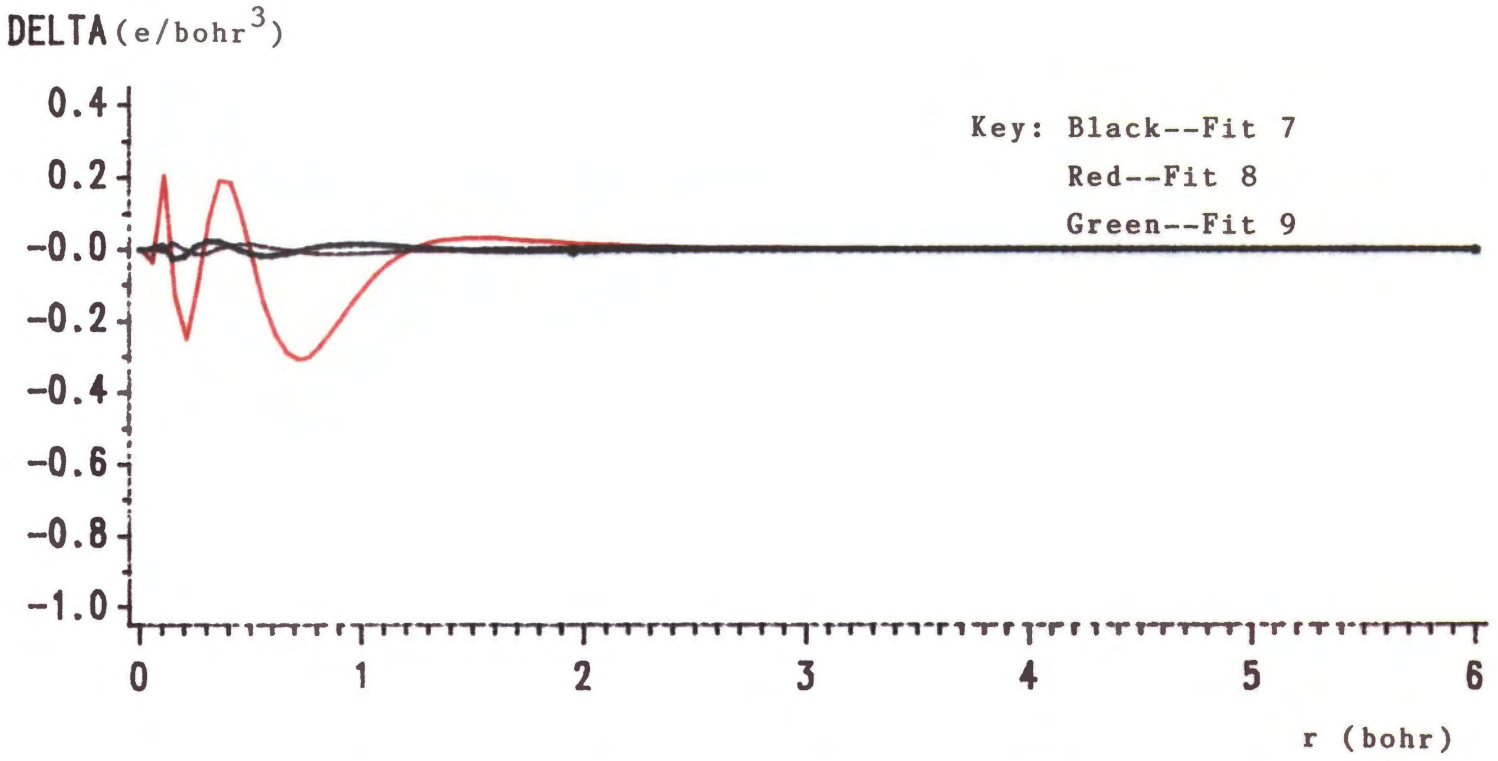

Figure 5. Plots of charge density difference ($\Delta\rho$) versus the radial distance (r) for Neon atom for three fits listed in Table III.

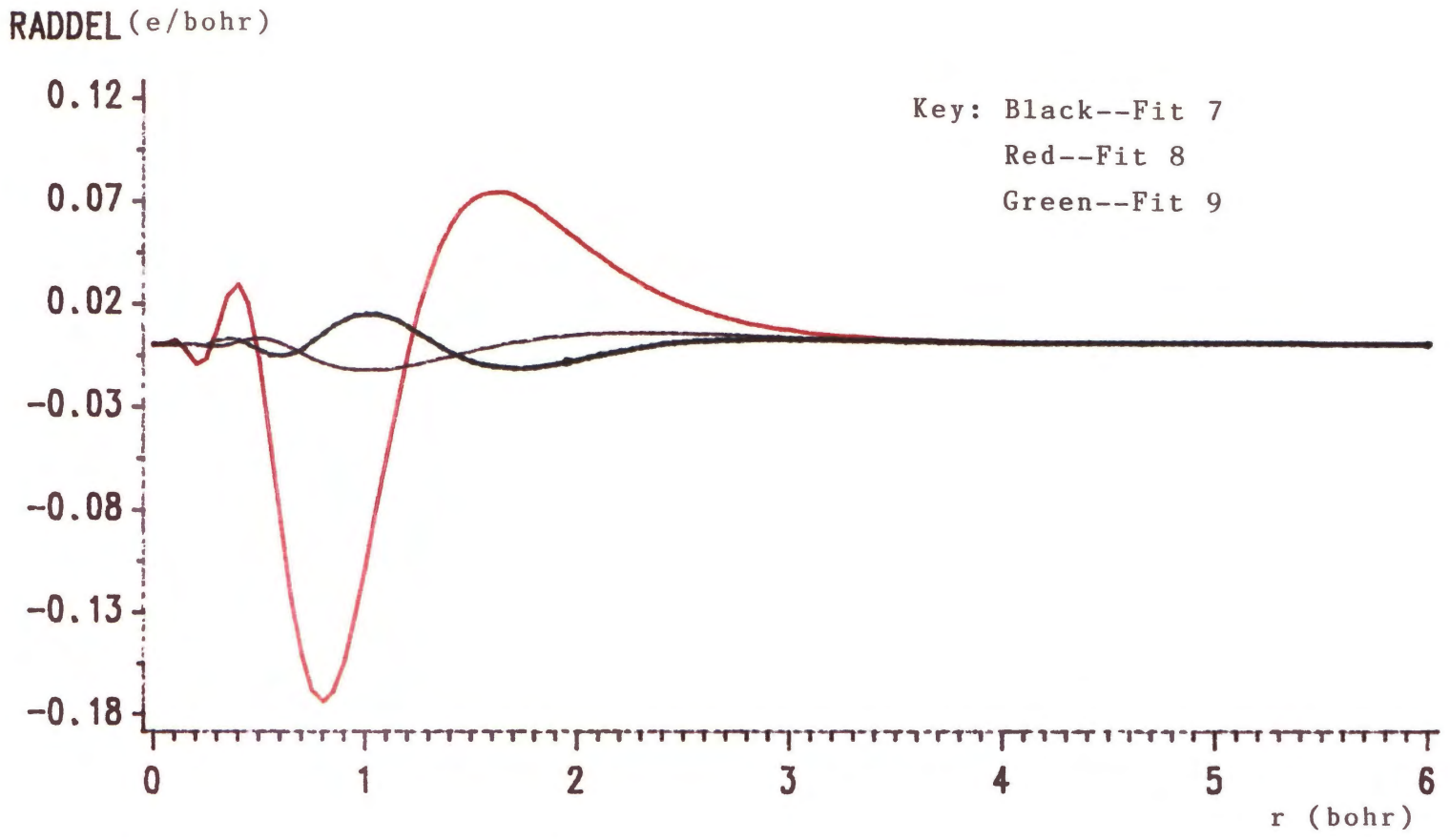

Figure 6. Plots of radial density difference ($r^2\Delta\rho$) versus the radial distance (r) for Neon atom for three fits listed in Table III.

role in determining the best fit.

Finally, Fit 10 thru 12 (Table IV) illustrate effect of using different types of Slater functions. The plots are shown in Figures 7 and 8. Fit 12 ($(\Delta\rho)_{RMS}$=0.3, in Green) may clearly be discarded. It appears that the L shell is not adequately represented by only one function with n=2. The other two fits appear equally good on these graphs. We have magnified these $\Delta\rho$ and $r^2\Delta\rho(r)$ graphs in Figures 9 and 10 to find that Fit 10 (in Red) is slightly better by visual inspection (Fit 12 (in Green) goes off-scale in these magnified graphs). Again this is borne out by the $(\Delta\rho)_{RMS}$ values in Table IV.

Note that these are only some of the fits that we have generated for the purpose of illustrating the factors affecting the convergence point in the parameter space. In fact, the fitting routine is very sensitive to slight changes in the factors listed above. Therefore, one can arrive at an almost endless number of different fits. With all these results, the question is how to select the best fit. There are two criteria used in choosing the best fit. The first criterion is to select the fit giving the lowest root mean square $(\Delta\rho)_{RMS}$ value, consistent with a good visual plot of $r^2\Delta\rho(r)$. This will at least tell us the best minimum that we obtained even though it might not be the global minimum that we are searching for. The second criterion is that all the q_j be less than the total number of electrons in the system. In other words, the charge is envisioned as divided among the Slater functions; in the atomic fits this corresponds to the shell-like structure. Note that this criterion was imposed based on our intuitive notion of more elegant

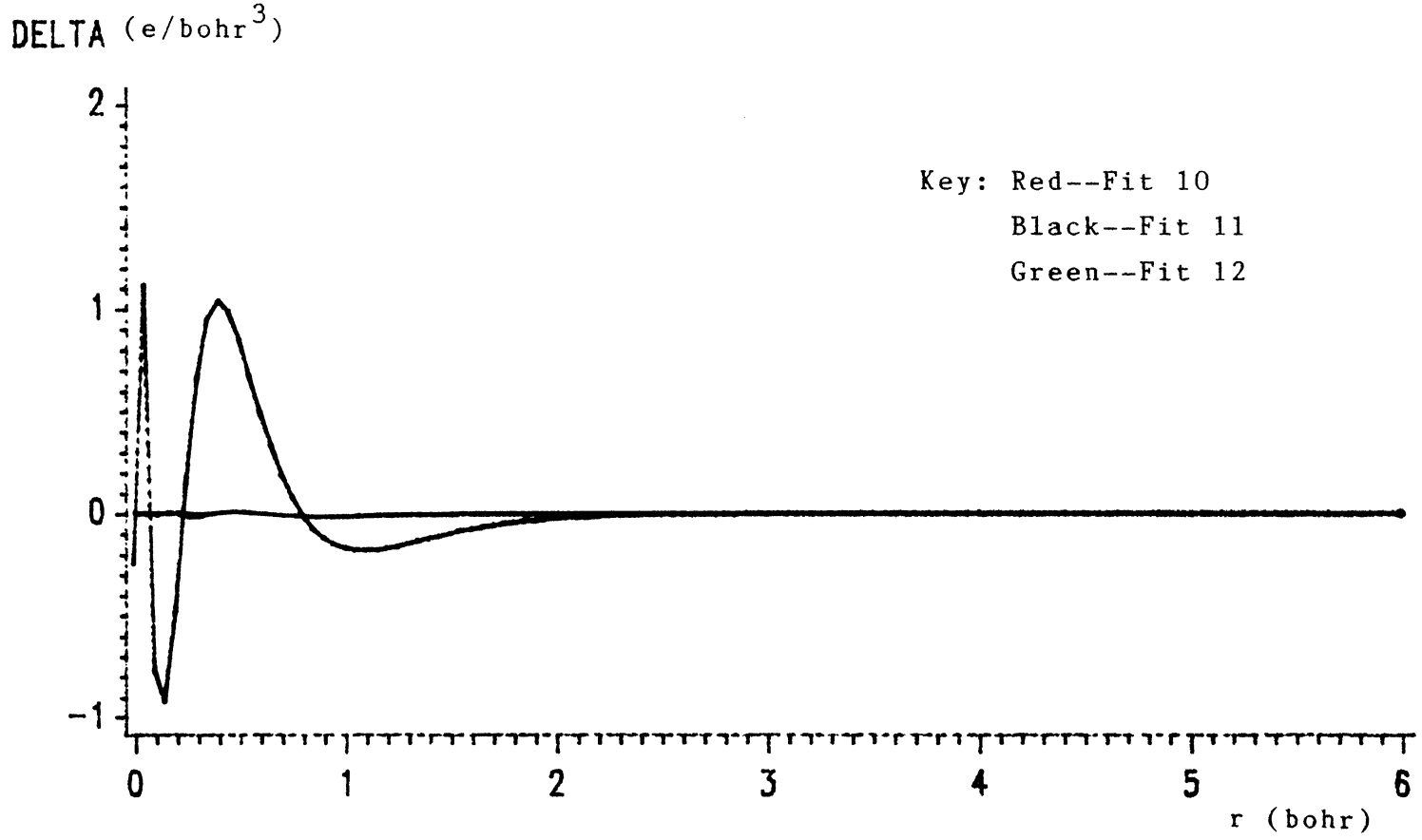

Figure 7. Plots of charge density difference ($\Delta\rho$) versus the radial distance (r) for Neon atom for three fits listed in Table IV.

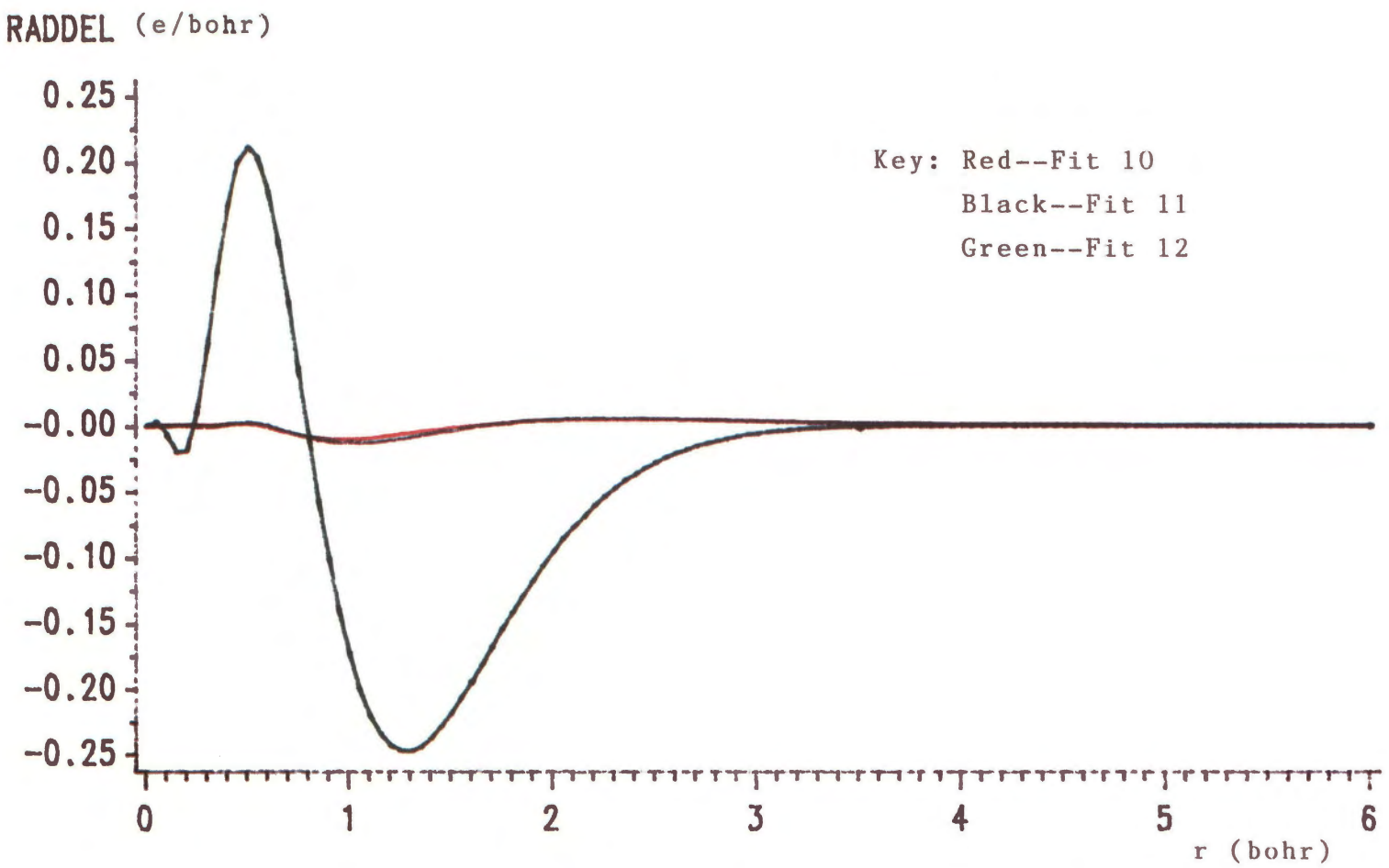

Figure 8. Plots of radial charge density difference ($r^2\Delta\rho$) versus the radial distance (r) for Neon atom for three fits listed in Table IV.

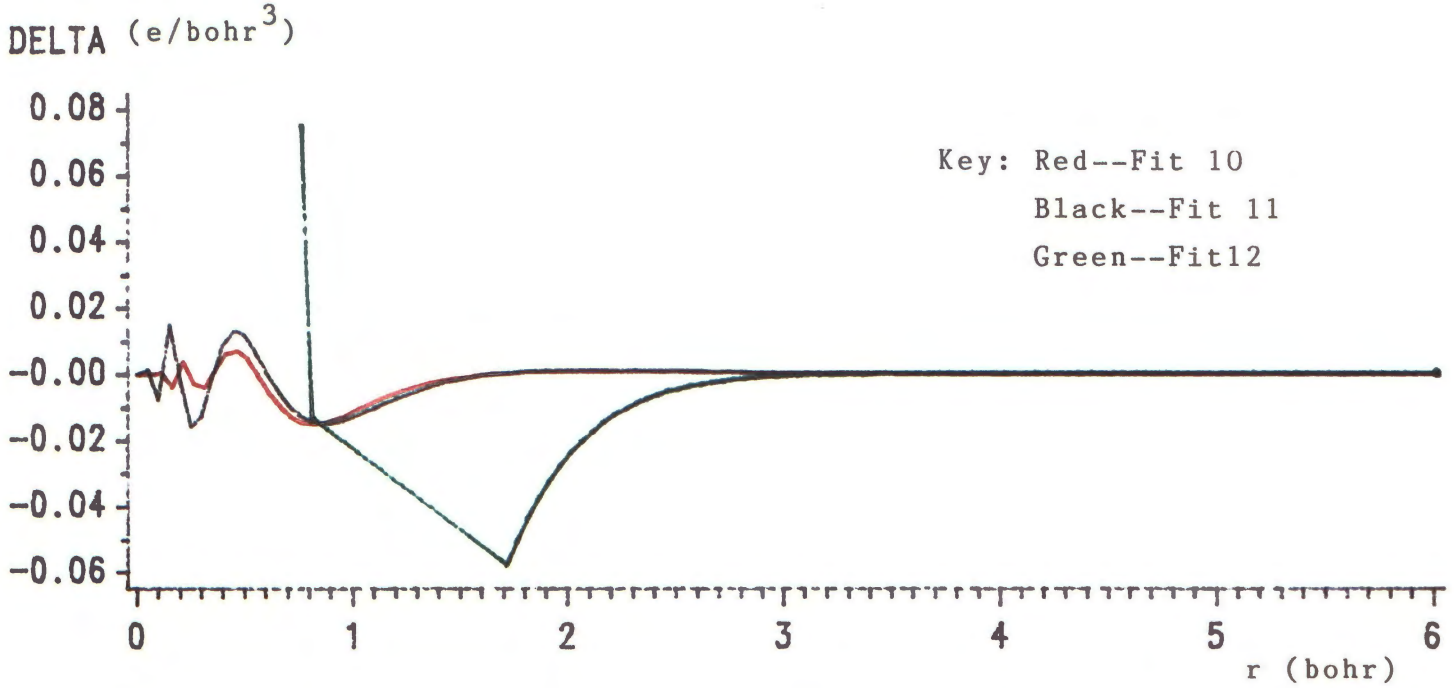

Figure 9. Plots of charge density difference ($\Delta\rho$) versus the radial distance (r) for Neon atom for three fits listed in Table IV. (magnified)

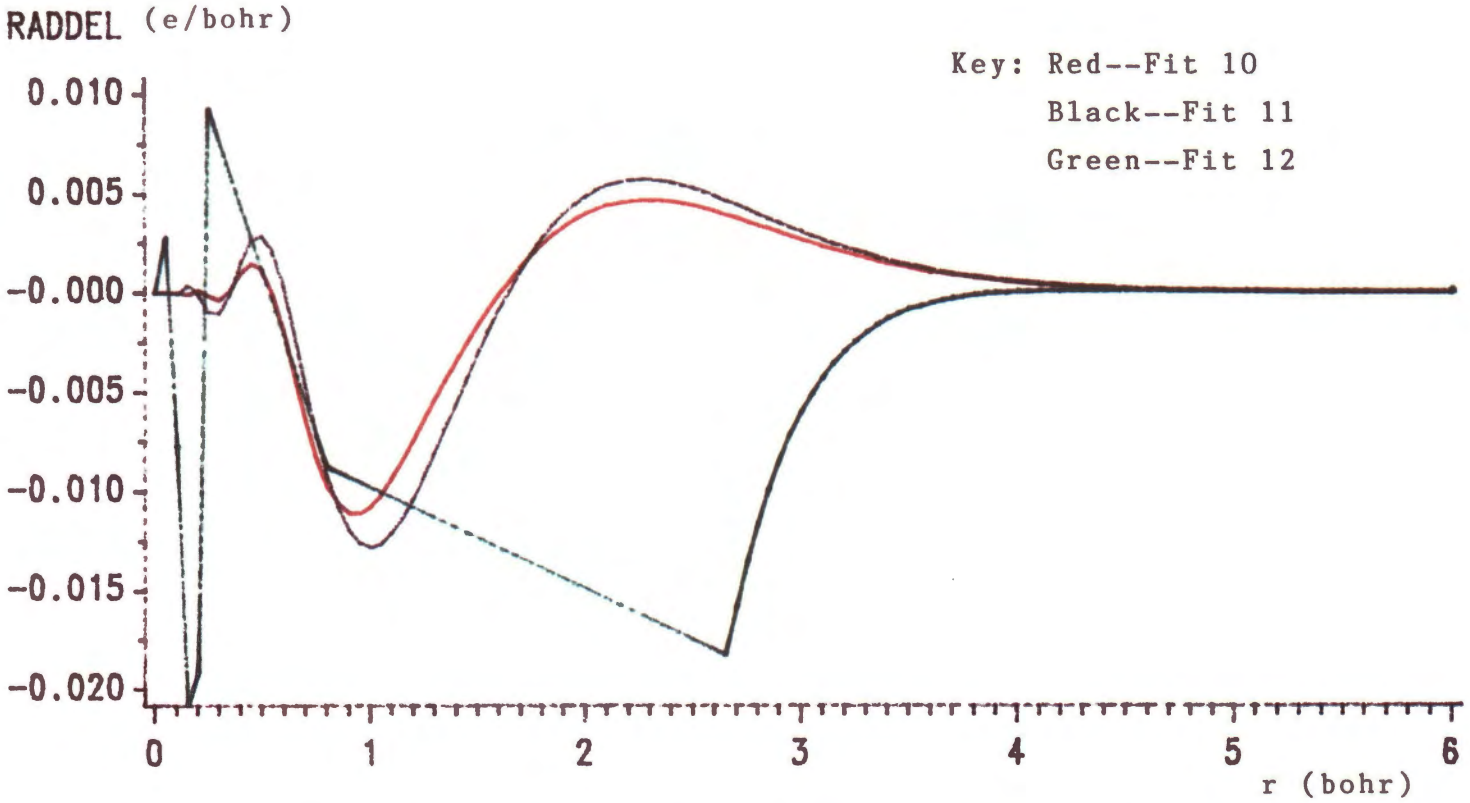

Figure 10. Plots of radial charge density difference ($r^2\Delta\rho$) versus the radial distance (r) for Neon atom for the three fits listed in Table IV. (Magnified)

results, something which cannot be required mathematically. Fits 2(=4=7=11), 3 and 10 all satisfy our intuitive notion that there are two K-shell and eight L-shell electrons in Neon. Of these three Fit 3 satisfies best our visual criterion and has the smallest $(\Delta\rho)_{RMS}$ and is selected as our best fit.

As a conclusion to this chapter let us mention again that fitting the charge densities for atom and molecules is not an easy task. There are still a lot of things that need to be done in order to understand better the structure of the multi-dimensional parameter space. With such understanding, hopefully one can determine even better algorithms in searching for the global minimum. On the other hand, we should also re-emphasize that since we are going to use the fits in the electrostatic energy calculation, picking the set of points to be fitted play a most important role. We must make sure that the number and the locations of the chose points in the molecular space are sufficient to represent the structure of the charge distribution. This assurance is rather difficult to pin down when one tries to fit the charge density of molecules. We did face what we believe to be this problem in trying to fit the charge density of the water molecule; it turns out that the dipole moments that we found for the fitted densities are always greater than the one obtained using the wave functions directly. Clearly, we need to explore the question of picking representative points further.

CHAPTER V

ELECTROSTATIC ENERGY CALCULATION FOR WATER DIMER

In this chapter we use our best fit to the charge density of the water molecule to find the electrostatic energy of interaction of a water dimer as a function of the configuration. To start with, we present the structure of a single water molecule used in the calculation. This geometry is shown in Fig 11 and remains fixed throughout the calculation. The wave function used to generate the charge density we are going to fit is given by Aung and Pitzer [32]. This wavefunction (designated III in reference 32) was calculated by the SCF method using atomic Slater-type orbital (STO) basis functions. Our interest is to find the electrostatic energy of interaction for a general orientation of two water molecules, but we present results only for the orientations where the dipole moments of each are either parallel or antiparallel. For each case we observe the change in the electrostatic energy as a function of the distance between the oxygen atoms R_{oo} for two choices (0^o and 90^o) of the dihedral angle ϕ, between the planes of the two molecules.

The number of points fitted is 576. The points are picked to lie on three spheres (radius r = 0.1, 0.5, 1.0 a.u.) centered at the oxygen nucleus, three spheres (r = 0.1, 0.25, 0.5 a.u.) around one hydrogen nucleus and two spheres (r = 0.25, 0.5 a.u.) centered approximately

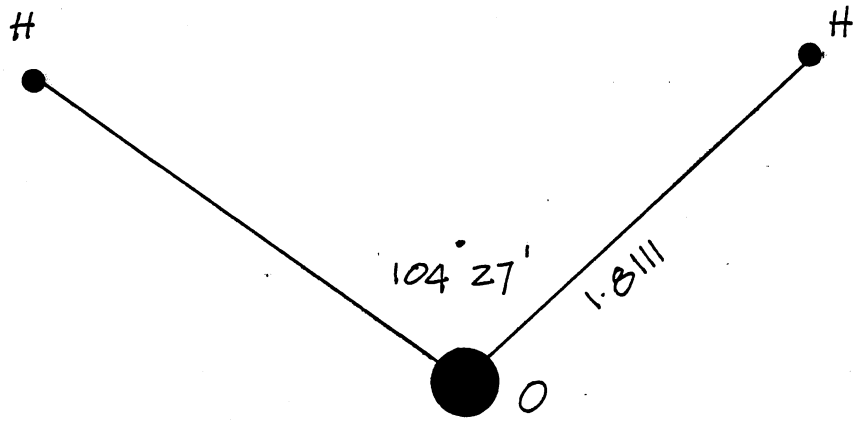

Figure 11. Geometry of a single water molecule.

half way along the OH bond. In addition we chose points along the OH bond line both between the two nuclei and with somewhat smaller density on the other side of each nucleus. Also points were chosen to cover trapezoidal figures lying in the molecular (xz) plane and the two perpendicular (xy and yz) planes. Finally a trapezoidal figure perpendicular to the molecular plane and containing the OH bond encloses another set of chosen points. Note that the selected points all favor just one region of the molecule. The correct symmetry of the fitted charge density is guaranteed by the constraints imposed in the fitting routine. A perspective plot of the points at which the density is tabulated is given in Figure 12. The number of Slater functions used to expand the charge density is eight: one at each of the hydrogen nuclei, four at the oxygen nucleus and one along each of the OH bonds. The functions centered at the nuclei remain fixed in place while the bond functions are allowed to slide back and forth along the bond direction seeking their optimum location. In Table V are the optimum Slater function parameters obtained for the fit. Note that the optimum positions of the bond functions are behind the oxygen nucleus ($z < 0$). The figures (13, 14, 15) present $\Delta\rho \equiv \rho_{fit} - \rho_o$, where both ρ's are the (negative valued) electron density in the xz, yz and xy planes respectively. Only half planes are presented, the remaining portion may be inferred from symmetry. It is clear from Fig. 13 that in the vicinity of the hydrogen nucleus ($x = 1.43$ a.u., $z = 1.11$ a.u.) there is more negative charge ($\Delta\rho < 0$) represented by ρ_{fit} than there should be according to ρ_o. This fact is also reflected in the expansion coefficient

TABLE V

RESULT OF FIT TO THE WATER MOLECULE CHARGE DENSITY
USING 8 SLATER FUNCTIONS

POSITION OF THE SLATER FUNCTIONS:

#	X-COORD	Y-COORD	Z-COORD
1	-1.4315	0.0000	1.1109
2	1.4315	0.0000	1.1109
3	0.0000	0.0000	0.0000
4	0.0000	0.0000	0.0000
5	0.0000	0.0000	0.0000
6	0.0000	0.0000	0.0000
7	-0.0933	0.0000	-0.0723
8	0.0933	0.0000	-0.0723

#	POWER(n_i)	CHARGE(q_i)	EXPONT(β_i)	RMS
1	0	-0.8152	1.95927	0.0821
2	0	-0.8152	1.95927	
3	0	-2.2222	14.9915	
4	1	0.0759	18.4195	
5	2	0.0612	18.8413	
6	2	0.0340	18.8239	
7	2	-3.1592	4.20211	
8	2	-3.1592	4.20211	

DIPOLE MOMENT IN X-DIRECTION = 0.000 A.U.
DIPOLE MOMENT IN Y-DIRECTION = 0.000 A.U.
DIPOLE MOMENT IN Z-DIRECTION = 0.867 A.U.

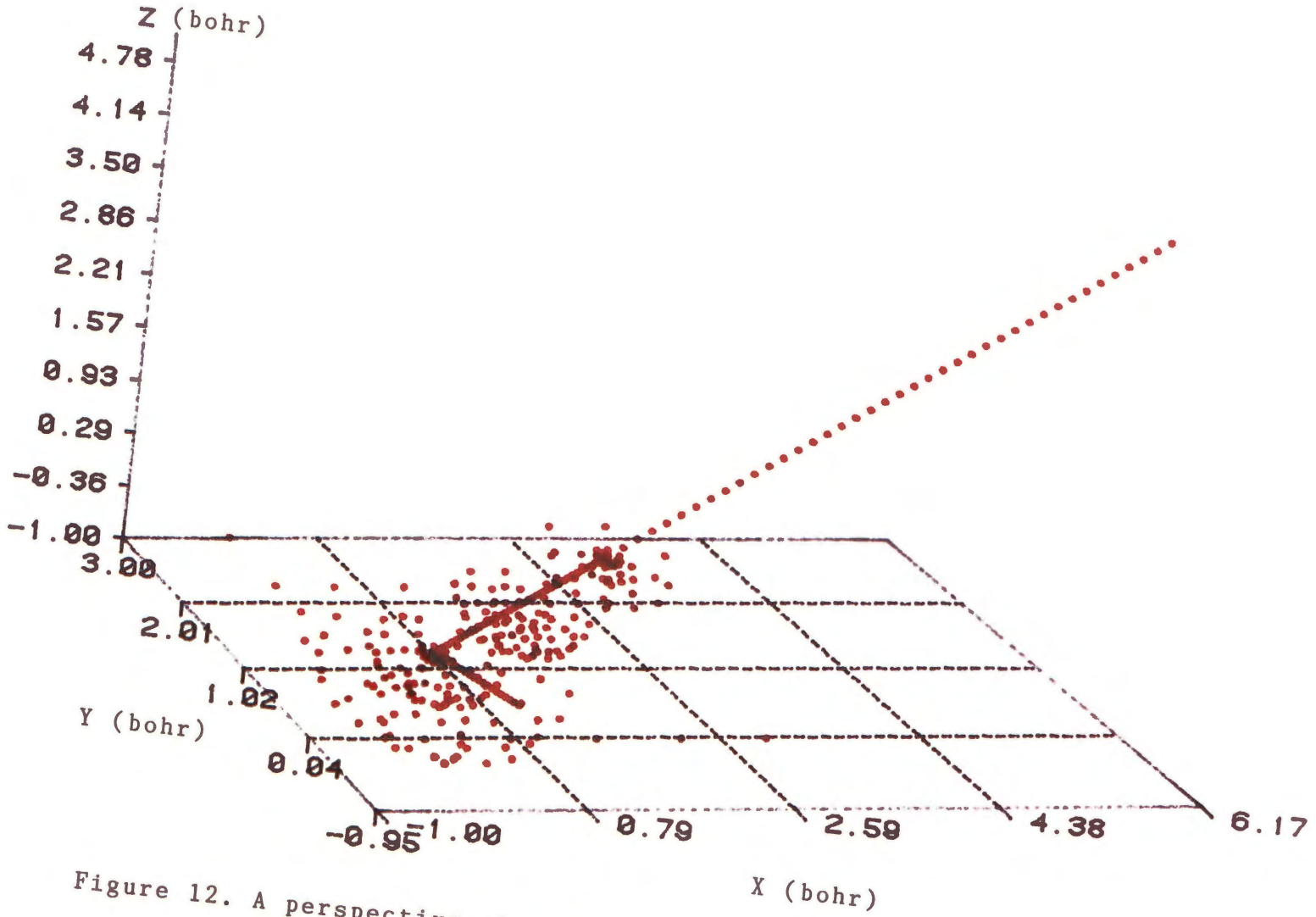

Figure 12. A perspective plot of points at which the charge density is tabulated.

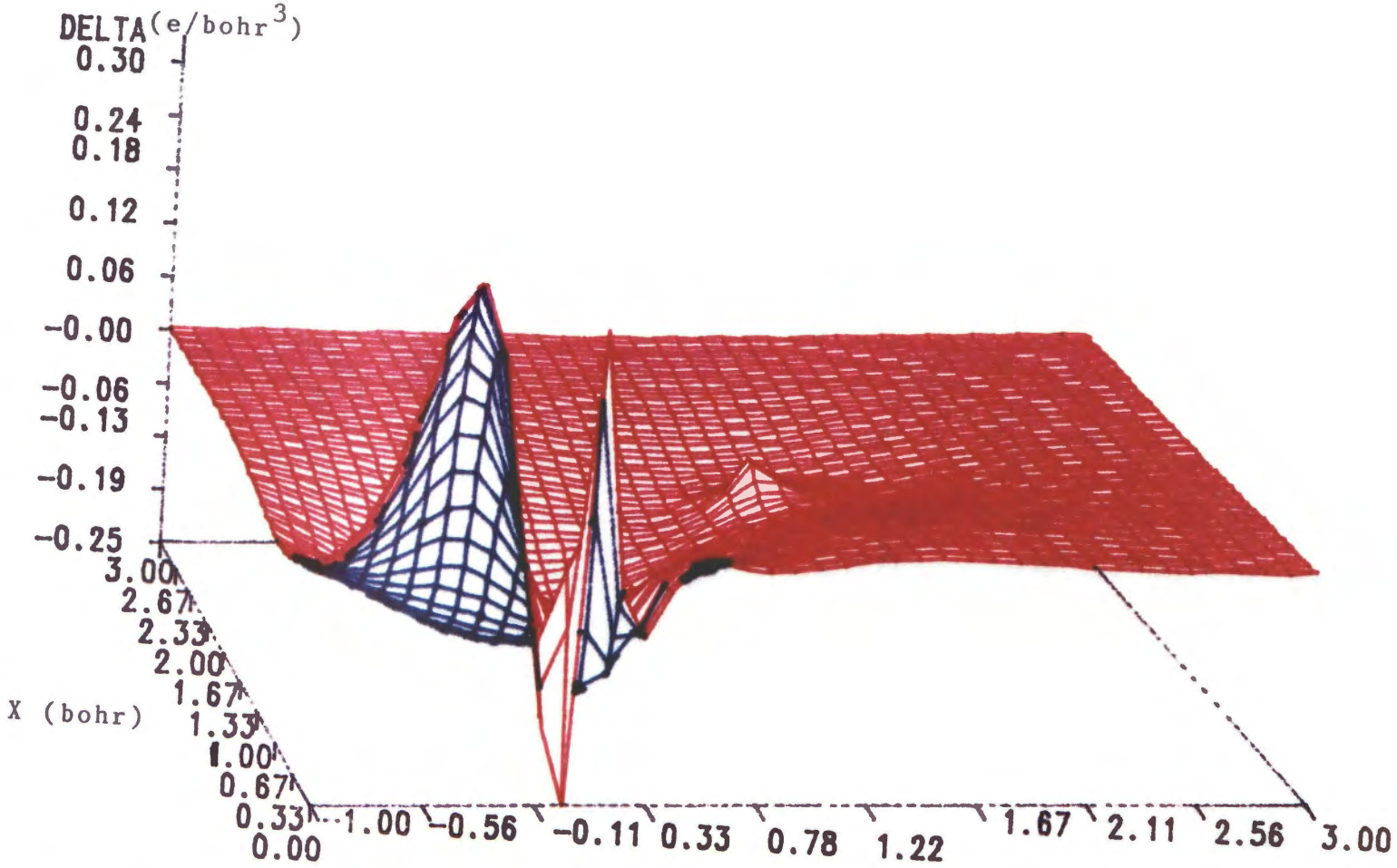

Figure 13. Plot of charge density difference ($\Delta\rho = \rho_{fit} - \rho_o$) at points in the x-z plane.

q_H = 0.8(-e) presented in Table V; generally population analysis place perhaps 0.5(-e) on the hydrogen nucleus. Furthermore there is a region where $\Delta\rho$ is strongly negative located along the extension of the OH bond behind the oxygen nucleus, that is in the region for which $z \simeq -0.11$ a.u. with 0.5 a.u. $< x <$ 2.0 a.u.. This excess negative charge is due to the position of the bond functions optimizing "behind" the oxygen nucleus. There is a smaller region near the z-axis where $\Delta\rho$ is positive indicating a depletion of electrons. The presence of the "bond functions" behind the oxygen we believe is an attempt to get into the lone pairs. Of course they are constrained to the xz plane and therefore cannot really simulate the lone pairs. In fact the presence of these excess negative charge behind the oxygen nucleus serves to increase the dipole moment of the water molecule. To be sure, the negative charge excess around the hydrogen would decrease the dipole moment and so the fact that we have an even larger moment than the wavefunction gives, indicates that the charge behind the oxygen in the xz plane is far excessive.

Looking in the yz plane (Fig. 14) we find the positive region of $\Delta\rho$ indicating that the lone pairs are not adequately represented by our expansion functions. In fact, we have not included any spherical Slater functions in the yz plane and have thus paid price for the absence.

In the xy plane (Fig 15) $\Delta\rho$ is always negative indicating more charge placed near the oxygen than is in the wavefunction description. Since the spherical Slater functions are centered at the atomic nucleus, this biased behavior of $\Delta\rho$ is not totally unexpected.

The dipole moment computed using the fit was 0.87 a.u.

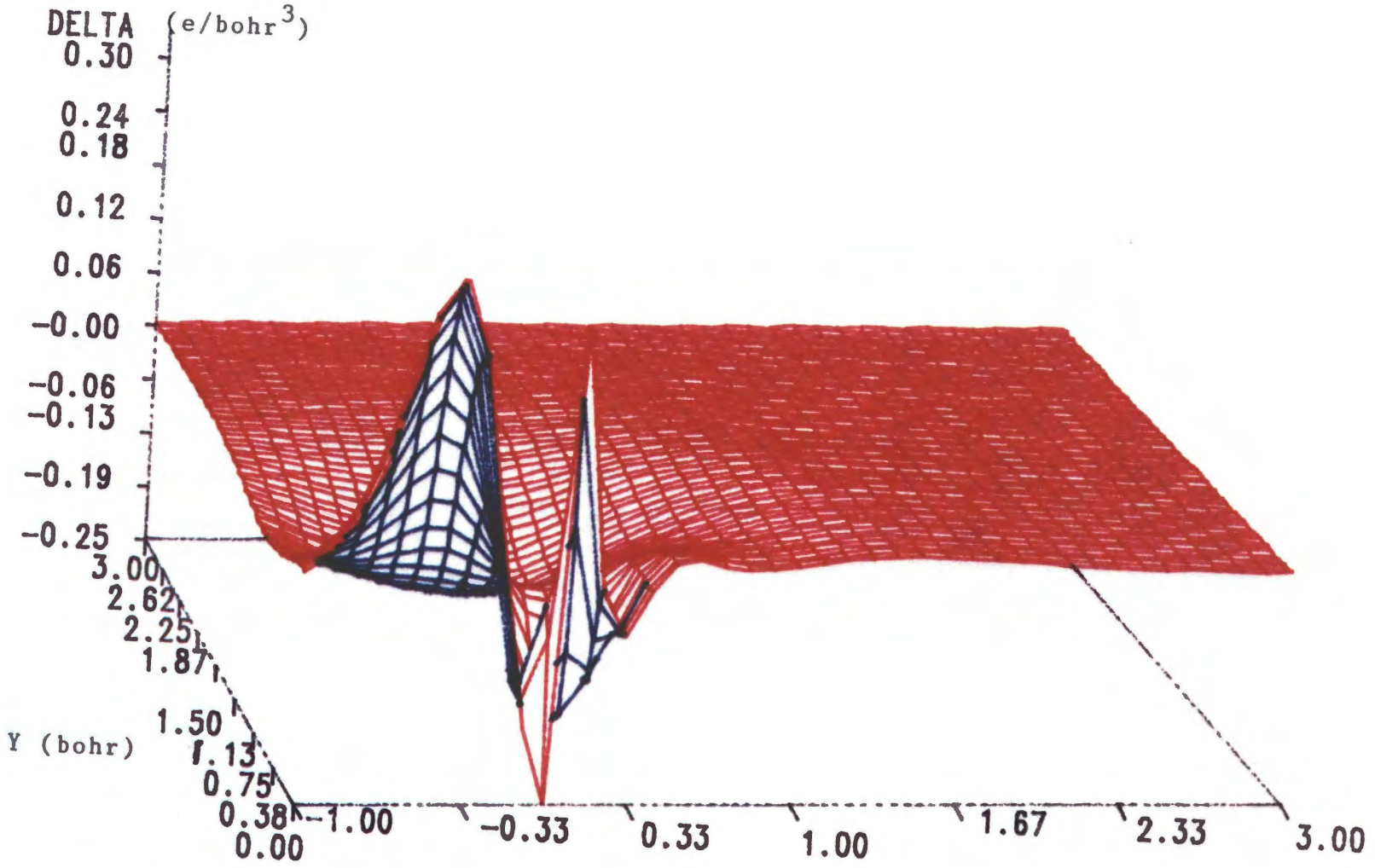

Figure 14. Plot of charge density difference ($\Delta\rho = \rho_{tot} - \rho_{\circ}$) at points in the y-z plane.

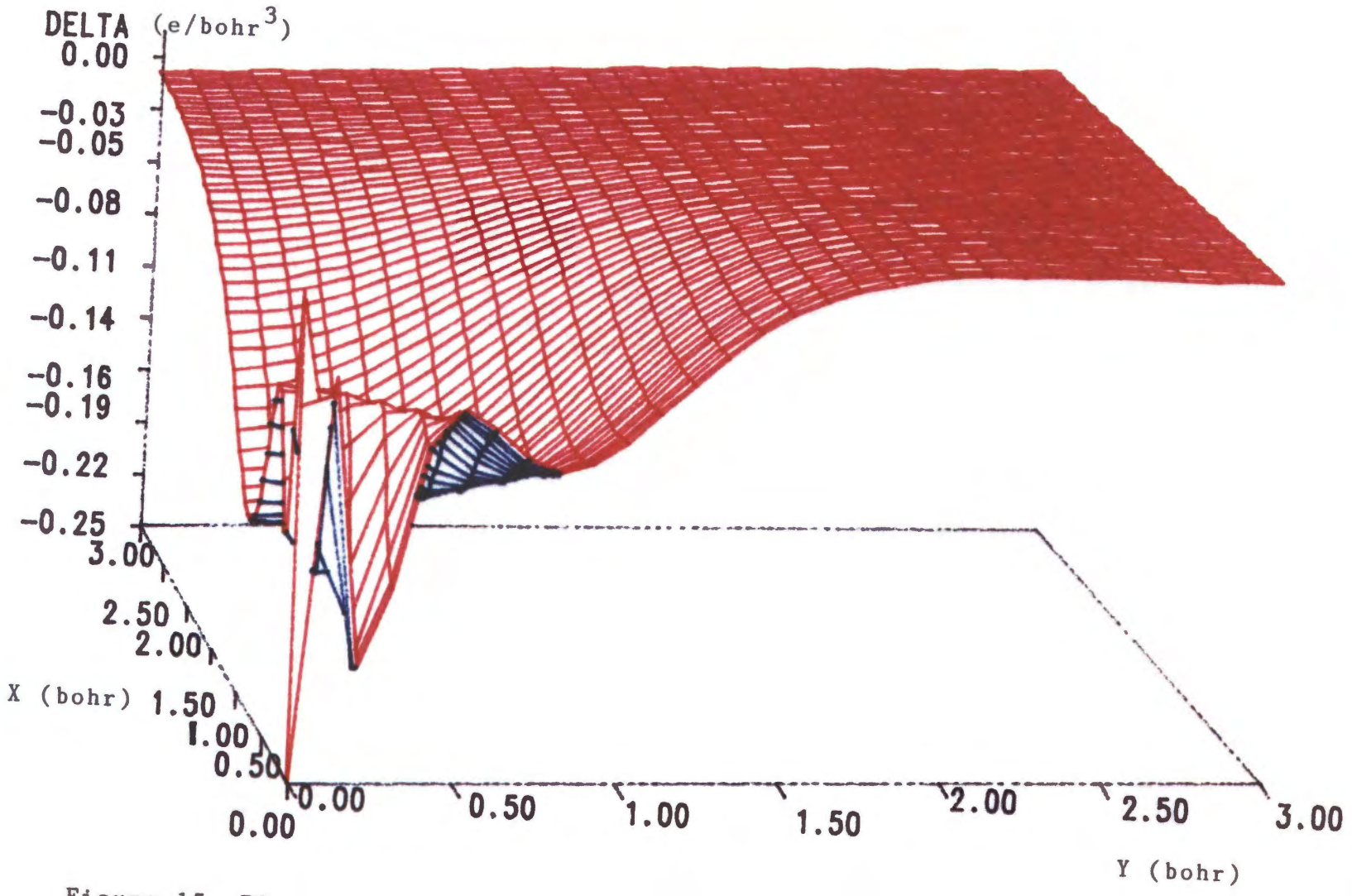

Figure 15. Plot of charge density difference ($\Delta\rho = \rho_{fit} - \rho_{o}$) at points in the x-y plane.

whereas the value that Aung and Pitzer obtained directly with their wave function was 0.75 a.u. The experimental dipole moment of H_2O is 0.71 a.u. The calculation of the dipole moment can be carried out easily when the charge density is expanded in terms of Slater-type functions. The electronic contribution to the dipole moment is

$$\vec{\mu}_{elect} = -Ne\langle\vec{r}\rangle = \int \vec{r}\,\rho(\vec{r})\,d^3r$$

$$= \int \vec{r}\left(\sum_{i=1}^{n} q_i \frac{\beta_i^{n_i+3}}{4\pi(n_i+2)!}\,|\vec{r}-\vec{R}_i|^{n_i} e^{-\beta_i|\vec{r}-\vec{R}_i|}\right) d^3r$$

$$= \sum_{i=1}^{n} \int (\vec{r}-\vec{R}_i)\,\frac{q_i\,\beta_i^{n_i+3}}{4\pi(n_i+2)!}\,|\vec{r}-\vec{R}_i|^{n_i} e^{-\beta_i|\vec{r}-\vec{R}_i|}\,d^3r$$

$$+ \sum_{i=1}^{n} \vec{R}_i \int q_i \frac{\beta_i^{n_i+3}}{4\pi(n_i+2)!}\,|\vec{r}-\vec{R}_i|^{n_i} e^{-\beta_i|\vec{r}-\vec{R}_i|}\,d^3r \qquad (5.1)$$

But for each term "i" the first integral vanishes since the integrand has odd parity with respect to inversion in the center $\vec{R}_i$. Therefore one is left with

$$\vec{\mu}_{elect} = \sum_{i=1}^{n} q_i \vec{R}_i \qquad (5.2)$$

The total dipole moment is, of course, the sum of the electronic and nuclear dipole moment

$$\vec{\mu}_{net} = \sum_{i=1}^{n} q_i \vec{R}_i + \sum_{\alpha=1}^{A} Z_\alpha e \vec{R}_\alpha \qquad (5.3)$$

The dipole moment of the molecule effects the leading (dipole-dipole) term in the asymptotic electrostatic interaction energy. The exact electrostatic energy of interaction for any molecular configuration

is given in Eqn (1.51). With the electronic charge densities expanded in terms of Slater functions we need to evaluate integrals such as

$$\int d^3r \int d^3r' \frac{|\vec{r}-\vec{R}_i|^{n_i} |\vec{r}'-R_j|^{n_j} e^{-\beta_i|\vec{r}-\vec{R}_i|} e^{-\beta_j|\vec{r}'-\vec{R}_j|}}{|\vec{r}-\vec{r}'|} \qquad (5.4)$$

and

$$\int d^3r \frac{|\vec{r}-\vec{R}_i|^{n_i} e^{-\beta_i|\vec{r}-\vec{R}_i|}}{|\vec{r}-\vec{R}_i|} \qquad (5.5)$$

These integrals can be evaluated in closed form and the result are given in Appendix A. A Fortran program has been written to compute the electrostatic energy of interactions based on the algebraic expressions.

The results of the calculation of the electrostatic energy of interaction are given in Tables VI and VII for various internuclear distances R_{oo} for the dipole moments parallel and antiparallel respectively. Each Table contains entries for both $\phi=0^o$ and $\phi=90^o$ cases For the dipole moments parallel we present in Fig. 16 the electrostatic interaction energy curves for $\phi=0^o$ (in Black) and $\phi=90^o$ (in Red) as a function of R_{oo}. Also on the same graph is plotted the dipole-dipole interaction energy (in Green), $E_{dd}= -2p^2/R_{oo}$, which of course, is independent of ϕ. In computing the dipole-dipole contribution to the energy we have used p=0.87 a.u., the dipole moment value obtained with the fit. It is apparent from Fig 16 that for $R_{oo} < 5.0$ a.u. the dipole-dipole contribution is only a fraction of the total electrostatic interaction energy. For $R_{oo} > 6.0$ a.u., however, this dipolar contribution is better than 93% of the total electrostatic interaction

TABLE VI

RESULTS FOR THE CALCULATION OF THE ELECTROSTATIC INTERACTION ENERGY FOR WATER-DIMER (PARALLEL DIPOLE MOMENTS)

PHI (RADIAN)	ROO (BOHR)	ENERGY (HARTREE)
0.00000D+00	0.40000D+01	-0.63123D-01
0.00000D+00	0.42000D+01	-0.47814D-01
0.00000D+00	0.44000D+01	-0.36631D-01
0.00000D+00	0.46000D+01	-0.28438D-01
0.00000D+00	0.48000D+01	-0.22405D-01
0.00000D+00	0.50000D+01	-0.17935D-01
0.00000D+00	0.52000D+01	-0.14596D-01
0.00000D+00	0.54000D+01	-0.12077D-01
0.00000D+00	0.56000D+01	-0.10154D-01
0.00000D+00	0.58000D+01	-0.86667D-02
0.00000D+00	0.60000D+01	-0.75002D-02
0.00000D+00	0.62000D+01	-0.65710D-02
0.00000D+00	0.64000D+01	-0.58193D-02
0.00000D+00	0.66000D+01	-0.52016D-02
0.00000D+00	0.68000D+01	-0.46864D-02
0.00000D+00	0.70000D+01	-0.42506D-02
0.00000D+00	0.72000D+01	-0.38771D-02
0.00000D+00	0.74000D+01	-0.35535D-02
0.00000D+00	0.76000D+01	-0.32700D-02
0.00000D+00	0.78000D+01	-0.30197D-02
0.00000D+00	0.80000D+01	-0.27969D-02
0.00000D+00	0.82000D+01	-0.25973D-02
0.00000D+00	0.84000D+01	-0.24175D-02
0.00000D+00	0.86000D+01	-0.22549D-02
0.00000D+00	0.88000D+01	-0.21071D-02
0.00000D+00	0.90000D+01	-0.19723D-02
0.00000D+00	0.92000D+01	-0.18490D-02
0.00000D+00	0.94000D+01	-0.17360D-02
0.00000D+00	0.96000D+01	-0.16321D-02
0.00000D+00	0.98000D+01	-0.15364D-02
0.00000D+00	0.10000D+02	-0.14481D-02
0.00000D+00	0.10200D+02	-0.13664D-02
0.00000D+00	0.10400D+02	-0.12907D-02
0.00000D+00	0.10600D+02	-0.12206D-02
0.00000D+00	0.10800D+02	-0.11554D-02
0.00000D+00	0.11000D+02	-0.10948D-02

TABLE VI (CONTINUE)

PHI (RADIAN)	ROO (BOHR)	ENERGY (HARTREE)
0.15708D+01	0.40000D+01	-0.62619D-01
0.15708D+01	0.42000D+01	-0.47505D-01
0.15708D+01	0.44000D+01	-0.36456D-01
0.15708D+01	0.46000D+01	-0.28350D-01
0.15708D+01	0.48000D+01	-0.22374D-01
0.15708D+01	0.50000D+01	-0.17939D-01
0.15708D+01	0.52000D+01	-0.14621D-01
0.15708D+01	0.54000D+01	-0.12114D-01
0.15708D+01	0.56000D+01	-0.10197D-01
0.15708D+01	0.58000D+01	-0.87113D-02
0.15708D+01	0.60000D+01	-0.75441D-02
0.15708D+01	0.62000D+01	-0.66129D-02
0.15708D+01	0.64000D+01	-0.58584D-02
0.15708D+01	0.66000D+01	-0.52376D-02
0.15708D+01	0.68000D+01	-0.47193D-02
0.15708D+01	0.70000D+01	-0.42804D-02
0.15708D+01	0.72000D+01	-0.39040D-02
0.15708D+01	0.74000D+01	-0.35776D-02
0.15708D+01	0.76000D+01	-0.32918D-02
0.15708D+01	0.78000D+01	-0.30392D-02
0.15708D+01	0.80000D+01	-0.28144D-02
0.15708D+01	0.82000D+01	-0.26131D-02
0.15708D+01	0.84000D+01	-0.24317D-02
0.15708D+01	0.86000D+01	-0.22676D-02
0.15708D+01	0.88000D+01	-0.21186D-02
0.15708D+01	0.90000D+01	-0.19827D-02
0.15708D+01	0.92000D+01	-0.18584D-02
0.15708D+01	0.94000D+01	-0.17445D-02
0.15708D+01	0.96000D+01	-0.16398D-02
0.15708D+01	0.98000D+01	-0.15434D-02
0.15708D+01	0.10000D+02	-0.14545D-02
0.15708D+01	0.10200D+02	-0.13722D-02
0.15708D+01	0.10400D+02	-0.12961D-02
0.15708D+01	0.10600D+02	-0.12254D-02
0.15708D+01	0.10800D+02	-0.11598D-02
0.15708D+01	0.11000D+02	-0.10988D-02

TABLE VII

RESULTS FOR THE CALCULATION OF THE ELECTROSTATIC INTERACTION ENERGY FOR WATER-DIMER (ANTIPARALLEL DIPOLE MOMENTS)

PHI (RADIAN)	ROO (BOHR)	ENERGY (HARTREE)
0.00000D+00	0.40000D+01	-0.30302D-01
0.00000D+00	0.42000D+01	-0.28599D-01
0.00000D+00	0.44000D+01	-0.23932D-01
0.00000D+00	0.46000D+01	-0.18540D-01
0.00000D+00	0.48000D+01	-0.13465D-01
0.00000D+00	0.50000D+01	-0.91235D-02
0.00000D+00	0.52000D+01	-0.56178D-02
0.00000D+00	0.54000D+01	-0.29012D-02
0.00000D+00	0.56000D+01	-0.86598D-03
0.00000D+00	0.58000D+01	0.61089D-03
0.00000D+00	0.60000D+01	0.16465D-02
0.00000D+00	0.62000D+01	0.23426D-02
0.00000D+00	0.64000D+01	0.27834D-02
0.00000D+00	0.66000D+01	0.30361D-02
0.00000D+00	0.68000D+01	0.31531D-02
0.00000D+00	0.70000D+01	0.31742D-02
0.00000D+00	0.72000D+01	0.31296D-02
0.00000D+00	0.74000D+01	0.30414D-02
0.00000D+00	0.76000D+01	0.29257D-02
0.00000D+00	0.78000D+01	0.27942D-02
0.00000D+00	0.80000D+01	0.26549D-02
0.00000D+00	0.82000D+01	0.25137D-02
0.00000D+00	0.84000D+01	0.23742D-02
0.00000D+00	0.86000D+01	0.22390D-02
0.00000D+00	0.88000D+01	0.21096D-02
0.00000D+00	0.90000D+01	0.19869D-02
0.00000D+00	0.92000D+01	0.18712D-02
0.00000D+00	0.94000D+01	0.17627D-02
0.00000D+00	0.96000D+01	0.16612D-02
0.00000D+00	0.98000D+01	0.15664D-02
0.00000D+00	0.10000D+02	0.14780D-02
0.00000D+00	0.10200D+02	0.13957D-02
0.00000D+00	0.10400D+02	0.13191D-02
0.00000D+00	0.10600D+02	0.12477D-02
0.00000D+00	0.10800D+02	0.11812D-02
0.00000D+00	0.11000D+02	0.11191D-02

TABLE VII (CONTINUE)

PHI (RADIAN)	ROO (BOHR)	ENERGY (HARTREE)
0.15708D+01	0.40000D+01	-0.56528D-01
0.15708D+01	0.42000D+01	-0.40735D-01
0.15708D+01	0.44000D+01	-0.28880D-01
0.15708D+01	0.46000D+01	-0.20002D-01
0.15708D+01	0.48000D+01	-0.13380D-01
0.15708D+01	0.50000D+01	-0.84711D-02
0.15708D+01	0.52000D+01	-0.48622D-02
0.15708D+01	0.54000D+01	-0.22387D-02
0.15708D+01	0.56000D+01	-0.35944D-03
0.15708D+01	0.58000D+01	0.96041D-03
0.15708D+01	0.60000D+01	0.18626D-02
0.15708D+01	0.62000D+01	0.24555D-02
0.15708D+01	0.64000D+01	0.28215D-02
0.15708D+01	0.66000D+01	0.30232D-02
0.15708D+01	0.68000D+01	0.31074D-02
0.15708D+01	0.70000D+01	0.31094D-02
0.15708D+01	0.72000D+01	0.30550D-02
0.15708D+01	0.74000D+01	0.29636D-02
0.15708D+01	0.76000D+01	0.28488D-02
0.15708D+01	0.78000D+01	0.27208D-02
0.15708D+01	0.80000D+01	0.25864D-02
0.15708D+01	0.82000D+01	0.24508D-02
0.15708D+01	0.84000D+01	0.23171D-02
0.15708D+01	0.86000D+01	0.21875D-02
0.15708D+01	0.88000D+01	0.20635D-02
0.15708D+01	0.90000D+01	0.19457D-02
0.15708D+01	0.92000D+01	0.18345D-02
0.15708D+01	0.94000D+01	0.17300D-02
0.15708D+01	0.96000D+01	0.16320D-02
0.15708D+01	0.98000D+01	0.15405D-02
0.15708D+01	0.10000D+02	0.14550D-02
0.15708D+01	0.10200D+02	0.13751D-02
0.15708D+01	0.10400D+02	0.13007D-02
0.15708D+01	0.10600D+02	0.12312D-02
0.15708D+01	0.10800D+02	0.11664D-02
0.15708D+01	0.11000D+02	0.11059D-02

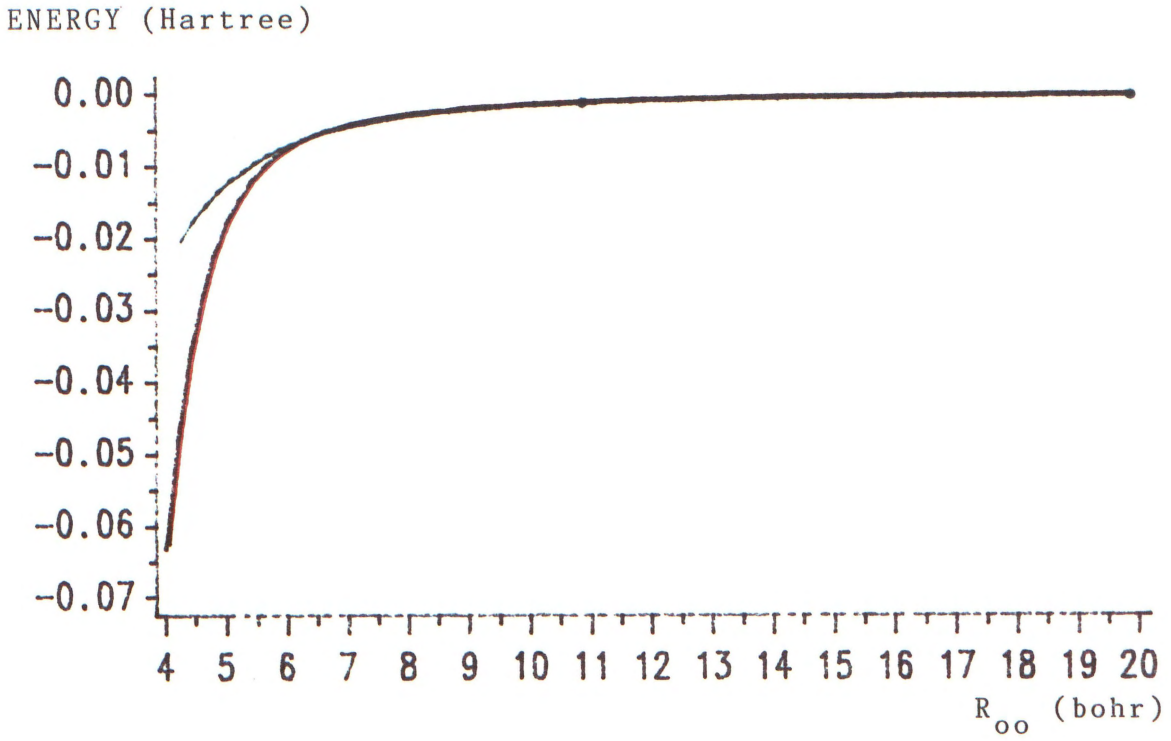

Figure 16. Total electrostatic interaction energy as a function of R_{oo} for ϕ=0° (Black), ϕ=90° (Red) and the dipole-dipole interaction energy for parallel dipole moments(Green).

energy. Moreover, the $\phi=0^{o}$and $\phi=90^{o}$ curves are essentially indistinguishable for this parallel dipole case. However, an important point to be made here is that such a conclusions cannot be extended to other orientations of molecules.

Consider the case of the dipoles being antiparallel, the corresponding three [$\phi=0^{o}$ (in Black) $\phi=90^{o}$ (in Red), dipolar (in Green)] graphs for which are presented in Fig. 17. Here, the total electrostatic energy for R_{oo} < 7.5 a.u. is significantly different from the dipole-dipole contribution alone. To be sure, for R_{oo} < 6.0 a.u. the dipolar and total electrostatic energies have opposite signs and are orders of magnitude different. The total electrostatic energy (for both the $\phi=0^{o}$ and $\phi=90^{o}$ orientations) for this antiparallel case rise through zero to reach a maximum at about 7.0 a.u.. The dipolar energy is still a factor of four times the total electrostatic energy at R_{oo}= 6.0 a.u..For this antiparallel case the two become comparable (within 10%) only for R_{oo} > 8.0 a.u.. Clearly the convergence of the multipole expansion of the interaction energy does depend on whether the dipoles are parallel or antiparallel. More generally we conclude that such multipole expansions are sensitive to the geometry of the interacting molecules, and thus must be used with caution in computing the electrostatic energy of interaction. Jeziorski and Van Hammet [33] have reported for yet another geometrical orientation of the water dimer that the dipolar energy contibution is only about 80% that of the total electrostatic interaction energy as distant as R_{oo}= 9.0 a.u..

Another clear orientation dependence is seen in comparing the

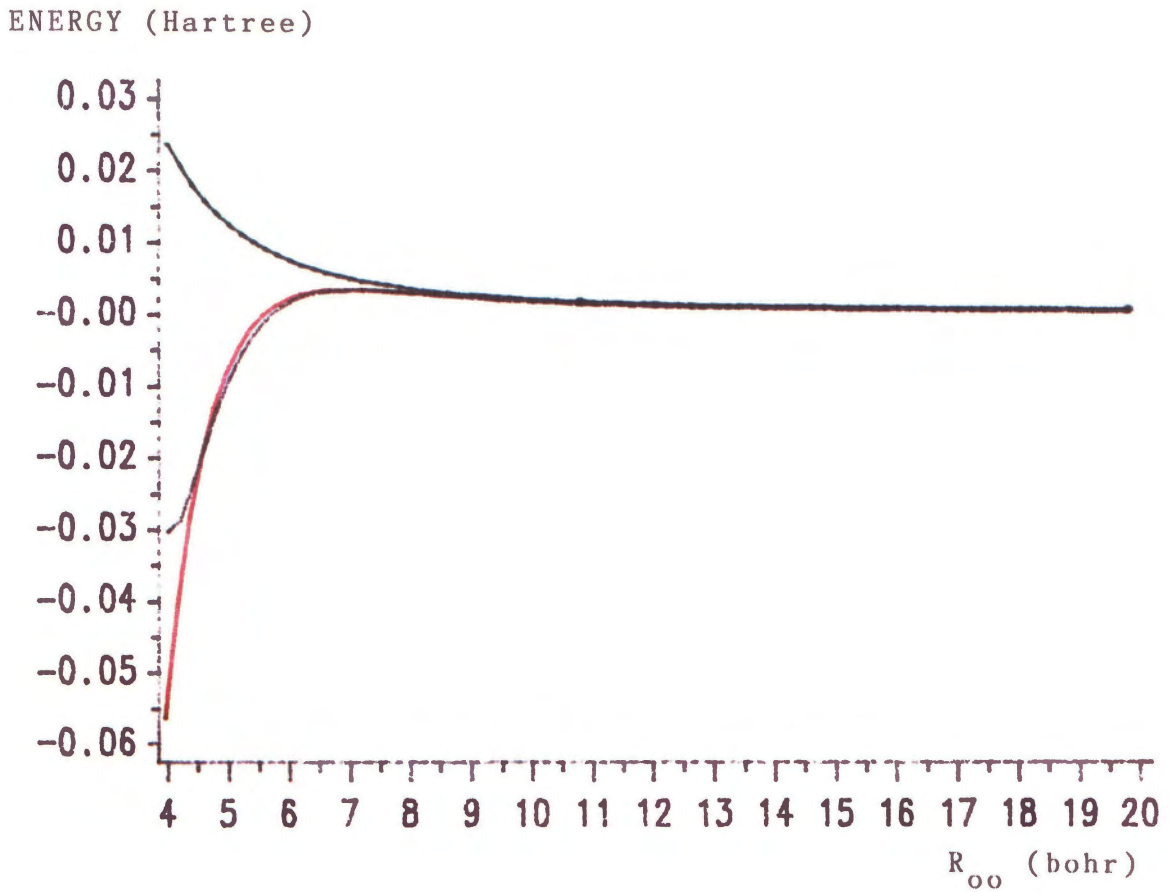

Figure 17. Total electroststic interaction energy as a function of R_{oo} for ϕ=0°(Black) ϕ=90° (Red) and the dipole-dipole interaction energy for antiparallal dipole moments (Green).

$\phi=0^{o}$ and $\phi=90^{o}$ curves for the parallel and antiparallel dipole cases. As mentioned before for the parallel dipole case the total interaction energy is essentially the same for these two ϕ's (viz the Red and the Black of Fig. 16). In fact, one finds that this apparent ϕ independence holds for R_{oo} as small as 2.0 a.u. Although no physical significance can be drawn from the electrostatic curves for R_{oo} values corresponding to the molecules overlapping, we have nevertheless presented the electrostatic energy curves down to R_{oo}= 1.0 a.u. in Figures 18 and 19 for the parallel and antiparallel dipole cases respectively. (As before, the $\phi=0^{o}$, 90^{o} and dipolar curves are presented in Black , Red and Green.) On the other hand for the antiparallel dipole situation the $\phi=0^{o}$ and $\phi=90^{o}$ curves begin to diverge below 4.0 a.u.. Investigating the curves in Fig. 19 for smaller values of R_{oo}, we find that they are in fact qualitatively different below R_{oo}= 4.0 a.u.. This is due, of course to the impending Coulombic singularity in the $\phi=0^{o}$ curve at R_{oo}= 2.2 a.u. as one pair of hydrogen nuclei approach the other. Clearly, this singularity is avoided in the $\phi=90^{o}$ (antiparallel) case. Once again the necessity for computing the total electrostatic interaction energy and avoiding the multipole moment expansion is apparent.

For 4.0 a.u. $< R_{oo} <$ 6.0 a.u. the electrostatic interaction energy is a significant portion of the potential energy of interaction. Still, the induction and quantum corrections (given by the kinetic and exchange-correlation energy functionals in the density functional formalism) are of the same order of magnitude in this range of R_{oo}.

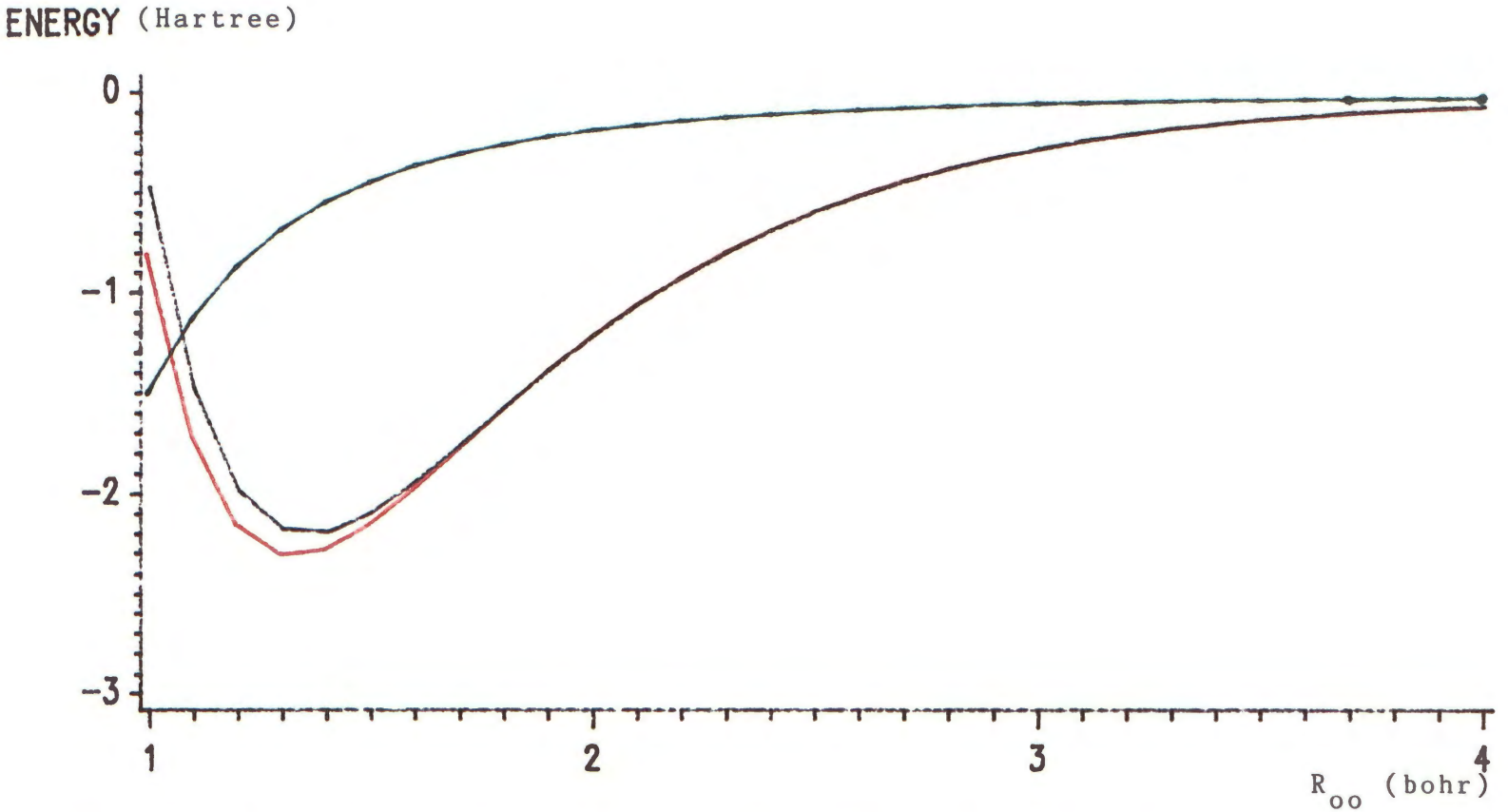

Figure 18. Total electrostatic interaction energy as a function of R_{oo} ($1<R_{oo}<4$) for ϕ=0° (Black), ϕ=90° (Red) and the dipole-dipole interaction energy for parallal dipole moments (Green).

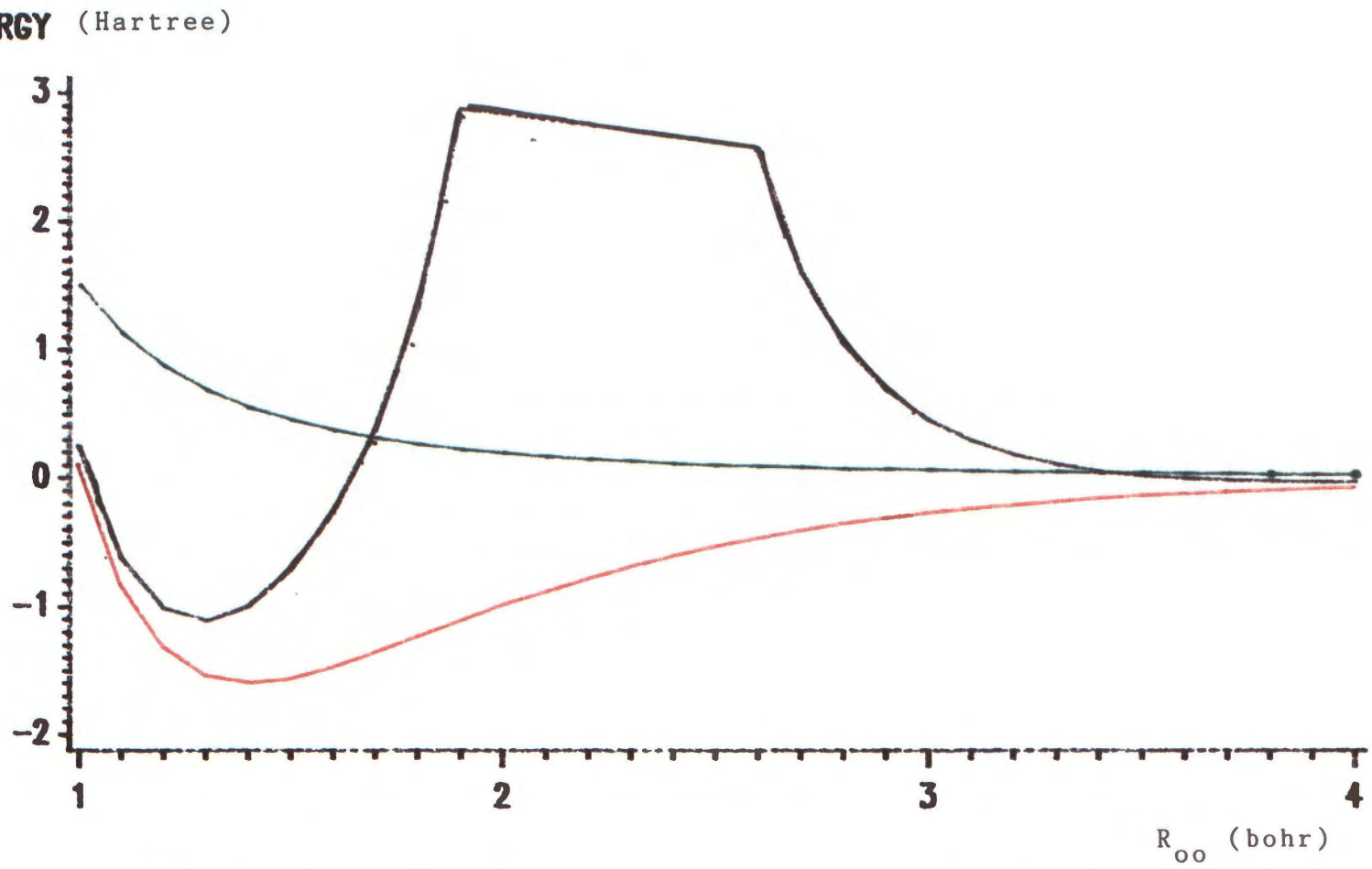

Figure 19. Total electrostatic interaction energy as a function of R_{oo} ($1<R_{oo}<4$) for $\phi=0°$ (Black), $\phi=90°$ (Red) and the dipole-dipole interaction energy for antiparallal dipole moments (Green).

For $R_{oo} > 6.0$ a.u. in the case of the strongly polar molecule (e.g. water), the electrostatic energy in fact is most prominent, although dispersion energy cannot be neglected until $R_{oo} > 10.0$ a.u. For $R_{oo} < 4.0$ a.u. the quantum corrections can surely not be ignored. Here, the kinetic and exchange-correlation functionals must be considered in the density functional formalism; the highly-repulsive part of the potential energy characterizing the short-range interaction must be associated with the kinetic and exchange energy contributions of these functionals, just as the long range dispersion energy ought to be obtained from the correlation energy functional. Of course, in the original Gordon -KIm model calculations, although the short-range repulsions between non-polar species was adequately described, the long-range dispersion energy could not be extracted from the model. This, of course, suggest only that the functionals employed in these calculations were not sufficiently accurate in treating the long-range forces, and does not discredit the density functional formalism itself.

In this thesis we have focused our attention on representing charge densities by an expansion in terms of Slater functions. These electrostatic energy calculations are easily done once these expansions are made. But the expansions are also the necessary input to our density functional programs which evaluate the quantum corrections. In a future time hopefully these calculations will be able to be done routinely and the potential energy surfaces mapped out.

REFERENCES

1. Hohenberg, P. and W. Kohn,. Phys. Rev. B., Vol. 136, 1964, p. 864.

2. Hirschfelder, J.O., C.F. Curtiss and R.B. Bird, Molecular Theory of Gases and Liquids., J. Wiley & Sons, New York: 1964.

3. Davidson, E.R. Reduced Density Matrices in Quantum Chemistry, Academic Press, New York: 1976

4. Merzbacher, W. Quantum Mechanics. New York: John Wiley & Sons, 1970.

5. Gilbert, T. L.. Phys. Rev. B., Vol. 12, 1975, p. 211.

6. Bamzai, A. S. and B.M. Deb . Rev. of Mod. Phys., Vol. 53, 1981, p. 95.

7. Levy, M.. Proc. Natl. Acad. Sci. (USA), Vol. 76, 1979, p. 6062; Phys. Rev. A., Vol. 29, 1982, p. 1200

8. Kim, Y.S. and R.G. Gordon J. Chem. Phys., Vol. 61, 1974, p. 1; Vol. 56, 1972, p. 3122.

9. Fetter, A.L. and Walecka Quantum Theory of Many-Particle Systems, Mcgraw Hill, San Francisco: 1971.

10. Parker, G. S., R.L. Snow, and R.T. Pack. J. Chem. Phys., Vol. 64, 1978, p. 1668.

11. Pearson, E. W. and Gordon R. G.. J. Chem. Phys., Vol. 82, 1985, p. 881.

12. Rae, A. I. M. Chem. Phys. Lett., Vol. 18, 1973, p. 574; Mol. Phys., Vol. 29, 1975, p. 467

13. Waldman, M. and Gordon, R. G. J. Chem. Phys., Vol. 71, 1975, p. 1325.

14. Parr. R. G. " Density Functional Theory." Annual Review of Physical Chemistry, Vol. 34, 1983, p. 631.

15. Thomas, L.H., Proc. Cambridge Philos Soc., Vol. 23, 1927, p. 542; Fermi, E. Z. Phys., Vol. 48, 1928

16. Von Weizacker, C. F.. Z. Physik, Vol. 96, 1935, p. 431.

17. Hodges, C. H. Can. J. Phys., Vol. 51, 1973, p. 1428

18. Dirac, P.A.M. Proc. Cambridge Philos Soc., Vol. 26 1930, p.376.

19. Slater, J.C. Quantum Theory of Molecules and Solids. Vol. 4. New York: Mcgraw-Hill, 1974.

20. Tomasi, J. " Electrostatic Molecular Potential and its Application to the Study of Molecular Aggregations." Molecular Interactions. Vol. 3. p. 119, New York: John Wiley and Sons, Inc., 1982.

21. Politzer, P. and Truhlar D. G. eds. Chemical Applications of Atomic and Molecular Electrostatic Potentials. New York: Plenum Press, 1981.

22. Richards, W.G. and Horsley Ab Initio Molecular Orbital Calculations for Chemists. Clarendon Press, Oxford: 1970.

23. Rys, J., King, H. F. and Coppens, P. Chem. Phys. Lett., Vol. 41, 1976, p. 617.

24. Yanez, M., Stewart, R. F. and Pople, J. A. Acta. Crystall. A., Vol. 34, 1978, p. 641.

25. Smith, C. M. and Hall, G. G. Theor. Chim. Acta., Vol. 69, 1986, p. 63.

26. Momany, F. A. J. Chem. Phys., Vol. 82, 1978, p. 592.

27. Cox, S. R. and Williams, D. E. J. Comp. Chem., Vol. 2, 1981, p. 304.

28. Ray, N. K., Shibata, M., Bolis, G. and Rein, R. Int. J. Quant. Chem., Vol. 27, 1985, p. 427.

29. Brobjer, J. T. and Murrell, J. N. J. Chem. Faraday Trans. 2., Vol. 78, 1982, p. 1853.

30. Bard, Y. Nonlinear Parameter Estimation. New York: Academic Press, 1974.; Marquardt, D. W. SIAM J., Vol. 11, 1963, p. 431.

31. Clementi, E. Tables of Atomic Functions. IBM, 1965.

32. Aung, S., Pitzer, M. and Chan, S. I. J. Chem. Phys., Vol. 49, 1968, p. 2071.

33. Jeziorski, B. and M.V. Hemert Mol. Phys., Vol. 31 1976, p. 713.

APPENDIX A

COULOMB INTEGRALS

The classical coulomb energy of interaction is given in terms of the six dimensional integral

$$\int d^3r_1 d^3r_2 \frac{\rho_A(\vec{r}_1)\,\rho_B(\vec{r}_2)}{|\vec{r}_1 - \vec{r}_2|} =$$

$$\sum_i \sum_j q_i \cdot q_j \cdot \frac{\beta_i^{n_i+3}}{4\pi(n_i+2)!} \cdot \frac{\beta_j^{n_j+3}}{4\pi(n_j+2)!} \times$$

$$\int d^3r_1 d^3r_2 \frac{|\vec{r}_1 - \vec{R}_i|^{n_i} \exp\{-\beta_i |\vec{r}_1 - \vec{R}_i|\} \cdot |\vec{r}_2 - \vec{R}_j|^{n_j} \exp\{-\beta_j |\vec{r}_2 - \vec{R}_j|\}}{|\vec{r}_1 - \vec{r}_2|}$$

(A.1)

where we have expanded ρ_A and ρ_B in spherical Slater functions. Thus the evaluation of the electrostatic Coulombic energy reduces to carrying out the six-dimensional integrals occuring under the doublesums.

The general form of the above integrals reduces in special cases to a somewhat simpler form when, for instance, one of the charges is a point charge so that the limit as $\beta \to \infty$ may be taken. In

fact will deal with this and other special cases on an individual basis. The results for the special cases really do not require a diiferent approach, but just a careful attention to the limiting values of the parameters used. In any event it is clear that the final expression for the Coulombic interaction energy of the two charge distributions is of the form

$$W_{AB} = \sum_{i\epsilon A} \sum_{j\epsilon B} q_i \cdot q_j \cdot C(n_i,\beta_i,\vec{R}_i,n_j,\beta_j,\vec{R}_j) \qquad (A.2)$$

where $C(n_i,\beta_i,\vec{R}_i,n_j,\beta_j,\vec{R}_j)$ contains the information about the parameters and positions defining the Slater functions:

$$C(n_i,\beta_i,\vec{R}_i;n_j,\beta_j,\vec{R}_j) = C_{ij} \equiv \frac{\beta_i^{n_i+3}}{4\pi(n_i+2)!} \cdot \frac{\beta_j^{n_j+3}}{4\pi(n_j+2)!} X$$

$$\int d^3r_1 d^3r_2 \frac{|\vec{r}_1-\vec{R}_i|^{n_i}\exp\{-\beta_i|\vec{r}_1-\vec{R}_i|\cdot|\vec{r}_2-\vec{R}_j|^{n_j}\exp\{-\beta_j|\vec{r}_2-\vec{R}_j|\}}{|\vec{r}_1-\vec{r}_2|}$$

(A.3)

The derivations have been given elsewhere; we here simply present the result for $C(n_i, \beta_i, \vec{R}_i, n_j, \beta_j, \vec{R}_j)$ both in its general form and for particular limiting values of the parameters. In general we have

$$C_{ij}(n_i,\beta_i,n_j\beta_j,R_{ij}) = \frac{1}{R_{ij}}\left\{1+\frac{1}{4(n_i+2)!\,(n_j+2)!}\times\left\{\right.\right.$$

$$e^{-\beta_i R_{ij}}.\left[\sum_{p=0}^{n_i+1}\sum_{q=0}^{p}\frac{(n_i+1)!\,(p-q+2)!\,(n_j+1+q)!}{(n_i+1-p)!\,q!\,(p-q)!}\cdot(\beta_i R_{ij})^{n_i+1-p}.\right.$$

$$\left[\frac{\beta_j}{\beta_i}\right]^{n_j+3}\left[\frac{1}{\left\{\frac{\beta_j}{\beta_i}+1\right\}^{n_j+2+q}}-\frac{(-1)^q}{\left\{\frac{\beta_j}{\beta_i}-1\right\}^{n_j+2+q}}\right]\Bigg]\Bigg]+$$

$$e^{-\beta_j R_{ij}}.\left[\sum_{p=0}^{n_j+1}\sum_{q=0}^{p}\frac{(n_j+1)!\,(p-q+2)!\,(n_i+1+q)!}{(n_j+1-p)!\,q!\,(p-q)!}\cdot(\beta_j R_{ij})^{n_j+1-p}.\right.$$

$$\left[\frac{\beta_i}{\beta_j}\right]^{n_i+3}\left[\frac{1}{\left\{\frac{\beta_i}{\beta_j}+1\right\}^{n_i+2+q}}-\frac{(-1)^q}{\left\{\frac{\beta_i}{\beta_j}-1\right\}^{n_i+2+q}}\right]\Bigg]\Bigg]\Bigg\}\Bigg\}$$

(A.4)

First consider the special case of $\beta_j \to \infty$ that is $\rho_B(\vec{r})$ is a point charge. We find

$$C_{ij}(n_i,\beta_i,n_j,\beta_j\to\infty,R_{ij}) = \frac{1}{R_{ij}}\cdot\left[1 - \frac{1}{(n_i+2)!}\cdot\exp(-\beta_i R_{ij})\cdot\left\{(\beta_i R_{ij})^{n_i+1} + \sum_{p=1}^{n_i+1}\frac{(n_i+1)!\,(p+1)}{(n_i+1-p)!}\cdot(\beta_i R_{ij})^{n_i+1-p}\right\}\right].$$

(A.5)

We note the expected result obtains if the second charge distribution becomes point-like, that is $\beta_i \to \infty$ also. Then the exponential factor goes to zero and $C_{ij} = 1/R_{ij}$.

Now we consider the special case in which $\beta_i = \beta_j$; with $\beta_i = \beta_j \equiv \beta$, we have

$$C_{ij}(n_i,\beta,n_j,\beta,R_{ij}) = \frac{1}{R_{ij}}\left\{1 + \frac{\exp(-\beta R_{ij})}{(n_i+2)(n_j+2)}\cdot\frac{1}{2}\cdot\right.$$

$$\left\{[-1]\sum_{p=0}^{n_i+n_j+3}\frac{(p+2)!}{2!\,p!\,((n_i+n_j+3-p)!}\cdot(\beta R_{ij})^{n_i+n_j+3-p} + \right.$$

$$\left.\left.\frac{1}{2^{n_i+3}}\cdot\left\{\sum_{p=0}^{n_j+1}\frac{(\beta R_{ij})^{n_j+1-p}}{(n_i+1)!\,(n_j+1-p)!}\left\{\sum_{q=0}^{p}\frac{(n_i+q+1)!\,(p-q+2)!}{2^q q!\,(p-q)!}\right\}\right\} + \right.\right.$$

$$\frac{1}{2^{n_j+3}}\cdot\left\{\sum_{p=0}^{n_i+1}\frac{(\beta R_{ij})^{n_i+1-p}}{(n_j+1)!\,(n_i+1-p)!}\left\{\sum_{q=0}^{p}\frac{(n_j+q+1)!\,(p-q+2)!}{2^q q!\,(p-q)!}\right\}\right\}\right\}$$

(A.6)

Thus we have considered all possible choices of β_i and β_j when the distance R_{ij} is different from zero. Each result is a simple algebraic expression involving at worst finite sums. When $R_{ij}=0$, but $\beta_i \neq \beta_j$ we get

$C_{ij}(n_i,\beta_i,n_j,\beta_j,R_{ij}=0) =$

$$\frac{\frac{1}{2}\beta_i \quad |}{(n_i+2)\,(n_j+2)}\left[\frac{\beta_j}{\beta_i}\right]^{n_j+3}\cdot\sum_{p=0}^{n_i+1}\left\{\frac{(n_i+2-p)\,(n_j+1+p)!}{p!\,(n_j+1)!}\right.$$

$$\left.\left[\frac{(-1)^p}{\left\{\frac{\beta_j}{\beta_i}-1\right\}^{n_j+2+p}}-\frac{1}{\left\{\frac{\beta_j}{\beta_i}+1\right\}^{n_j+2+p}}\right]\right\} \quad +$$

$$\frac{1/2\beta_j}{(n_i+2)\,(n_j+2)}\left[\frac{\beta_i}{\beta_j}\right]^{n_i+3}\cdot\sum_{p=0}^{n_j+1}\left\{\frac{(n_j+2-p)\,(n_i+1+p)!}{p!\,(n_i+1)!}\right.$$

$$\left.\left[\frac{(-1)^p}{\left\{\frac{\beta_i}{\beta_j}-1\right\}^{n_i+2+p}}-\frac{1}{\left\{\frac{\beta_i}{\beta_j}+1\right\}^{n_i+2+p}}\right]\right\}\cdot$$

(A.7)

The special case with one of the β's $\to \infty$ may be obtained from (A.7) For instance, if $\beta_i \to \infty$ only the second set of terms survive with the limit

$$C_{ij}(n_i,\beta_i\to\infty,n_j,\beta_j,R_{ij}=0) = \frac{\beta_j}{(n_j+2)} \qquad (A.8)$$

We note that any power n_i can be used in representing the point charge since no remnant remains in the final result. Obviously, if the second charge becomes more and more localized by having $\beta_j \to \infty$ the results itself becomes singular as it indeed must.

The final special case to be considered is that with $R_{ij}=0$ and $\beta_i = \beta_j \equiv \beta$. This time the integral is

$$C(n_i,\beta,n_j,\beta,R_{ij}=0) = \frac{\beta}{(n_i+2)\,(n_j+2)} \left\{ \frac{(n_i+n_j+4)}{2} \right.$$

$$- \frac{1}{2^{n_i+3}} \sum_{p=0}^{n_j+1} \frac{(n_j+2-p)\,(n_i+1+p)!}{p!\,(n_i+1)!\,2^p}$$

$$\left. - \frac{1}{2^{n_j+3}} \sum_{p=0}^{n_i+1} \frac{(n_i+2-p)\,(n_j+1+p)!}{p!\,(n_j+1)!\,2^p} \right\} . \qquad (A.9)$$

APPENDIX B

BIBLIOGRAPHY

I GORDON-KIM MODEL AND REFINEMENTS

1. Kim Y.S. and R.G. Gordon. J. Chem. Phys., Vol. 61, 1974, p.1.
2. Gordon R.G. and Yok Sik Kim. J. Chem. Phys., Vol 56, 1972, p. 3122.
3. Waldman Marvin and Roy G. Gordon. J. Chem. Phys., Vol. 71, 1979, p.1325.
4. Waldman Marvin and Roy G. GOrdon. J. Chem. Phys., Vol. 71, 1979, p.1340.
5. Waldman Marvin and Roy G. GOrdon. J. Chem. Phys., Vol. 71, 1979, p.1353.
6. Rae A.I.M.. Chem. Phys. Lett., Vol. 18, 1973, p.574.
7. Lloyd J. and D. Pugh. J. Chem. Soc. Faraday Trans. II, Vol.73, 1977, p.234.
8. Lloyd J. and D. Pugh. Chem. Soc. Lett., Vol. 26, 1974, p.281.
9. Rae A.I.M.. Mol. Phys., Vol. 29, 1975, p.467.
10. Muhlhausen Carl and Roy G. Gordon. Phys. Rev., Vol.B23, 1981, p.900.
11. Muhlhausen Carl and Roy G. Gordon. Phys. Rev., Vol.B24, 1981, p.2147.
12. LeSar R. and R. G. Gordon. Phys. Rev., Vol.B25, 1982, p.7221.
13. Pearson E.W. and R. G. Gordon. J. Chem. Phys., Vol.82, 1985, p.1.

II CALCULATIONS

1. Dreyfus C., d. Balou, and N. Brigot-Dutarte. J. Chem. Phys., Vol.80, 1984, p.5393.
2. Parker G. A. and R. T. Pack. J. Chem. Phys., Vol.69, 1978, p.3268.
3. Nelson Glen C. and Gregory A. Parker. J. Chem. Phys., Vol.66, 1977, p.1396.
4. Parker G. A., Richard L. Snow, R. T. Pack. J. Chem. Phys., Vol.64, 1976, p.1668.
5. Parker G. A., R. L. Snow, R. T. Pack. Chem. Phys Lett., Vol.33, 1975, p.399.
6. Clugston M. J. and N. C. Pyper. Chem. Phys. Lett., Vol.63, 1979, p.549.
7. Lloyd J. and D. Pugh. J. Chem. Soc. Faraday Trans. II, Vol.73, 1977, p.234.

8. Pyper W. C., I. P. Grant, R. b. Gerber. Chem. Phys. Lett., Vol.49, 1977, p.479.
9. Clugston M. J. and N. C. Pyper. Chem. Phys. Lett., Vol.58, 1978, p.457.
10. Clugston M. J.. Adv. Physic, Vol.27, 1978, p.893.
11. Schneider B., A. M. Boring, J. s. Cohen, Chem. Phys. Lett., Vol.27, 1974, p.576.
12. Tabsiz, Chem. Phys. Lett., Vol.52, 1977, p.125.
13. Shih C. C.. Mol. Phys., Vol.38, 1980, p.1225.

III HISTORICAL

1. Gaydaenko W. I. and V. K. Nikulin. Chem. Phys. Lett., Vol.7, 1970, p.360.
2. Nikulin V. K. and Yu N. Tsarev. Chem. Phys., Vol.10, 1975, p.433.
3. Abrahamson A. Adolf, Robert D. Hatcher, G. H. Vineyard, Phys. Rev., Vol.121, 1961, p.159.
4. Firsov O. B., J. Exptl. Theoret. Phys. (USSR), Vol.32, 1975, p.1464. Soviet Phys., JEPT Vol.5, 1957, p.1192.
5. Firsov O. B., J. Exptl. Theoret. Phys. (USSR), Vol.33, 1975, p.669. Soviet Phys., JEPT Vol.6, 1958, p.534.
6. Abrahmanson A. Adolf. Phys. Rev., Vol.130, 1963, p.693.
7. Abrahmanson A. Adolf. Phys. Rev., Vol.131, 1963, p.a990.
8. Thomas L. H.. Proc. Cambridge Phil. Soc., Vol.23, 1927, p.542.
9. Fermi E.. Z. Physik, Vol.48, 1928, p.73.
10. Dirac P. A. M.. Proc. Cambridge Phil. Soc., Vol.26, 1930, p.376.
11. Gombas P.. Die Statistiche Theories des Atoms und Ihre Anwendugen, (Springer, Berlin 1949).
12. Wedepohl P. T., Proc. Phys. Soc., Vol.92, 1976, p.79.
13. Wedepohl P. T., J. Phys., Vol.B1, 1968, p.307.
14. Gundhen K.. Analen der Physik, Vol.14, 1964, p.296.
15. Gombas P.. Rev. Mod. Phys., Vol.35, 1963, p.572.

IV FUNCTIONAL

1. Thomas L. H.. Proc. Cambridge Phil. Soc., Vol.23, 1927, p.542.
2. Fermi E.. Z. Physcik, Vol.48, 1928, p.73.

KINETIC

1. Von Weizacker C. F.. Z. Physik, Vol.96, 1935, p.431.
2. Acharya P. K., L. J. Barolotti, S. B. Sears, R. G. Parr. Proc. Natl. Acad. Sci. (USA), Vol.77, 1980, p.6978.
3. Le Counter K. J.. Proc. Phys. Soc., Vol.84, 1964, p.837.

4. Golden Sidney. Phys. Rev., Vol.A105, 1957, p.604; ibid Vol.A107, 1957, p.1283
5. Golden Sidney. Rev. Mod. Phys., Vol.32, 1960, p.322.
6. Deb B. M. and S. K. Ghosh. Int. J. Quant. Chem., Vol.XXIII, 1983, p.1.

EXHANGE

1. Dirac P. A. M.. Proc. Cambridge Phil. Soc., Vol.26, 1930, p.376.
2. Kohn W., and L. J. Sham. Phys. Rev., Vol.A140, 1966, p.1333.
3. Gunnarson O. and B. I.. Lundquist. Phys. Rev., Vol.B13, 1976, p.4274.
4. Bartolotti L. J.. J. Chem. Phys., Vol.76, 1982, p.6057.

GENERAL CONSIDERATIONS

1. Englert Berthold-Georg and Julian Schwinger. Phys. Rev., Vol.A29, 1984, p.2331. p.2339, p.2353.

GENERAL THEORY AND REVIEW ARTICLES

1. Honenberg P. and W. Kohn, Phys. Rev., Vol.B136, 1964, p.864.
2. Bamzai Anjuli S. and B. M. Deb. Rev. of Mod. Phys., Vol.53, 1981, p.95.
3. H. Leib Elliot. Rev. of Mod. Phys., Vol.53, 1981, p.803.
4. Bader R. F. W. and H. Essen. J. Chem. Phys., Vol.80, (1984), 1943 and reference therein.
5. The Force Concept in Chemistry, ed. by Deb B. M. (Van Nostrand-Reinhold, New York, 1981).

VITA 2

Iskhandar Md Nasir

Candidate for the degree of

Master of Science

Thesis: NUMERICAL ASPECTS OF DENSITY FUNCTIONAL THEORY: CHARGE DENSITY EXPANSIONS AND CALCULATIONS OF ELECTROSTATIC INTERACTION ENERGIES

Major Field: Physics

Biographical:

Personal Data: Born in Johor Bahru, Malaysia, January 17, 1962, the son of Mohammad Nasir Haji Marzuki and Jamilah Abdul Hamid. Married to Norizan Ishak on May 4, 1984, with one child Azzakirah.

Education: Graduated from Dato' Jaafar School, Johor Bahru in November 1979. Received Bachelor of Science from Oklahoma State University in 1984. Completed the requirements for Master of Science degree at Oklahoma State University in July, 1987.

Professional Experience: Teaching Assistant, Department of Physics, Oklahoma State University, August 1984 to May 1987.